

1-egged in 6/28/84

WM RECORD COPY

Cyda

Unit Evaluation at Yucca Mountain, Nevada Test Site: Summary Report and Recommendation

J. Keith Johnstone, Ralph R. Peters, Paul F. Gnirk

Prepared by
Sandia National Laboratories
Albuquerque, New Mexico 87185 and Livermore, California 94550
for the United States Department of Energy
under Contract DE-AC04-76DP00789

HYDROLOGY DOCUMENT NUMBER 222

SAND83-0372
Distribution Category UC-70
Unlimited Release
Printed June 1984

UNIT EVALUATION AT YUCCA MOUNTAIN, NEVADA TEST SITE:
SUMMARY REPORT AND RECOMMENDATION

J. Keith Johnstone and Ralph R. Peters
NNWSI Repository Assessments Division 6312
Sandia National Laboratories
Albuquerque, NM 87185

and

Paul F. Gnirk
RE/SPEC Inc.
Under Sandia Contract: 37-3278

*1) NO RELEASE
FIRST 1000 YEARS.
∴ NO HOAT CONSIDERED*

Abstract

By the end of FY81, at least four potential repository units were identified at Yucca Mountain, as part of the Nevada Nuclear Waste Storage Investigations project. Two potential units--the welded, devitrified portions of the Bullfrog and Tram Members of the Crater Flat Tuff--are below the water table. The welded, devitrified Topopah Spring Member of the Paintbrush Tuff and the nonwelded, zeolitized Tuffaceous Beds of Calico Hills are above the water table. In this report, Sandia National Laboratories and its subcontractors, Pacific Northwest Laboratory and RE/SPEC, Inc., report the results of a study of the four potential repository units to provide a technical basis for selecting a single target repository unit for future test and evaluation. The unit evaluation studies compared the units rather than provided an absolute assessment. The four ranking evaluation criteria used were 1) radionuclide isolation time, 2) allowable repository gross thermal loading, 3) excavation stability, and 4) relative economics. Considered the most important of the criteria as well as the most difficult, radionuclide isolation times (including groundwater travel times) were estimated using the limited existing data. The allowable repository gross thermal loadings determined from near-field calculations, were nearly the same for all four units. The gross thermal loading supported other criteria by providing the heat source for succeeding thermally related evaluation studies. A large number of studies evaluated excavation stability, including near-field mechanical and thermomechanical finite element code calculations, rock matrix property evaluation, and rock mass classification. Relative economics, a minor criterion, did not play an explicit role in the final ranking. Based on all of the analyses, the final recommendation was that the Topopah Spring be selected as the target unit, followed, in order, by the Calico Hills, Bullfrog, and Tram.

CONTENTS

	<u>Page</u>
Abstract	i
1.0 INTRODUCTION	1
2.0 UNIT EVALUATION STUDIES	5
2.1 Constructibility	5
2.1.1 Definitions	5
2.1.2 Mineability	5
2.1.3 Excavation Stability	6
2.1.3.1 Near-Field Thermal, Mechanical, and Thermomechanical Evaluation	6
2.1.3.2 Rock Matrix Property Evaluation	14
(a) Analysis of Unconfined Mechanical Property Data	15
(b) Analysis of Ratio of Compressive Strength to Overburden Stress	15
(c) Pillar Safety Factor	17
(d) Effect of Stress Concentrations	17
(e) Effect of Waste Decay Heating	18
2.1.3.3 Rock Mass Classification	18
2.2 Far-Field Thermal/Mechanical Evaluation	21
2.3 Groundwater Travel Time Estimates	23
2.3.1 Unsaturated Zone	23
2.3.2 Saturated Zone	24
2.3.3 Radionuclide Transport	26
3.0 SUMMARY OF RANKINGS	27
4.0 RECOMMENDATION	30
5.0 REFERENCES	30
FIGURES	34

TABLES

<u>Table No.</u>	<u>Title</u>	<u>Page</u>
1	Description of Potential Repository Units in USW-G1	3
2	Relationship Between Ranking Criteria and Unit Evaluation Studies	4
3	Average and Limit Properties for Tuff	8
4	Optimized Repository Gross Thermal Loading	10
5	Factor of Safety for Rock Mass	16
6	Rock Mass Classification Estimates of Unsupported Roof Span Size and Standup Time	20
7	Estimate of Groundwater Travel Time from Unsaturated Repository Horizons Vertically Downward to the Transmissive Zones (at G-1)	24
8	Average Hydraulic Conductivity (m/day)	25
9	Preliminary Hydraulic Conductivity Distribution Measured in USW-H1	25
10	Estimates of Groundwater Travel Times From Saturated Repository Horizons Vertically Upward to the Transmissive Zone	26
11	Average Sorption Ratios from Batch and Circulating System Sorption Experiments on Crushed Tuff	28
12	Summary of Unit Rankings	29

FIGURES

<u>Figure No.</u>	<u>Title</u>	<u>Page</u>
1	Comparison of the Lithologic and Thermal/Mechanical T/M) Stratigraphies	35
2	C-C' Cross Section of the Thermal/Mechanical Stratigraphy	36
3	Map of Yucca Mountain Showing the Location of the C-C' Cross Section and Its Relation to Various Drill Holes	37
4	A Portion of the Finite-Element Mesh Used in Near-Field Thermal/Mechanical Calculations	38
5	Preliminary Technical Constraints for the Near Field	39
6	Ratio of Horizontal to Vertical Stress (K_0) as a Function of Depth	40
7	Joint Movement in Calico Hills Due to Excavation	41
8	Cumulative Joint Movement in Calico Hills Due to 100 Years of Heating	41
9	Joint Movement at 50-Year Time Step in the Calico Hills	42
10	Joint Movement at 100-Year Time Step in the Calico Hills	43
11	Cumulative Joint Movement in First 100 Years in Calico Hills	44
12	Calico Hills Matrix Fracturing Due to Excavation (None) and 100 Years of Heating (Average properties)	45

FIGURES (continued)

<u>Figure No.</u>	<u>Title</u>	<u>Page</u>
13	Calico Hills Matrix Fracturing Due to Excavation and 100 Years of Heating (Limit properties)	45
14	Matrix Factor of Safety Contours for the Calico Hills (Average properties) at Excavation	46
15	Matrix Factor of Safety Contours for the Calico Hills (Average properties) at 50 Years	46
16	Matrix Factor of Safety Contours for the Calico Hills (Limit properties) at Excavation	47
17	Matrix Factor of Safety Contours for the Calico Hills (Limit properties) at 50 Years	47
18	Fractured Matrix Regions for the Calico Hills (Limit properties) at Excavation (No joints)	48
19	Fractured Matrix Regions for the Calico Hills (Limit properties) at 100 Years (No joints)	48
20	Joint Movement for Topopah Spring at Excavation	49
21	Cumulative Joint Movement for Topopah Spring to 100 Years	49
22	Fractured Matrix Regions for Topopah Spring to 100 Years (Limit properties)	50
23	Matrix Factor of Safety Contours for Topopah Spring (Average properties) at Excavation	51
24	Matrix Factor of Safety Contours for Topopah Spring (Average properties) at 50 Years	51
25	Matrix Factor of Safety Contours for Topopah Spring (Limit properties) at Excavation	52

FIGURES (continued)

<u>Figure No.</u>	<u>Title</u>	<u>Page</u>
26	Matrix Factor of Safety Contours for Topopah Spring (Limit properties) at 50 Years	52
27	Joint Movement for Bullfrog at Excavation	53
28	Cumulative Joint Movement for Bullfrog to 100 Years	53
29	Matrix Factor of Safety Contours for Bullfrog (Average properties) at Excavation	54
30	Matrix Factor of Safety Contours for Bullfrog (Average properties) at 50 Years	54
31	Matrix Factor of Safety Contours for Bullfrog (Limit properties) at Excavation	55
32	Matrix Factor of Safety Contours for Bullfrog (Limit properties) at 50 Years	55
33	Joint Movement for Tram at Excavation	56
34	Cumulative Joint Movement for Tram to 100 Years	56
35	Fractured Matrix Region for Tram to 100 Years (Limit properties)	57
36	Matrix Factor of Safety Contours for Tram (Average properties) at Excavation	58
37	Matrix Factor of Safety Contours for Tram (Average properties) at 50 Years	58
38	Matrix Factor of Safety Contours for Tram (Limit properties) at Excavation	59

FIGURES (continued)

<u>Figure No.</u>	<u>Title</u>	<u>Page</u>
39	Matrix Factor of Safety Contours for Tram (Limit properties) at 50 Years	59
40	Joint Movement for Grouse Canyon at Excavation	60
41	Comparison of Regions of Predicted Joint Movement in the Four Potential Units With Grouse Canyon at Excavation	61
42	Sample Mechanical Properties Versus Sample Depth for the Calico Hills (Tests on saturated samples at room temperature)	62
43	Frequency Plots of Unconfined Compressive Strength	63
44	Pillar Factor of Safety Determined According to Two Different Techniques	64
45	Schematic Showing the Manner in Which the Average Factor of Safety for the Room was Calculated	65
46	Average Factor of Safety for an Unheated Room Expressed as a Function of the Ratio of the Reduced Unconfined Compressive Strength to the Vertical Stress	66
47	Average Factor of Safety for a Heated Room Expressed as a Function of the Ratio of the Reduced Unconfined Compressive Strength to Sum of the Vertical and Thermal Stresses	67
48	Tunneling Quality Index for the Four Units at Yucca Mountain and the Two Units at G-Tunnel	68
49	Finite Element Mesh Used in Far-Field Thermal/Mechanical Calculations	69

FIGURES (continued)

<u>Figure No.</u>	<u>Title</u>	<u>Page</u>
50	Schematic Diagram Showing Position of Boundaries	70
51	Far-Field Preliminary Technical Constraints	71
52	Thermal Model Conceptualized	72
53	Thermal History of the 15% Boundary Below the Repository Horizons (Average properties)	73
54	Thermal History of the 15% Boundary Below the Repository Horizons (Limit properties)	73
55	Thermal History of the 15% Boundary Below the Topopah Spring Repository Horizon	74
56	Thermal History of the 85% Boundary Below the Repository Horizons (Average properties)	74
57	Thermal History of the 85% Boundary Below the Topopah Spring Repository Horizon	75
58	Thermal History 3 m Below Ground Surface When the Repository is Located in the Topopah Spring Horizon	75
59	Mechanical Model Conceptualized	76
60	Far-Field Joint Opening With the Repository in the Topopah Spring (Average properties throughout the section)	77
61	Far-Field Joint Opening With the Repository in the Topopah Spring (Limit properties throughout the section)	78

FIGURES (continued)

<u>Figure No.</u>	<u>Title</u>	<u>Page</u>
62	Surface Uplift Resulting From a Repository Emplaced in the Designated Units (Average properties throughout the section)	79
63	Surface Uplift Resulting From a Repository Emplaced in the Designated Units (Limit properties throughout the section)	79
64	Conceptual Model for Groundwater Flow	80
65	Conceptual Steady-State Infiltration Model for the Unsaturated Zone	81

1.0 INTRODUCTION

The Nevada Nuclear Waste Storage Investigations (NNWSI) Project, managed by the Nevada Operations Office of the U.S. Department of Energy, is examining the feasibility of siting a repository for high-level nuclear wastes at Yucca Mountain on and adjacent to the Nevada Test Site. The work presented here was funded by the NNWSI Project. The expected result of this work was to provide a technical basis for selecting a single target repository horizon upon which to concentrate future activities.

Historically, the NNWSI Project focused on characterizing potential repository units below the water table at Yucca Mountain. By mid FY81, two such units had been identified. They were the welded, devitrified portions of the Bullfrog and Tram Members of the Crater Flat Tuff. Late in FY81, attention turned to the unsaturated zone, above the water table, which also contained two potential repository units; the welded, devitrified Topopah Spring Member of the Paintbrush Tuff, specifically limited to the zone containing 10% lithophysae or less, and the nonwelded, highly zeolitized (clinoptilolite) Tuffaceous Beds of Calico Hills. Within the repository block, the Topopah Spring lies entirely above the static water level while portions of the Calico Hills drop below the static water level toward the east. Thus, as a consequence of the exploratory program at Yucca Mountain, at least four potential repository units had been identified by the end of FY81.

At the beginning of FY82, we began a formal unit evaluation activity, which was originally scheduled for completion in December 1982, and later revised to February 1983. The activity was intended to provide a relative comparison of the four potential repository horizons using existing data and codes, supplemented by engineering and scientific judgment when necessary, and was aimed at identifying the one zone most suitable for repository placement. The activity was not a site performance assessment and should not be interpreted as such. Note that in July 1982, in the midst of the unit evaluation study, a programmatic decision, prompted by exploratory shaft design needs, was made selecting the Topopah Spring as the reference case target horizon.

The unit evaluation studies were limited to those which we anticipated would provide discrimination between units and which we had a reasonable probability of being able to complete successfully considering the availability of real and estimated data. Some studies were performed in spite of a nearly complete absence of real data or by using very preliminary data because they were deemed crucial to the evaluation. The water travel time estimates are an example of such a study. For these cases, we strived to pursue a conservative analysis. An example of a nondiscriminating study is movement along a fault since the consequence of fault movement should be substantially the same for each unit. Another nondiscriminator is the waste package. Since it is a totally engineered subsystem of the repository, we assumed that it could be made equally effective in all horizons even though, in fact, that may be more easily (and, hence, less expensively) accomplished in the unsaturated units. Nevertheless, we could not identify any factors that would severely compromise the waste package in any of the units. Finally, at the time the unit evaluation studies were initiated, reference waste package designs for tuff were not available.

We used the most current information we could, within the time limitations available for the study. In an attempt to bound the results, we performed calculations with average and limit material properties whenever possible. The limit properties were taken as either $\pm 2\sigma$ from average values, the sign being chosen on a worst-case basis. Because of the very limited data base, we have the most confidence in the results obtained with the average material properties because, as the data base expands, a consistent value for an average property often converges faster than the value for a limit property.

Our approach to unit evaluation was divided into six steps: 1) define the system, 2) develop preliminary technical constraints, 3) establish unit ranking criteria, 4) obtain a relative optimized gross thermal (waste) loading for a repository in each unit, 5) evaluate the repository behavior in each unit relative to the technical constraints using the optimized gross thermal loading, and 6) rank each potential repository emplacement zone. To define the system, we replaced the lithologic description of the strata with an appropriate stratigraphy based on zones having similar thermal/mechanical, hydrological, or geochemical properties. An example is shown in Figure 1 (figures grouped following text) which compares the formal lithologic stratigraphy and the thermal/mechanical stratigraphy developed for drill hole USW-G1.^{1,2} Note that the boundaries on the zones in the thermal/mechanical stratigraphy do not necessarily coincide with those of the formal lithologic stratigraphy.

The position of the four potential repository horizons within the thermal/mechanical stratigraphic zones are shown in the C-C' cross section² in Figure 2. The C-C' cross section runs approximately east-west across Yucca Mountain through hole UE25A-1 as shown on the map in Figure 3. For comparison, the estimated position of the static water level is also included in Figure 2. Descriptive information for each of the four repository horizons relative to drill hole USW-G1 is shown in Table 1. Included in the table is the depth of each repository, the thickness of the zone in which the repository is placed, the distance of the repository from the static water level, and the ambient temperature at each repository horizon.

We made six assumptions at the beginning of the unit evaluation activity which simplified the total system. First, we considered only repository behavior under expected conditions, i.e., we did not consider the effects of earthquake, volcanism, meteor impact, etc. Next, we assumed that the repositories were parallel to the stratigraphy and that waste was emplaced in boreholes located in the drift floor. Another tuff repository design concept calls for emplacement of waste canisters in long (~180 m), horizontal holes bored into the pillars³ rather than as assumed in this study. While we have not addressed the horizontal emplacement scheme in detail, preliminary analyses indicate that it would not affect the relative comparison of the potential repository zones. We assumed, due to the limited data base, that the material properties were laterally uniform throughout a given zone. Note, however, that possible extremes in material properties were accounted for by the limit material properties. The last two assumptions were that spent fuel was the waste form and that all waste was emplaced immediately. The latter assumption eliminated the need for three-dimensional code analysis.

Table 1

Description of Potential Repository Units in USW-G1

	<u>Topopah Spring</u>	<u>Calico Hills</u>	<u>Bullfrog</u>	<u>Tram</u>
Repository Depth	348 m	478 m	745 m	881 m
Thermal/Mechanical Zone	2B	4A	6	8
Zone Thickness	88 m	104 m	63 m	79 m
Distance from Repository to Static Water Level ^a	225 m	94 m	-173 m	-309 m
Ambient Temperature	26°C	30°C	38°C	41°C

^a Positive and negative values indicate distance above and below static water level, respectively.

The ranking criteria were also established at the beginning of the activity. We attempted to keep them simple and to limit their number, yet, at the same time, cover the significant technical discriminators among the alternative horizons. The criteria that were established were 1) radionuclide isolation time, 2) allowable repository gross thermal loading, 3) excavation stability, and 4) relative economics.

Radionuclide isolation time (generally, the longer the better) was considered by far to be the most important of the criteria. It is dependent on water travel times and radionuclide sorption factors, among others, none of which is well understood at the present. Some care must be exercised in these studies because of the potentially long times calculated using relatively poor-quality data. The longer the calculated times the less the discrimination when compared to other long times.

We expected that allowable repository gross thermal loading (the higher the better) would discriminate between units according to the relative quantity of waste each was capable of accepting, which would, in turn, affect economics. One of the main concerns addressed by this criteria was to ensure that each unit could accept the designated 70,000 metric tons of uranium (MTU) waste equivalent for the first waste repository. These studies showed that each of the four units could accept the 70,000 MTU of waste. Determination of the allowable gross thermal loading also provides the heating source term for all subsequent thermally related evaluation studies.

Excavation stability received considerable attention in this activity even though it is not directly related to waste isolation. Excavation stability, instead, relates to worker safety and maintaining the option to retrieve the

waste. Evaluation of the stability of the underground openings depends, in large part, on the repository gross thermal loading. Nevertheless, as with all the studies carried out in the unit evaluation activity, we studied excavation stability as thoroughly as possible using every approach at our disposal.

Relative economics (the cheaper the better, consistent with satisfactory waste isolation) was the last criterion to be considered. We made no attempt to carry out a cost analysis or attach actual dollar costs to repository components. In fact, the extent of the economic analysis was only to assume, for example, that the deeper the repository, the greater the cost. In general, economics would have been considered only in the case of a tie in technical ranking between two or more repository units. In such a case, the cheaper repository would be considered the most desirable. As it turned out, no such tie occurred and economics did not play an explicit role in the final ranking.

Based on the foregoing discussions, the studies included in the unit evaluation activity were the mineability, relative gross thermal loading, excavation stability, far-field thermal/mechanical behavior, and groundwater/radionuclide travel time for a repository in each of the four zones. Excavation stability was evaluated by near-field thermomechanical calculations, rock matrix property evaluation, and rock mass classification. The relationship between the ranking criteria and the evaluation studies is shown in Table 2. In several cases, a particular study supports more than one of the ranking criteria. The remainder of this report summarizes each of the studies individually, and ends with a summary of the rankings and a final recommendation.

Table 2

Relationship Between Ranking Criteria and Unit Evaluation Studies

1. Radionuclide Isolation Time
 - o Groundwater travel time
 - o Radionuclide travel time
 2. Allowable Repository Gross Thermal Loading
 - o Gross thermal loading determinations
 - o Near-field thermal evaluations
 - o Far-field thermal and thermomechanical evaluations
 3. Excavation Stability
 - o Near-field thermal, mechanical, and thermomechanical finite element code evaluations
 - o Rock matrix property evaluation
 - o Rock mass classification
 4. Relative Economics
 - o Mineability
 - o Gross thermal loading determinations
-

2.0 UNIT EVALUATION STUDIES

2.1 Constructibility

2.1.1 Definitions

The construction of a system of underground openings, involving shafts, tunnels, drifts, and rooms, requires two processes: rock excavation and rock stabilization. Rock excavation, or mining, is commonly accomplished either by conventional drilling and blasting or by use of a machine that mechanically cuts the rock in a continuous fashion. The relative ease with which a rock mass can be excavated, with the associated influence of rock temperature, water influx, rock mass variability, and depth, is defined herein as mineability. Rock mass stabilization by artificial means, such as rockbolts and wire mesh, steel sets and lagging, etc., may be necessary if the rock around the opening is unable to accommodate the existence of the opening. That is, the response of the rock mass to the surrounding in situ and thermal stresses may be such that it is unable to support itself over the intended operational lifetime of the opening. This aspect of constructibility is defined herein as excavation stability, and involves consideration of rock mass properties, such as matrix strength, joint properties, thermal properties, and the existence of water, in relation to the opening geometry and state of stress.

2.1.2 Mineability

On the basis of observations of drill core and G-tunnel (located in Rainier Mesa on the NTS) excavations, as well as evaluations of relevant geologic reports and laboratory test data, it was the consensus from three groups of consultants that underground openings could be constructed in all four potential emplacement zones at Yucca Mountain (Ash and Craig;⁴ Gnirk and Ratigan;⁵ Hustrulid⁶). From the strict viewpoint of mineability, as defined above, the relative ease of excavation would correspond closely with the degree of welding in the tuff. Specifically, the excavation of underground openings in the Calico Hills, which is nonwelded, could be accomplished with a continuous mining machine. The use of continuous mining in the Bullfrog and Tram, which are partially to moderately welded, appears to be possible, although with more difficulty than expected for the Calico Hills. Due to dense welding and relatively high compressive strength of the Topopah Spring, excavation by drilling and blasting would be required.

Recently, continuous mining machines with rotary cutter heads have been used to excavate underground openings in rocks with compressive strengths comparable to moderately and densely welded tuffs. Thus, it may be feasible in the near future to use continuous mining machines in all of the potential emplacement zones at Yucca Mountain. However, the rate of advance in tunnel excavation would still be strongly governed by the compressive strength of the rock and the existence of joints. From a practical view, the use of continuous mining machines for underground excavation would be preferred to conventional drilling and blasting because it causes less disturbance to the rock mass around an opening.

Tunnel excavation in the potential emplacement zones above the water table would also be easier due to relatively less groundwater influx during excavation. Extensive water influx during excavation detrimentally influences the performance of both personnel and equipment, and sometimes imposes difficulties with ground support in the immediate vicinity of headings. Furthermore, large or continuous influxes of water must be handled and removed from the facility during both mining and operation.

Based on data from exploratory drill holes from the surface, the ambient rock temperature appears to increase approximately 10 to 20% with depth from one emplacement zone to the next. Increasing temperature with depth directly affects the amount of ventilation, and possibly cooling, required during both excavation and operation of underground openings. For this reason, it would be preferable to construct underground openings in the shallowest and, hence, coolest emplacement zone.

Due to the fact that in situ compressive stresses in the rock mass increases with depth, it would not be unreasonable to anticipate some increase in construction difficulties with depth. These difficulties may be unexpected tunnel roof and rib slabbing during the actual excavation process, particularly in potential regions of localized faults and rubblized rock. Note, however, that such difficulties can occur in underground openings at any depth. Therefore, from a mineability point of view, in situ stress was nondiscriminating.

Upon consideration of all of the factors mentioned above, excavation of underground openings in the tuffs above the water table would be preferable to excavation below the water table. More specifically, mineability of the Calico Hills would be ranked as best on a relative basis, followed by the Topopah Spring, Bullfrog, and Tram in that order. We must emphasize, however, that underground openings could be constructed in all four emplacement zones.

2.1.3 Excavation Stability

2.1.3.1 Near-Field Thermal, Mechanical, and Thermomechanical Evaluation

The near-field thermal/mechanical calculations were carried out by Johnson,⁷ Thomas,⁸ and Melo and Parrish.⁹ The purposes of this study were to determine relative optimized gross thermal loadings, and to examine the near-field (room and pillar) response to repository excavation and heating due to waste emplacement within the framework of the technical constraints. Determination of the relative optimized gross thermal loading for each unit also addresses, indirectly, the economic ranking criteria since a greater gross thermal loading corresponds to greater economic efficiency of the repository. In addition, it provides the basis for all the following near- and far-field thermal and thermomechanical analyses.

The model thermal, mechanical, and physical input parameters are described by Peters and Lappin,^{10,11} Peters,¹²⁻¹⁴ and Price,¹⁵ many of which are based on the data collected by Lappin.¹⁶⁻¹⁸ The thermal/mechanical average and limit properties for the four potential emplacement zones are given in

Table 3. Both the near- and far-field thermal/mechanical calculations were carried out using state-of-the-art, finite element computer codes. The thermal fields were determined using ADINAT¹⁹ and SPECTROM-41.²⁰ The thermomechanical studies were carried out with continuum elastic/plastic stress analysis codes (Sandia-ADINA²¹ and SPECTROM-11²²) containing ubiquitous vertical joints (aligned parallel to the axis of the drift for near-field calculations).

A portion of the two-dimensional, planar, finite-element mesh used for these calculations is shown in Figure 4. The plane of the two-dimensional model was normal to the axis of the room. The volumetric heat output was determined by the canister pitch and by generalizing the individual waste canisters to a continuous trench whose dimensions were determined by the canister height and diameter. Vertical adiabatic symmetry planes are located at the pillar centerline on the right and at the drift centerline on the left. Mechanically, these planes correspond to zero horizontal displacement. The upper and lower horizontal boundaries are isothermal. No vertical displacement occurs at the lower boundary. The initial conditions were that all temperatures were equal to the ambient temperature, all stresses were equal to the in situ stresses, and all displacements were zero.

The near-field technical constraints considered in optimizing the thermal loadings in the four emplacement zones are summarized in Figure 5. A detailed description of the constraints are summarized elsewhere.²³ The operational period includes all underground operations such as mining, waste emplacement, monitoring and retrieval (if required) until closure of the repository. The operational period may last as long as 110 years or as short as 50 years. In this study we assumed the 110-year value. The containment period is the time after closure in which the radionuclides are totally contained within the waste package. The containment period may extend as long as 1,000 years after closure. The isolation period applies to times after the containment period and is concerned mainly with the release of radionuclides from the repository. The constraints in the near field are primarily limited to the operational period and almost half the constraints are a consequence of maintaining the retrievability option. For the studies reported here, we assumed that during the operational period the rooms remained open, that is, they were not backfilled until final repository closure.

Of particular interest is the 100°C maximum temperature limitation for the drift floor, a preliminary constraint based on the ability of men and equipment to reenter a storage room and retrieve waste canisters. The current value of 100°C for this constraint is somewhat arbitrary, but we believe it is a maximum value. In the absence of a waste package or backfill, it was found to be the controlling constraint in optimizing the repository gross thermal loading. While open rooms could be cooled by continuous ventilation or blast ventilation in the case where the room had been sealed off, the extent of cooling into the rock is expected to be tens of centimeters at most. For the case of backfilled rooms, blast ventilation would not accomplish a significant, in-depth temperature reduction in the backfill. Thus, serious threat to worker safety exists if large quantities of tunnel backfill, at temperatures near 100°C, must be removed and transported during retrieval operations. This

Table 3

Average and Limit Properties for Tuff

Ambient Temperature and Tuff Thermal Properties

		<u>Average Case</u>				<u>Limit Case</u>			
		<u>Topopah Spring</u>	<u>Calico Hills</u>	<u>Bullfrog</u>	<u>Tram</u>	<u>Topopah Spring</u>	<u>Calico Hills</u>	<u>Bullfrog</u>	<u>Tram</u>
Temperature Ranges (°C)	Sat ^a	<100	<100	<100	<100	<100	<100	<100	<100
	Trans ^b	100-125	100-150	100-125	100-125	100-125	100-150	100-125	100-125
	Dry	>125	>150	>125	>125	>125	>150	>125	>125
Conductivity (W/m°C)	Sat	1.8	1.3	2.0	2.2	1.5	1.2	2.0	2.0
	Trans	1.7	1.1	1.7	2.05	1.45	1.0	1.7	1.8
	Dry	1.6	0.9	1.4	1.9	1.40	0.8	1.4	1.6
Heat Capacity (cal/cm ³ °C)	Sat	0.52	0.65	0.63	0.62	0.53	0.67	0.63	0.63
	Trans	2.47	3.93	5.32	4.49	3.15	4.44	5.51	5.71
	Dry	0.42	0.32	0.40	0.43	0.40	0.29	0.39	0.38
Thermal Expansion (°C ⁻¹ 10 ⁻⁶) (Temp Range, °C)		10.7 (32-200)	6.7 (32-100)	8.0 (32-100)	8.0 (32-100)	14.1 (32-200)	-0.4 (32-100)	5.2 (32-100)	5.2 (32-100)
		31.8 (200-350)	-56.0 (100-150)	-12.0 (100-125)	-12.0 (100-125)	53.6 (200-350)	-115.0 (100-150)	-20.0 (100-125)	-20.0 (100-125)
		15.5 (350-400)	-4.5 (150-300)	11.0 (125)	11.0 (125)	23.1 (350-400)	-9.3 (150-300)	9.4 (125)	9.4 (125)
Initial Temp (°C) (near field)		26	30	38	41	29	34	40	44

Table 3 (Cont'd)

In Situ Stress and Tuff Mechanical Properties

	<u>Average Case</u>				<u>Limit Case</u>			
	<u>Topopah Spring</u>	<u>Calico Hills</u>	<u>Bullfrog</u>	<u>Tram</u>	<u>Topopah Spring</u>	<u>Calico Hills</u>	<u>Bullfrog</u>	<u>Tram</u>
E (MPa)	26.7	8.1	15.5	21.8	18.2	6.3	14.3	13.3
ν	0.14	0.16	0.19	0.19	0.16	0.14	0.18	0.18
Unconfined Compressive Strength (MPa)	91	29	54	75	63	22	50	47
σ_v (MPa) (near field)	8.6	10.3	16.8	20	11.3	15.4	20.6	23.7
σ_h/σ_v (near field)	0.96	0.87	0.72	0.70	0.96	0.87	0.72	0.70
Matrix Cohesion (MPa)	28.5	10.9	18.1	24.0	20.7	9.0	17.0	16.1
Angle of Internal Friction (Deg)	26	15.9	22.1	24.7	23.4	12.3	21.4	20.8
Matrix Tensile Strength (MPa)	12.8	0.1	7.7	11.1	9.4	0.1	6.9	6.0
Joint Cohesion (MPa)	1	0.4	1	1	0	0	0	0
Coeff. of Stable Sliding Friction	0.8	0.55	0.8	0.8	0.8	0.55	0.8	0.8
Joint Tensile Strength(MPa)	0.1	0.	0.1	0.1	0.1	0	0.1	0.1

^a Eighty percent saturated in Topopah Spring.

^b Transition from saturated to dry rock.

constraint is undergoing continuous evaluation and may be revised as new information and better understanding of the thermal environment becomes available.

The results of the gross thermal loading optimization studies are shown in Table 4. Average thermal rock properties and no drift ventilation were used in the calculations. The maximum relative gross thermal loading was determined so that the drift floor temperature reached 100°C at 110 years. The calculations considered both boiling, with the removal of the vaporization energy from the system, and nonboiling of the pore water in the rock. The most interesting results of this study are the similarity in maximum loading for all four units regardless of the initial ambient temperature and the fact that how the water was treated had virtually no effect on the final result.

Table 4

Optimized Repository Gross Thermal Loading
(Using the Maximum Room Floor Temperature 100°C
from 0 to 110 Years as the Controlling Constraint)

	Gross Thermal Loading (kW/acre)	
	Pore Water (boiling)	Pore Water (not boiling)
Topopah Spring	57	57
Bullfrog	56	55
Tram	55	54
Calico Hills	54	53

At 50 years, the drift floor temperatures vary from 95 to 97°C. Consequently, optimizing the gross thermal loading at 50 instead of 110 years would result in little, if any, increase in the present values and would not affect the rankings. For practical purposes, the calculated thermal loadings in the four repository zones appear identical and do not provide any means of discrimination. Nevertheless, for the thermal and thermomechanical calculations discussed below, the individual gross thermal loading was used for each unit, that is, 57 kW/acre was used for the Topopah Spring, 56 kW/acre for the Bullfrog, 55 KW/acre for the Tram, and 54 KW/acre for the Calico Hills.

We turn now to the near-field mechanical and thermomechanical studies. The ratio of the average horizontal stress to vertical stress as a function of depth, used in both the near- and far-field mechanical calculations, is shown by the dotted line in Figure 6. At the time we began these studies, no in situ stress measurements had been made at Yucca Mountain. The stress ratio curve, shown in Figure 6, was determined by Langkopf after a literature review of stress ratios at Rainier Mesa and other tuffs not on the NTS.²⁴

Recently, Healy et al. have reported minimum horizontal stress values determined by hydrofracturing techniques.²⁵ For comparison, stress ratios based on these data are also plotted on Figure 6 as bars. The right limit on each bar was determined by assuming that the maximum horizontal stress was equal to the vertical stress. The left limit was determined by assuming that the maximum horizontal stress was equal to the minimum horizontal stress, that is, that the horizontal stresses were isotropic. An estimate of the maximum horizontal stress was made using the minimum stress measured by hydrofracturing, the tensile strength of the rock, and assuming a hydrostatic pore pressure fixed by the static water level. The values of stress ratio corresponding to the estimated maximum horizontal stress lie near the center of each bar.

As mentioned above, we monitored the calculated behavior of both ubiquitous vertical joints and the rock matrix in the rock mass surrounding the mined opening for the cases of excavation (no heating) and later time, thermally induced stresses due to waste emplacement. Joint movement was characterized by either shear along the joints, opening normal to the joint plane, or, in many cases, both. Similarly, rock matrix fracturing could occur by shear or tensional failure. Joint movement and matrix fracture were determined according to individual Mohr-Coulomb criteria which are described elsewhere.^{7,9}

The calculated mechanical response of the rock surrounding a room is summarized for each of the four units in the figures that follow. Figure 7 shows the response of joints in the Calico Hills to excavation. The solid line encloses the regions of calculated joint movement (shear or opening) using average material properties. The dotted line represents similar regions for limit material properties. Figure 8 shows the accumulated regions of thermally induced joint movement in the Calico Hills through a period of 100 years. Note in this case that the regions of calculated joint movement penetrate more than half the pillar width.

The next several figures demonstrate how these regions of joint movement were determined. The same method is used to describe the regions of matrix fracturing. Figure 9 shows the actual finite element code output at the 50-year time step using limit material properties. The output is in the form of Xs and Os where X denotes slip along a joint and O denotes opening normal to the joint. Figure 10 shows the code output for the 100-year time step for comparison. Note in this case that a considerably larger number of joints show opening instead of slip. Figure 11 shows the accumulated thermally induced joint behavior from the onset of heating to 100 years. In this case, a solid O indicates that a joint showed both opening and slip at some time during the 100-year time interval. The region of joint movement was determined by simply drawing a boundary around this summary plot of the accumulated computer code output. The region defined in Figure 11 corresponds to the dotted line region in Figure 8.

Figure 12 shows the response of the rock matrix in the Calico Hills for average material properties. No matrix fracturing was calculated for the excavation case, but regions of rock matrix fractured in the floor and in the roof during heating. Figure 13 shows the rock matrix behavior in the Calico Hills for limit material properties. Small regions of fracturing were

calculated to develop upon excavation at the corners of the room. During heating, matrix fracture was predicted to continue, particularly in the floor and around the waste canisters. Rock matrix factor of safety contours at excavation and at 50 years for average and limit material properties are shown in Figures 14 through 17 where the factor of safety is the ratio of the rock matrix shear strength as determined by the Mohr-Coulomb failure surface to the calculated maximum shear stress (in situ plus thermally induced stresses).

We should point out that the Calico Hills is not a highly fractured rock and the ubiquitous joint model may not be an accurate representation for the expected behavior of this rock. These calculations were rerun after deleting the ubiquitous joints from the model. With average material properties, no matrix fracturing was observed in the pillars between the rooms while the same amount of matrix fracturing was observed in the floor and roof of the room as for the ubiquitous joint calculations. With limit material properties, small regions of matrix fracturing occurred at the corners of the room at excavation as shown in Figure 18. During heating, these regions enlarged slightly (Figure 19). Small regions of fracturing (not shown) also developed around the waste package. In general, calculated damage to the rock around the room and in the pillar is minor when joints are absent.

Figures 20 through 22 summarize the finite element calculations for the near field in the Topopah Spring. A minor amount of joint movement was observed at the corners of the room upon excavation. When heat was added, the calculated regions of joint movement extended farther into the pillar. No matrix fracturing at excavation was calculated for the Topopah Spring for either average or limit material properties. A small amount of matrix fracturing, shown in Figure 22, occurred at the corners of the room for the limit material properties at 50 and 100 years after waste emplacement. Calculated rock matrix factor of safety contours for the Topopah Spring are shown in Figures 23 through 26.

The calculated regions of joint movement for excavation and during heating for the Bullfrog are shown in Figures 27 and 28. No matrix failure was calculated at any time in the Bullfrog. Calculated rock matrix factor of safety contours are shown in Figures 29 through 32.

Figures 33 and 34 show similar calculated joint behavior for the Tram. Like the Topopah Spring, no matrix failure was calculated for the Tram except for limit properties late in time as shown in Figure 35. Calculated rock matrix factor of safety contours are shown in Figure 36 through 39.

Very little has been done to correlate the results of finite element code calculations with observed responses of actual underground openings. In an attempt to try to understand the significance of the finite element calculations, we performed a similar excavation calculation for an opening in the highly fractured, welded Grouse Canyon tuff in G-tunnel. The properties of the Grouse Canyon are reasonably well known and the in situ stress has been measured in the vicinity of existing openings.²⁶ The result of the excavation calculation is shown in Figure 40. The calculation shows regions of joint movement at the corners of the room similar to those in the Yucca Mountain units. Examination of the corners of rooms in the Grouse Canyon that

have been open for two years or more show no evidence of preferential rock falls. In fact, completely unsupported drifts up to 30 ft in length have stood for periods of a week or more during drilling and blasting mining operations with no evidence of rock fall at the corners (or anywhere else). Consequently, we conclude from at least this one observation that finite element code prediction of joint movement does not necessarily correlate with room instability. The regions of joint movement calculated for average material properties for each of the four potential repository units are compared with those of the Grouse Canyon in Figure 41. Note that the Calico Hills is the only unit that shows behavior significantly different from the Grouse Canyon.

The ubiquitous joint model used in this study yields conservative results. The model assumes vertical, planar, parallel, noninteracting joints much like a deck of cards. No attempt is made to account for the mitigating effects of joint orientation dispersion or intersecting joints and the subsequent pinning that would be expected in reality. Consequently, we expect that the regions of joint movement observed in the field would be less than those calculated in this study.

The calculated regions of joint movement in the three welded units are very similar in size and shape and lie well within standard rockbolt and wire mesh support capabilities. Little or no rock matrix fracturing was predicted in the welded units. Calculated regions of joint movement in the Calico Hills are much larger than for the welded units and the joints have a greater tendency to open, particularly between 50 and 100 years. This is due mainly to the negative coefficients of thermal expansion measured for the Calico Hills. When the ubiquitous joints were removed from the model, no new matrix fracturing was calculated for average material properties and relatively minor regions of matrix fracturing extending into the pillar were calculated for limit material properties.

For all units, joints exhibited an increased tendency to open between 50 to 100 years. Intuitively, joint opening appears to be a worse condition than joint slip. Using the previous analogy, a deck of cards can support a substantial load on its ends as long as the deck is held together and individual cards are constrained to move by slip only. However, once the cards are allowed to separate, i.e., joints open, the load bearing capacity diminishes rapidly. As an aside, these results may provide the beginnings of a technical insight for why maintaining very long (in excess of 50 years) retrievability could be undesirable.

Comparison of the calculated regions of joint movement for the four units, either by size or by depth of penetration into the pillar, provides a clear distinction between the welded (Topopah Spring, Bullfrog, and Tram) and the nonwelded (Calico Hills) units, especially in view of the tendency toward joint opening in the Calico Hills later in time. But the comparison provides little or no distinction between the three welded units. If, as is likely the case, the ubiquitous joint model is inappropriate for the Calico Hills, then all four units appear suitably stable for openings. Comparison of regions of matrix rock fracturing do not eliminate any units, but it still provides the welded units with an edge over the nonwelded Calico Hills.

A number of trends become apparent when the factor of safety contours for the rock matrix are compared for the four units. Comparison of the calculated factor of safety contours at excavation for average and limit material properties shows that they are significantly lower for the limit cases. This is primarily due to the reduction (ranging from 7 to 37%) in rock strength when changing from the average to limit values. There is also a trend toward lower factors of safety with increasing depth due to the increasing overburden-induced stress. If all the units had the same strength, this trend would be obvious; since they do not, the trend is less apparent. For excavation, the figures show the Topopah Spring to be clearly superior to the other units. Note, however, that only the Calico Hills and Tram limit cases show contours as low as 1.5 and only the Calico Hills showed matrix fracturing ($FS < 1.0$) at the corners of the opening. In all other cases, 3 is the lowest contour observed. While the Topopah Spring is the best, the other welded units still appear entirely acceptable and the damage calculated in the Calico Hills appears minor, well within standard support technology.

Comparison of the contours after 50 years of heating suggests that for the average cases all of the units are quite stable but that the Calico Hills has the lowest factor of safety values. Comparison of the 50-year limit case contours is less straightforward. The Bullfrog appears the best behaved of the units while the Topopah Spring still maintains the strongest pillars. However, the Topopah Spring exhibits a decrease in the factor of safety in the room floor and roof. The Tram and Calico Hills exhibit safety factors of < 1.5 (but > 1.0) for regions extending from the rib into the pillar.

Based on this study, all of the units appear acceptable with regard to stability of underground openings. The Topopah Spring appears clearly superior to the other units while the Calico Hills is the poorest. After the Topopah Spring, the Bullfrog is ranked, followed by the Tram.

As a matter of interest, even if no joint movement was observed in the welded units, damage extending a meter or more into the pillar would be expected if these units were excavated by drilling and blasting.²⁷ The damaged region almost entirely encompasses the regions of joint movement caused by excavation in the welded units and overlaps a large fraction of the regions of thermally induced joint movement.

2.1.3.2 Rock Matrix Property Evaluation

A less sophisticated, but more common process of evaluating the stability of an underground opening on the basis of rock matrix properties commonly involves consideration of the stress concentration factors around openings of particular geometrical shapes, the state of in situ stress, the unconfined compressive strength of the rock, and suitable case history analogs. In the discussions to follow, the case history analogs are those that exist for excavations in welded and nonwelded tuff in the G-tunnel complex. In all instances, the vertical in situ stress is assumed to be equal to the weight of the overburden. The ratio of the horizontal in situ stress to the vertical in situ stress is assumed to fall in the range of 0.5 to 1.0. The stress concentration factors are appropriate for underground openings with a height to

width ratio of 1.0 to 1.5, as determined by previous finite element calculations.²⁸ Evaluations of pillar stability are based on empirical relationships proposed by Obert and Duvall²⁹ and Hustrulid³⁰ for application to the design of underground room and pillar systems. The unconfined compressive strengths of the tuff members are based on data compiled by Price.¹⁵

(a) Analysis of Unconfined Mechanical Property Data

The unconfined compressive strength data, appropriate for saturated test samples of approximately 2.5-cm diameter and 5-cm length, were plotted as a function of depth in each of the four potential repository units in accordance with the stratigraphy for USW-G1 given by Spengler et al.¹ An example of this type of plot is shown in Figure 42 for Calico Hills. The strength and elastic modulus data were determined on core from USW-G1. The depth interval between the dashed arrows designated T/M denotes the thermal/mechanical emplacement zone within which the actual repository horizon might be located. The unconfined compressive strength data are plotted in Figure 43 in the form of frequency distributions for the four emplacement zones and the Grouse Canyon welded tuff in G-tunnel. For purposes of room stability evaluation, values of the unconfined compressive strength have been selected on the basis of the mean of the range of greatest frequency of laboratory test results,⁵ and on the basis of a correlation with bulk physical properties¹⁵ within a thermal/mechanical zone. In all instances, this approach yields a range of unconfined compressive strength within which the mean and median values of a test data set are contained. A similar approach was followed to obtain the appropriate range on modulus of elasticity for each of the four emplacement zones.

(b) Analysis of Ratio of Compressive Strength to Overburden Stress

To obtain some insight into the anticipated stability of the underground excavation,⁵ we considered the simple ratio of unconfined compressive strength to overburden stress. The tabulation of calculated results is given in Table 5. The ratio varies from about 2 to 4 in the Calico Hills, Bullfrog, and Tram, to in excess of 10 in the Topopah Spring, for the particular range of unconfined compressive strengths obtained in the laboratory. Similar calculations for the welded and nonwelded units in G-tunnel are comparable to the Topopah Spring and the Calico Hills, respectively.

Rock often exhibits an apparent size or scale effect in both strength and deformation properties. In general, the strength of the rock will decrease with an increase in some characteristic dimension such as sample diameter, to the one-half to one-fourth power, until the characteristic dimension obtains a value of approximately 0.5 to 1.5 m.³¹⁻³³ Currently, there are no data available to indicate that tuff will or will not exhibit such a size effect. For conservatism, we arbitrarily decreased laboratory strength values by 50% to account for the potential size effect under isothermal conditions. This value is based on our best judgment, but the reduction factor could conceivably be either greater or smaller. The influence of this reduction in compressive strength in relation to the overburden stress is also shown in Table 5. A strength to stress ratio on the order of 1.0 indicates that the rock exists in an incipient state of failure where the horizontal stress is 0,

Table 5

Factor of Safety for Rock Mass
(Ratio of unconfined compressive strength, C_0 , to overburden stress)

<u>Greatest^a Unit/Ratio</u>	<u>No C_0 Reduction</u>		<u>50% C_0 Reduction</u>	
	<u>Physical Prop.^b Frequency</u>	<u>Correlation</u>	<u>Greatest Frequency</u>	<u>Physical Prop. Correlation</u>
Topopah Spring	17.2	10.5	8.6	5.2
Calico Hills	2.3	2.8	1.2	1.4
Bullfrog	1.8	3.2	0.9	1.6
Tram	2.0	3.8	1.0	1.9
G-Tunnel, Welded (Grouse Canyon)	15.8	---	7.9	---
G-Tunnel, Nonwelded	3.5	---	1.8	---

^a Mean of the range of greatest frequency.

^b Based on Price's¹⁵ recommendation.

e.g., at the drift wall. This implies that artificial support of a drift or room would be required, probably in some substantial fashion, immediately after excavation. When the ratio is only slightly > 1 , the rock at the corners of the tunnel can be expected to fracture shortly after excavation. This expectation is based on a magnification of stresses around the periphery of an opening due to stress concentrations which result from the creation of an opening in an initially stressed medium. On the basis of the results given in Table 5, it is possible that rock stabilization by means of artificial support measures would be required for rooms and tunnels excavated in the Calico Hills, Bullfrog, and Tram. Relatively speaking, rock stabilization measures would be less critical in the Topopah Spring. Based on observations of tunnel stability in the welded and nonwelded tuffs of G-tunnel, these conclusions appear to be reasonable and consistent.

(c) Pillar Safety Factor

It is not uncommon in mining practice to size pillars on the basis of empirical relationships, which involve geometrical dimension, unconfined compressive strength (C_0), overburden stress (σ_v), and a factor to account for the sample size effect. The vertical stress in the pillar is simply taken as enhancement of the overburden stress, which must be accommodated by the pillar as a consequence of mining. Employing the relationships proposed by Obert and Duvall²⁹ and Hustrulid,³⁰ pillar factors of safety for an extraction ratio of 20%, a pillar width of 20 m, and room height of 7 m are shown in Figure 44. Note that these empirical relationships assume a system of alternating rectangular pillars and parallel rooms. The cross-sectional dimensions are constant, and the length of a pillar is much greater than its width. Thus, the stress distribution across a pillar is considered to be two-dimensional in nature.

The calculated results given in Figure 44 indicate that the factors of safety for pillars constructed in the Calico Hills, Bullfrog, and Tram range from < 1.0 to a maximum of approximately 2.5. Comparatively, the factor of safety for a pillar in the Topopah Spring unit ranges from at least 2 to in excess of 10. These results reflect the corresponding ratios of unconfined compressive strength to overburden stress as discussed previously. This form of calculation yields conservative results, and a calculated factor of safety of < 1.0 should not be construed to mean instantaneous collapse of a pillar. Rather, it is an indication that the average vertical stress in the pillar is comparable to the reduced compressive strength of the rock, and that additional load imposed by heating, for example, could lead to loss of load bearing capacity over some period of time.

(d) Effect of Stress Concentrations

To further assess the stability of excavated openings in the four emplacement zones, consideration was given to stress concentrations around the periphery of an opening, the in situ stress state, and the unconfined compressive strength of the rock. By using previously calculated stress concentration factors around the peripheries of rooms of various shapes and for various states of in situ stress, it is possible to obtain an average stress concentration factor for a particular geometry and in situ stress

state. Specifically, the stress concentration factors at individual points on the periphery are integrated with respect to position, and that result is divided by the perimeter. A schematic diagram of the reference room geometry is shown in Figure 45. Variations in room height to room width ranges from 1.0 to 1.5. Consideration was also given to ratios of the horizontal to vertical in situ stresses ranging from 0.5 to 1.0.

For the case in which a room or tunnel is unheated, a factor of safety for the entire room has been calculated as the ratio of the unconfined compressive strength to the product of the integrated average stress concentration factor and vertical in situ stress. The results are shown in Figure 46 as a function of the ratio of the unconfined compressive strength to the overburden stress, where the laboratory values of unconfined compressive strength have been reduced by 50% as before. For the Calico Hills, Bullfrog, and Tram, the factors of safety range from approximately 0.5 to 1.5. Comparatively, the factor of safety for a room constructed in the Topopah Spring ranges from approximately 3 to 7. As discussed previously, a value of 1 for the factor of safety does not imply immediate collapse of a tunnel or room on excavation, but rather that support measures should be applied to stabilize the rock as soon as possible after excavation.

(e) Effect of Waste Decay Heating

A similar plot evaluating the effect of temperature on opening stability is shown in Figure 47, where we assumed the rock temperature increased uniformly to 100°C. In this case, the additional stress due to heating is calculated simply on the basis of coefficient of thermal expansion, the modulus of elasticity, and the temperature rise. In this case, the unconfined compressive strength and modulus of elasticity, as determined from laboratory tests at room temperature, have been arbitrarily reduced by 60% to account for sample size and elevated temperature effect. The results indicate that the factors of safety for a tunnel or room under elevated temperature conditions in the Calico Hills, Bullfrog, and Tram are < 1.0 , while the Topopah Spring exhibits values ranging from 1.5 to 2.5. Under the assumed conditions, a safety factor of considerably < 1.0 would indicate that stability problems could be anticipated in the absence of rather substantial support measures.

This evaluation of excavation stability indicates that tunnels and rooms in the Topopah Spring would be expected to be considerably more stable than those constructed in the Calico Hills, Bullfrog, and Tram. Based on the results of the nonheated situation, comparisons of tunnel stability and support measures from the tuffs surrounding G-tunnel appear to be comparable to those anticipated for the Topopah Spring and Calico Hills tuffs in Yucca Mountain.

2.1.3.3 Rock Mass Classification

Another commonly used method for estimating opening stability and support requirements for underground excavations is based on rock mass classification. This technique involves consideration of unconfined compressive

strength, RQD,^a joint properties, groundwater conditions, and in situ stress in relation to a large data base on the stability of underground openings in a diverse collection of rock types. Somewhat comparable techniques have been proposed and applied by Barton³⁵ and Bieniawski.³⁶ These techniques are commonly known as the NGI Tunneling Quality Index and the CSIR Geomechanics Classification of Jointed Rock Masses, respectively. Langkopf et al.³⁷ used these methods to evaluate the tuffs.

The results of the approach outlined by Barton, for four emplacement zones at Yucca Mountain and two units at the G-tunnel complex are shown in Figure 48. The tunneling quality index, Q, has been estimated to range from approximately 10 to 50 for the Topopah Spring and the G-tunnel tuffs, and from about 0.15 to 0.75 for the Calico Hills, Bullfrog, and Tram. The diagonal line in the figure indicates the crossover point from which "no support measures" are required to "support measures are required." Thus, one can estimate the minimum roof span or room height for which no support is required by consideration of the equivalent dimension on the figure ordinate. Commonly the excavation support ratio (ESR) factor ranges from 1.6 for permanent mine openings to 1.3 for storage rooms to 1.0 for major road and railway tunnels as derived from a wide variety of case history situations, none of which involve extreme rock heating. The results from Figure 48 are summarized on Table 6 in terms of maximum unsupported roof span for an ESR of 1.0. The results indicate a range of roof span widths of approximately 6 to 10 m in the Topopah Spring and 1 to 2 m in the Calico Hills, Bullfrog, and Tram. Evaluations of the welded and nonwelded tuffs in G-tunnel indicate reasonable agreement between observed, unsupported span width, and those derived from the tunnel quality index.

The second approach to rock mass classification by Bieniawski (CSIR) provides a measure of stand-up time for various (unsupported) roof span widths in relation to rock mass quality. The results of evaluations by this technique are also given in Table 6, and indicate a rather wide range of stand-up times for unsupported roof span of 5 m. Generally speaking, the Topopah Spring and Calico Hills appear to have somewhat longer predicted stand-up times for the roof span of concern than the Bullfrog and Tram.

On the basis of the results from the two techniques of rock mass classification as discussed above, the requirements for roof support measures in units above the water table appear to be less severe than those units below the water table. In general, the support measures envisioned here would include rockbolts and wire mesh for all four tuff units. The intensity of bolting, i.e., distance between bolts and depth of bolts, would vary from unit to unit. Specifically, the spacing between bolts in the tuff units above the water table would conceivably be greater than the spacing for those units below the water table.

^a The rock quality designation (RQD) is based on a modified core recovery procedure that is obtained by summing the total length of core recovered by counting only those pieces 10 cm in length or longer and that are hard and sound.³⁴

Table 6
 Rock Mass Classification Estimates of Unsupported
 Roof Span Size and Standup Time

Yucca Mountain Unit	NGI Tunneling Quality Index Maximum unsupported roof span or room height (m)	CSIR Geomechanics Classification Standup time of unsupported roof span of 5 m (days)
Topopah Spring	5.8 - 9.9	10 - 85
Calico Hills	1.7 - 1.8	45
Bullfrog	1.1 - 2.0	2 - 55
Tram	1.4 - 2.0	5 - 70
G-Tunnel, Welded	5.8 - 9.9	15 - 70
G-Tunnel, Nonwelded	5.0 - 10.0	45

Both rock mass classification schemes rank excavation stability in the Topopah Spring superior to the other units. The NGI system shows the Topopah Spring to be significantly better than the other three. The results of the NGI technique are more realistic, in our opinion, because the overburden stress and joint alteration characteristics are included in the evaluation. These considerations are not explicit in the CSIR technique. The CSIR system ranks the Calico Hills nearly as high as the Topopah Spring, followed by the Bullfrog and Tram.

2.2 Far-Field Thermal/Mechanical Evaluation

The purpose of the far-field thermal/mechanical study was to confirm that none of the far-field technical constraints were violated by the calculated rock response to the relative optimized repository gross thermal loading for each of the four potential units. These studies were carried out by Brandshaug.³⁸ The finite element mesh used for these calculations is shown in Figure 49. The mesh was designed to reflect the thermal/mechanical functional stratigraphy described earlier with the additional feature that several of the near vertical lines representing faults have been zoned so that fault behavior can be studied with future calculations. Average and limit material properties cases were defined for each of the zones.^{10,11}

The far-field boundary is shown in Figure 50 and is adopted from Reference 39. The boundary is defined in terms of the repository depth and includes the rock mass and groundwater regimes as well as the shafts and boreholes. This domain encompasses the significant thermal and mechanical effects of the host rock. In particular, notice the boundaries that are 15 and 85% of the depth above and below the repository. These boundaries enclose the 70% regions above and below the repository which are the so-called "intact zones."

The far-field constraints are shown in Figure 51. The operational, containment, and isolation periods have the same definitions as before. The far-field constraints are primarily associated with the post-operational time periods, and are probably the ones we are least able to assess since compliance must be almost exclusively demonstrated with computer code calculations. The constraints with an asterisk apply to the intact rock mass discussed above. The temperatures in this region are constrained to 150°C or less and the intact zone should not exhibit any new fractures. Surface uplift and subsidence, and surface temperature increase are both constraints associated with the environment and are not specifically associated with nuclear waste isolation.

The conceptualized thermal model used for the far-field thermal calculations is shown in Figure 52. The geothermal flux, Q , was altered so that it predicted the same ambient temperatures at the repository horizons as measured in the drill holes. For units below the water table, boiling was assumed to occur at atmospheric pressure from 0 to 110 years, and was controlled by hydrostatic pressure after 110 years (closure and flooding of the facility).

Figure 53 shows the thermal history at the 15% boundary (along the repository midline) below the repository horizons using average material

properties. (The temperatures at the 15% boundary below the repository will be slightly higher than those at the 15% boundary above the repository due to the increasing ambient temperature.) The maximum temperature achieved at the boundary is about 83°C at approximately 1,000 years. Similar temperatures are achieved for all four repository horizons. Figure 54 shows the thermal history at the same boundary calculated with limit material properties. For this case, the maximum temperature is about 88°C and, as before, nearly the same results are obtained for all four repository horizons. Figure 55 compares the thermal history for the average and limit material properties at the same boundary for the Topopah Spring horizon. Note that the thermal histories are almost identical.

As a matter of interest, since no constraint currently applies, the thermal history at the 85% boundary below the repository horizons calculated using average material properties are shown in Figure 56. The maximum temperature is 72°C. Figure 57 compares the thermal history for the average and limit properties at 85% boundary below the Topopah Spring horizon. As before, the results are almost identical.

Figure 58 shows the thermal history 3 m below the ground surface when the repository is located in the Topopah Spring horizon. The maximum temperature increase is 0.6°C at about 3,000 years.

The conceptualized mechanical model used for the far-field thermomechanical calculations is shown in Figure 59. As in the case for the near-field calculations, the horizontal stresses are assumed to be isotropic and the model includes ubiquitous vertical joints. The same assumptions and initial conditions used for the near-field calculations apply. Figures 60 and 61 show the far-field joint behavior calculated using average and limit material properties for a repository in the Topopah Spring horizon. In these cases, the Xs correspond to joint opening which arises from the bowing of the surface caused by the thermally induced uplift. The 15 and 85% boundaries are defined by the minimum depth at the west end of the repository, the most conservative approach. The 85% boundary is conservatively defined by applying the same 15% depth increment at both the west and the east ends of the repository rather than calculating the 15% depth at the west end of the repository and drawing the boundary parallel to the repository. The result is a boundary that diverges slightly from the repository in an easterly direction. The number of joints opening in both the average and the limit cases are almost identical, and at only one point in the limit case does it drop below the 85% boundary toward the easterly edge of the repository. No matrix fracturing or new joint formation was observed for any of the four units. The Topopah Spring results were shown here because Topopah exhibited the most joint opening of all four units.

The calculated surface uplift caused by a repository in each of the four units for average and limit material properties is shown in Figures 62 and 63. For average material properties, all four units show similar results, with the maximum uplift being about 37 cm for a repository located in either the Bullfrog or the Topopah Spring. For the limit material properties, a repository in the Topopah Spring still causes about 36 cm of surface uplift while the other units show a significant decrease in uplift. This result is

significant because of the previously unknown impact of potential heat induced contraction (limit values) in the Calico Hills on the far-field rock mass behavior. While the calculated surface uplift due to repositories located in the three units below the Topopah Spring is reduced when using limit material properties, there is no indication of adverse effects.

The results of the far-field thermal and mechanical studies were benign. All of the units exhibited very similar far-field behavior for both average and limit material properties. None of the far-field technical constraints were exceeded and most were not even approached. Because of the similarity in results, this study does not provide a means to discriminate between the four units. All of the emplacement zones are equally acceptable.

2.3 Groundwater Travel Time Estimates

The groundwater travel time provides a conservative estimate of the time of first release of radionuclides to the accessible environment. The approach taken to estimate the relative groundwater travel times from each of the four emplacement horizons is shown schematically in Figure 64. In this study we assumed, based on the limited hydrologic information available, that a transmissive zone containing flow in an easterly direction existed near the static water level. We reasoned that once a nuclide reached the transmissive zone and began its horizontal movement, it could no longer be determined from which repository unit it had originated and, therefore, the horizontal section of the pathway was of no value in discriminating between candidate repository units. Consequently, to provide a relative comparison of the four emplacement zones, we needed only to estimate the vertical travel times either downward to the static water level from the unsaturated units or upward to the transmissive zone from the saturated units.

LOG/BA

The current hydrologic data from Yucca Mountain do not include information about fracture flow nor are the existing transport codes capable of explicit treatment of fracture flow, especially in the unsaturated zone. Therefore, the travel time estimates in both the saturated and unsaturated zones were based on the assumption of porous flow.

We made no attempt to include the possible effects of heat on the travel time estimates. Since we considered expected repository behavior, radionuclides would not be released to the rock until after approximately 1,000 years. This is well past the thermal peak in the rock immediately surrounding the waste where, at 1,000 years, temperatures will be less than 100°C and decreasing. Temperatures will still be increasing in the far field but generally at a very slow rate approaching maximums well below 100°C. More importantly, the thermal gradients are very small, on the order of tenths of a degree per meter, suggesting that the thermal impact on flow behavior would be minor. Finally, we do not currently have at our disposal the analytical capability to calculate the effects of heat on the far-field groundwater flow.

2.3.1 Unsaturated Zone

One of the advantages of the Yucca Mountain site is its location in an arid region in Nevada resulting in particularly low infiltration rates through

the unsaturated zone. In addition, the water table is very deep (Table 1) which enhances isolation potential. The conceptual steady-state infiltration model^{40,41} for the unsaturated zone is shown in Figure 65. We assumed a steady-state, vertical infiltration flux of 3 mm/year which we presume to be a conservative estimate. The water velocity is obtained by dividing the flux by the effective porosity. The estimated groundwater travel time vertically downward to the transmissive zone at USW-G1 is shown in Table 7. For effective porosities equal to the total rock matrix porosities in each of the intervening zones, the travel time from the Topopah Spring is 21,000 years and from the Calico Hills is slightly over 11,000 years. If, for example, the effective porosity is equal instead to 10%, the travel time from the Topopah Spring is 7,500 years and the travel time from the Calico Hills is slightly over 3,100 years. Note that the travel times will increase when moving westward and decrease when moving eastward from USW-G1.

Table 7

Estimate of Groundwater Travel Time from
Unsaturated Repository Horizons Vertically
Downward to the Transmissive Zone (at G-1)

	$\phi_e = \phi$ (yr)	$\phi_e = 0.10$ (yr)
Topopah Spring	21,000	7,500
Calico Hills	11,100	3,130

2.3.2 Saturated Zone

A similar approach was used to calculate the vertically upward travel times from the units below the water table. Three cases were considered. They included average hydraulic conductivities for the saturated units measured in USW-H1⁴² and UE25b1H⁴³ given in Table 8 and a detailed hydraulic conductivity distribution⁴³ measured in USW-H1 given in Table 9. Note that all three sets of hydraulic conductivities are preliminary data and are subject to change. The calculations used a vertically upward head difference of 3 m which was measured in H1 between a piezometer (elevation ~ 189 m) located near the base of the Tram and another, above the first, near the top of the Bullfrog (elevation ~ 563 m).⁴² Examination of the hydraulic conductivity distribution in Table 9 suggests that the upper piezometer lies in an interval of relatively high conductivity, approximately 0.1 m/day. For the calculations in H1, the flux was calculated between the two piezometers and the travel times were calculated from the repository level to the upper piezometer.

Table 8

Average Hydraulic Conductivity (m/day)

	USW-H1 ⁴²	UE25b1H ⁴³
Prow Pass	1×10^{-2}	9.1×10^{-1}
Bullfrog	7×10^{-6}	1.1
Tram	2×10^{-6}	$<10^{-3}$
Flow Breccia	3×10^{-6}	
Lithic Ridge	2×10^{-7}	$<10^{-3}$

Table 9

Preliminary Hydraulic Conductivity Distribution
Measured in USW-H1⁴³

Elevation Interval (m)	Hydraulic Conductivity (m/day)
730-705	3
705-686	1
686-650	1
650-649	18
649-614	≤ 0.003
614-608	0.001
608-566	$\leq 2 \times 10^{-4}$
566-561	0.1
561-544	0.001
544-510	3×10^{-4}
510-491	$\leq 2 \times 10^{-4}$
491-376	4×10^{-5}
376-102	$\leq 7 \times 10^{-6}$

For the calculations in B1, we used the same 3-m-head difference and assumed it extended from the base of the Tram to the base of the Bullfrog (a depth interval of about 328 m). The travel time from a repository in the Tram was calculated to the base of the Bullfrog, which because of its high hydraulic conductivity, was assumed to be a transmissive zone with horizontal flow. The repository locations were determined from the C-C' cross section and we assumed an effective porosity of 10%. The travel times are given in Table 10. Also included in Table 10 are the vertical fluxes for each set of hydraulic data and the possible error in travel time associated with each meter of uncertainty in repository elevation.

Table 10

Estimates of Groundwater Travel Times from Saturated Repository Horizons
Vertically Upward to the Transmissive Zone

	<u>Avg. Hydraulic Conductivity</u>	<u>Hydraulic Cond. Distribution</u>	<u>UE25b1</u>
Bullfrog Travel Time (yr)	225,000	46,300	0
Tram Travel Time (yr)	2,260,000	433,000	2,200
Flux (L/m ² yr)	0.00712	0.0367	3.33
Repository Location Uncertainty ^a (yr/m)	±14,000	±2,720	±30

^a Potential error in travel time associated with each meter of
uncertainty in repository elevation.

The vertical travel times from a repository in the Bullfrog range from < 1 year in B1 where the Bullfrog lies within the transmissive zone, up to approximately 225,000 years, a variation of 5 orders of magnitude. Travel times from a repository in the Tram range from 2,200 years to more than 2,260,000 years. Note, however, that initial testing in USW-G4 and USW-H6 indicates that water production occurs in the Tram while the Prow Pass is tight. Consequently, the vertical travel times from the Tram at that location may be very short, < 1 year, giving rise to variations in travel time estimates of up to 6 orders of magnitude or more. It is clear from these calculations that there is virtually no stratigraphic correlation of the hydrology between holes for the limited number tested so far. The evidence suggests that portions of both repository units below the water table potentially lie within a transmissive zone. The most conservative conclusion is that there is no vertical transport, it is all horizontal in these units. These large uncertainties in the groundwater travel times for the saturated units cause them to be ranked well below the unsaturated units.

2.3.3 Radionuclide Transport

In the absence of retardation effects, radionuclides would be expected to move at approximately the same rate as the water. However, most radionuclides interact with the geology so that they are slowed relative to the water movement. Table 11 lists average sorption ratios (R_d) reported by Daniels et al.⁴⁴ for a sampling of radionuclides in the units of interest. For this discussion we chose the lowest values from a relatively large amount of data.

The retardation factor, B, is given by

$$B = 1 + \frac{\rho_b}{\phi} R_d$$

where ρ_b is the bulk density of the rock and ϕ is the porosity. Assuming that this, or a similar expression, applies to the unsaturated zones, the retardation factor ranges from $(1 + 4.8 R_d)$ to $(1 + 18.7 R_d)$. For R_d 's equal to 1, the radionuclide transport times will be lengthened over the water transport times by a factor of about 6 to 20 times. For R_d 's equal to 10, the transport times are lengthened by a factor of about 50 to almost 200.

Similar arguments apply to the saturated units where the retardation factor equals approximately $20 R_d$. In this case an R_d of 1 or 10 result in transport times lengthened by factors of 20 or 200, respectively. Examination of the sorption ratios in Table 11 show that the nuclide travel times should be significantly longer than the water travel times. In most cases, the sorption ratios are > 10 and in many cases, much > 10 . The Calico Hills consistently show values > 100 . Only technetium has values < 1.0 in some units.

The preceding discussion of water and radionuclide travel times suggests considerable uncertainty in predicting such times in any of the potential units. Nevertheless, the greatest variability appears associated with the hydrology of units below the water table. Evaluation of credible variations in parameters in the unsaturated zone still indicate travel times of thousands of years just to reach the water table. Furthermore, preliminary code calculations indicate that heavy rains and initial fracture flow are not necessarily a factor in the water travel times from the unsaturated repository zones to the static water level. Based on these considerations, we ranked the four units in the following order: Topopah Spring, Calico Hills, Tram, and Bullfrog.

3.0 SUMMARY OF RANKINGS

A summary of the individual rankings is given in Table 12. Mineability relates specifically to the mining process. The Calico Hills is a clear choice at this time because of the ability to use continuous miners as opposed to drilling and blasting for the welded units. However, the distinction may disappear shortly if developmental continuous miners for hard rock continue to prove successful. The main result from this study is that no units were eliminated. All units can be mined successfully using conventional techniques.

The optimized gross thermal loading determinations turned out to be a nondiscriminator between the four units. Within the property variability, the units must be considered identical.

Excavation stability was evaluated using three different approaches. The near-field finite element thermomechanical code calculations indicated a clear superiority of the welded to the nonwelded units and a subranking among the three welded units with the Topopah Spring ranked best. Rock matrix property evaluation provided a more traditional approach to evaluation of room and

Table 11

Average Sorption Ratios^a from Batch and Circulating System
Sorption Experiments on Crushed Tuff^b

Unit	R_d (ml/g)									
	Sr	Cs	Ba	Ce	Eu	Am	Pu	U	Tc	Np
Topopah Spring	27.	290.	120.	66.	140 ^b	1200.	64.	1.8	0.30	7.0
Tuffaceous Beds of Calico Hills	3900.	7800.	94000.	760.	1600.	4600.	140.	5.3	--	11.0
Prow Pass	22.	187.	182.	140.	970.	2200.	56.	--	0.15	6.4
Bullfrog	41.	123.	130.	82.	90.	130.	80.	2.2	4.2	---
Tram	68 ^c	610.	760.	100 ^b	200 ^b	3300.	290.	4.6	--	28.

^a The values presented are the lowest average values given in Daniels, W. R., et al.⁴⁴

^b Ambient conditions, air, 20 \pm 4°C; fractions do not contain <75- μ m-diameter particles except those designated by c.

^c Average of data for <500- μ m-diameter particle size (contains some <75- μ m-particles); no other data available.

Table 12

Summary of Unit Rankings

MINEABILITY

1. CH
2. TS
3. BF
4. TR

GROSS THERMAL LOADING

1. TS, BF, TR, CH

EXCAVATION STABILITY

Near-Field Thermal/Mechanical	Rock Mass/ Rock Matrix Properties	Classification	
		(NGI)	(CSIR)
1. TS	1. TS	1. TS	1. TS,CH
2. BF	2.	2.	2. BF,TR
3. TR	3.	3.	
4. CH	4. CH,BF,TR	4. CH,BF,TR	

FAR-FIELD
THERMAL/MECHANICAL

1. TS,CH,BF,TR

GROUNDWATER TRAVEL
TIME (vertical)

1. TS
2. CH
3. TR
4. BF

pillar stability. This study showed a clear preference for the Topopah Spring over the other units. Two rock mass classification techniques, the NGI and CSIR systems, were used to evaluate excavation stability in the units. The NGI system ranked the Topopah Spring clearly superior to the other three units while the CSIR system was less dramatic but still ranked the Topopah Spring first.

The far-field finite element thermal and thermomechanical code calculations provided no discrimination between units. All of the units affected the far field in virtually the same, benign way.

The groundwater travel time estimates suffer from a variety of problems. In the unsaturated zone, the virtual lack of data and the poor understanding of the transport phenomena certainly limit our ability to calculate credible transport times. Nevertheless, one reasonable estimate based on the low infiltration rates representative of the arid region and the long distance to the water table, identified the Topopah Spring with long travel times. For units in the saturated zone, extreme variability in the hydraulic parameters yield travel time estimates that vary by up to 6 orders of magnitude. Other results suggest that repositories in either the Bullfrog or the Tram may be located, at least in part, in transmissive zones.

4.0 RECOMMENDATION

Based on the preceding studies and their inherent limitations, we believe that a clear first choice for the target horizon is the Topopah Spring, with the understanding that a comprehensive, timely program to characterize the hydrology should be a high priority activity. The second choice is the Calico Hills with the caveat that matrix contraction during heating may degrade the stability of underground openings. The third and fourth choices are the Bullfrog and the Tram, respectively, but only if the hydrology can be sufficiently well characterized to support a definitive performance assessment.

5.0 REFERENCES

1. R. W. Spengler, F. M. Byers Jr., and J. B. Warner, "Stratigraphy and Structure of Volcanic Rocks in Drill Hole USW-G1, Yucca Mountain, Nye County, Nevada," USGS Open-File Report 81-1349, Denver, U.S. Geological Survey, 1981.
2. B. S. Langkopf, Sandia National Laboratories, to Distribution, "Discussion of Thermomechanical Cross-Section C-C' as Given to RE/SPEC for Far-Field Unit Selection Calculations;" Memorandum dtd July 23, 1982.
3. L. W. Scully and A. J. Rothman, "Repository and Engineering Barriers Design," Proceedings of the 1982 NWTs Program Information Meeting, Las Vegas, Nevada, December 1982.
4. J. L. Ash and W. E. Craig, Scott-Ortech, Inc., to J. K. Johnstone, Sandia National Laboratories, "Mineability of Four Candidate Lithologic Units in Yucca Mountain," Letter Report dtd September 1982.
5. P. F. Gnirk and J. L. Ratigan, RE/SPEC Inc., to J. K. Johnstone, Sandia National Laboratories, "Constructibility Analysis of Welded and Nonwelded Tuff Members at Yucca Mountain," Technical Letter Memorandum RSI-0078 dtd October 20, 1982.

6. W. A. Hustrulid, Colorado School of Mines, to J. K. Johnstone, Sandia National Laboratories, "Constructibility of a Nuclear Waste Disposal Facility at Yucca Mountain," Letter Report dtd October 18, 1982.
7. R. L. Johnson, "NNWSI Unit Evaluation at Yucca Mountain, Nevada Test Site: Near Field Thermal and Mechanical Calculations Using the SANDIA ADINA Code," SAND83-9939, Albuquerque, Sandia National Laboratories, in preparation.
8. R. K. Thomas, "NNWSI Unit Evaluation at Yucca Mountain, Nevada Test Site: Near Field Mechanical Calculations Using a Continuum Jointed Rock Model in the JAC Code," SAND83-0070, Albuquerque, Sandia National Laboratories, in preparation.
9. A. Melo and D. K. Parrish, "NNWSI Unit Evaluation at Yucca Mountain, Nevada Test Site: Near Field Thermal-Rock Mechanics Analysis," RSI-0205, Rapid City, RE/SPEC Inc., in preparation.
10. R. R. Peters and A. R. Lappin, Sandia National Laboratories, to T. Brandshaug, RE/SPEC Inc., "Revised Far Field Thermomechanical Calculations for Four Average Property Cases," Memorandum dtd August 17, 1982.
11. R. R. Peters and A. R. Lappin, Sandia National Laboratories, to T. Brandshaug, RE/SPEC Inc., "Revised Far Field Thermomechanical Calculations for Four "Limit" Property Cases," Memorandum dtd September 22, 1982.
12. R. R. Peters to R. K. Thomas, Sandia National Laboratories, "Thermomechanical Calculations for Unit Evaluation," Memorandum dtd October 25, 1982.
13. R. R. Peters, Sandia National Laboratories, to S. W. Key, RE/SPEC Inc., "Thermomechanical Calculations for Unit Evaluation," Memorandum dtd October 25, 1982.
14. R. R. Peters to R. D. Krieg, Sandia National Laboratories, "Near Field Thermomechanical Calculations in the Welded, Devitrified Portion of the Grouse Canyon Member of the Belted Range Tuff (G-Tunnel Tuff)," Memorandum dtd November 29, 1982.
15. R. H. Price, "Analysis of Rock Mechanics Properties of Volcanic Tuff Units from Yucca Mountain, Nevada Test Site," SAND82-1315, Albuquerque, Sandia National Laboratories, in preparation.
16. A. R. Lappin, Sandia National Laboratories, to Distribution, "Bulk and Thermal Properties of the Functional "Tuffaceous Beds", Here Defined to Include the Basal Topopah Spring, All of the Tuffaceous Beds of Calico Hills, and the Upper Portion of the Prow Pass, Memorandum dtd March 26, 1982.
17. A. R. Lappin, Sandia National Laboratories, to Distribution, "Bulk and Thermal Properties for the Welded, Devitrified Portions of the Bullfrog and Tram Members, Crater Flat Tuff," Memorandum dtd April 19, 1982.

18. A. R. Lappin, Sandia National Laboratories, to Distribution, "Bulk and Thermal Properties of the Potential Emplacement Horizon Within the Densely Welded, Devitrified Portion of the Topopah Spring Member of the Paintbrush Tuff," Memorandum dtd June 30, 1982.
19. K. J. Bathe, "ADINA T - A Finite Element Program for Automatic Dynamic Incremental Nonlinear Analysis of Temperatures," Report 82448-5, Cambridge, Massachusetts Institute of Technology, Revised 1978.
20. D. K. Svalstad, "User's Manual for SPECTROM-41: A Finite Element Heat Transfer Program," Topical Report RSI-152, Rapid City, RE/SPEC Inc., 1981.
21. K. J. Bathe, "ADINA - A Finite Element Program for Automatic Dynamic Incremental Nonlinear Analysis," Report 82448-1, Cambridge, Massachusetts Institute of Technology, Revised 1978.
22. S. E. Yamada, "User's Manual for SPECTROM 11: A Finite Element Thermo-elastic/Plastic Stress Analysis Program," Topical Report RSI-158, Rapid City, RE/SPEC Inc., 1981.
23. J. K. Johnstone and P. F. Gnirk, "Preliminary Technical Constraints for a Repository in Tuff," SAND82-2147, Albuquerque, Sandia National Laboratories, in preparation.
24. B. S. Langkopf, Sandia National Laboratories to Distribution, "Suggested Bounds for In Situ Stress Ratios for Use in Yucca Mountain Unit Selection Calculations," Memorandum dtd March 26, 1982.
25. J. H. Healy, S. H. Hickman, M. D. Zoback, and W. L. Ellis, "Deep-Borehole Stress Measurements at the Nevada Test Site," (abs.), EOS, Vol. 63, no. 45, p. 1099, 1982.
26. R. M. Zimmerman and W. C. Vollendorf, "Geotechnical Field Measurements, G-Tunnel, Nevada Test Site," SAND81-1971, Albuquerque, Sandia National Laboratories, May 1982.
27. W. A. Hustrulid, Colorado School of Mines, to J. K. Johnstone, Sandia National Laboratories, Personal Communication, January 25, 1983.
28. T. Brandshaug and P. F. Gnirk, "Stability Analysis of CAES Caverns in Hard Rocks: I. Influence of In Situ Stress State and Cavern Geometry on the Post-Excavation Elastic Stress State," RE/SPEC Project Summary Report RSI-0123, prepared for Pacific Northwest Laboratories of Battelle Memorial Institute, 1980.
29. L. Obert and W. Duvall, "Design and Stability of Excavations in Rock--Subsurface," SME Mining Engineering Handbook, Vol. 1, Section 7.2, pp. 7-10--7-49, 1973.
30. W. A. Hustrulid, "A Review of Coal Pillar Strength Formulas," Rock Mechanics, Vol. 8, pp. 115-145, 1976.

31. Z. T. Bieniawski and W. L. Van Heerden, "The Significance of In Situ Tests on Large Rock Specimens," *Int. J. Rock Mech. Min. Sci.*, Vol. 12, pp. 101-113, 1975.
32. R. E. Goodman, Introduction to Rock Mechanics, John Wiley and Sons, New York, pp. 85-88, 1980.
33. E. Hoek and E. T. Brown, Underground Excavations in Rock, The Institution of Mining and Metallurgy, London, pp. 155-156, 1980.
34. D. U. Deere, "Geological Considerations," from Rock Mechanics in Engineering Practice, edited by K. G. Stagg, and O. C. Zienkiewicz, J. Wily and Sons, 1968.
35. N. Barton, "Recent Experiences with the Q-System of Tunnel Support Design," Proceedings of the Symposium on Exploration for Rock Engineering, Johannesburg, Vol. 1, pp. 107-117, 1976.
36. Z. T. Bieniawski, "Rock Mass Classification in Rock Engineering," Proceedings of the Symposium on Exploration for Rock Engineering, Johannesburg, Vol. 1, pp. 97-106, 1976.
37. B. S. Langkopf and P. F. Gnirk, "Preliminary Rock Mass Classification Ratings of Four Potential Repository Units at Yucca Mountain," SAND82-2034, Albuquerque, Sandia National Laboratories, in preparation.
38. T. Brandshaug, "NNWSI Unit Evaluation at Yucca Mountain, Nevada Test Site: Far Field Thermal-Rock Mechanics Analyses," RSI-0209, Albuquerque, RE/SPEC, Inc., in preparation.
39. NWTS Working Group on Far Field Performance Constraints, "Repository Performance Constraints in the Far Field Domain," NWTS-25, Washington, DC, NWTS Program Office and U.S. Department of Energy, in draft form, 1981.
40. R. R. Peters and J. K. Johnstone to L. D. Tyler, Sandia National Laboratories, "Bounding Calculations for Radionuclide Movement in the Unsaturated Zone," Memorandum dtd September 13, 1982.
41. F. H. Dove, W. A. Rice, J. L. Devary, F. W. Bond, and P. G. Doctor, "Hydrologic and Transport Considerations for Horizon Selection at Yucca Mountain, Nevada," Richland, Pacific Northwest Laboratory, in preparation.
42. J. H. Robison and F. E. Rush, "Hydrologic Site Characterization of Yucca Mountain, Nevada," U.S. Geological Survey presented at the 1982 NWTS Program Information Meeting, Las Vegas, Nevada, December 1982.
43. F. E. Rush, U.S. Geological Survey, to J. K. Johnstone, Sandia National Laboratories, "Preliminary Hydraulic Conductivities in Wells USW-H1 and UE25a-B1," Personal Communication, January 21, 1983.
44. W. R. Daniels, K. Wolfsberg, R. S. Rundberg, A. E. Ogard, J. F. Kerrisk, C. J. Duffy, T. W. Newton, J. L. Thompson, et al., "Summary Report on the Geochemistry of Yucca Mountain and Environs," LA9328-MS, Los Alamos, Los Alamos National Laboratories, December 1982.

FIGURES

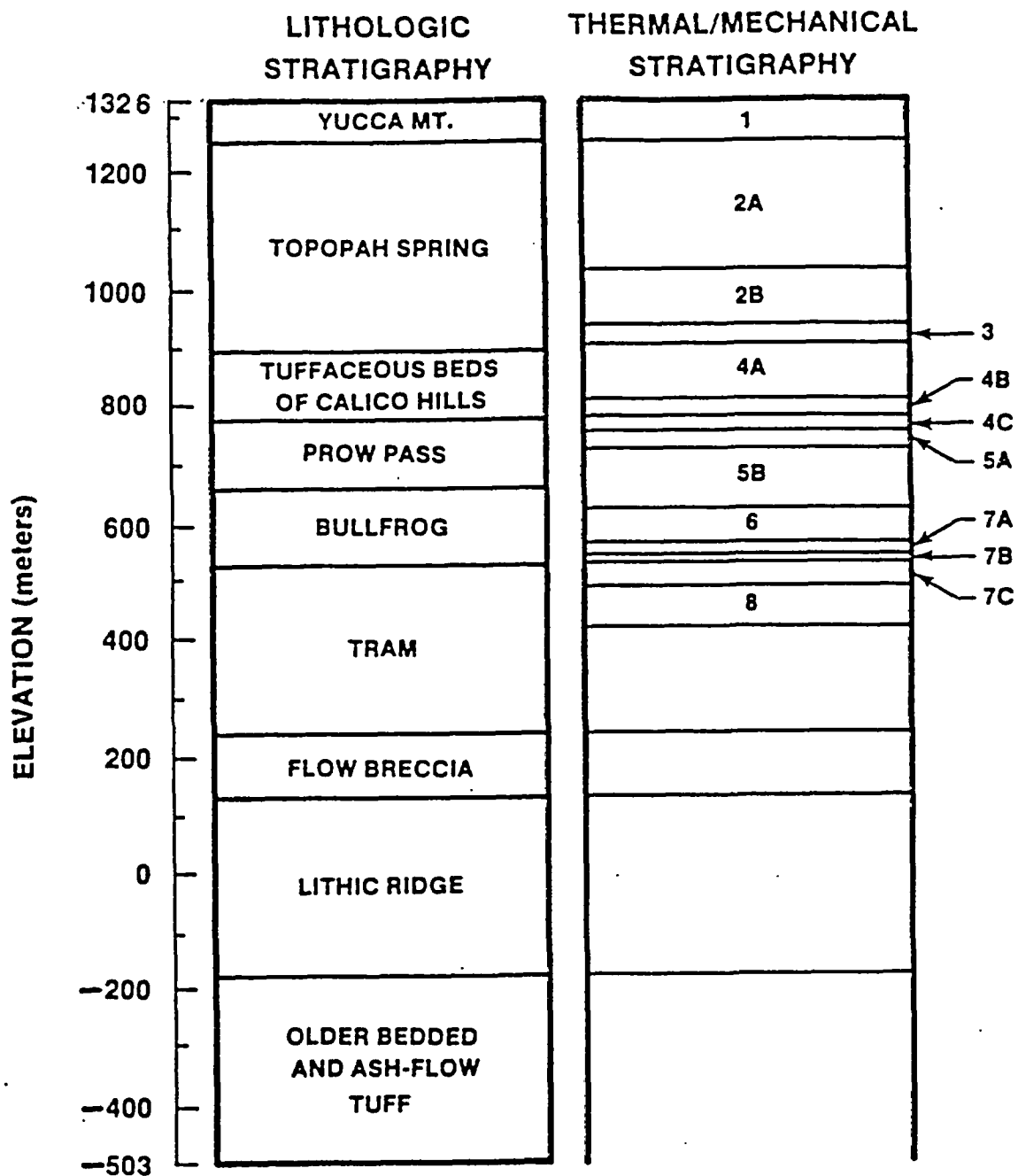


Figure 1. Comparison of the Lithologic and Thermal/Mechanical (T/M) Stratigraphies. (The T/M stratigraphy provides a model of the vertical variation in the thermal and mechanical properties of tuff used for the unit evaluation studies. Each zone in the T/M stratigraphy includes material with similar thermal and mechanical properties. Other property stratigraphies, such as hydrologic and geochemical, were also used in these studies.)

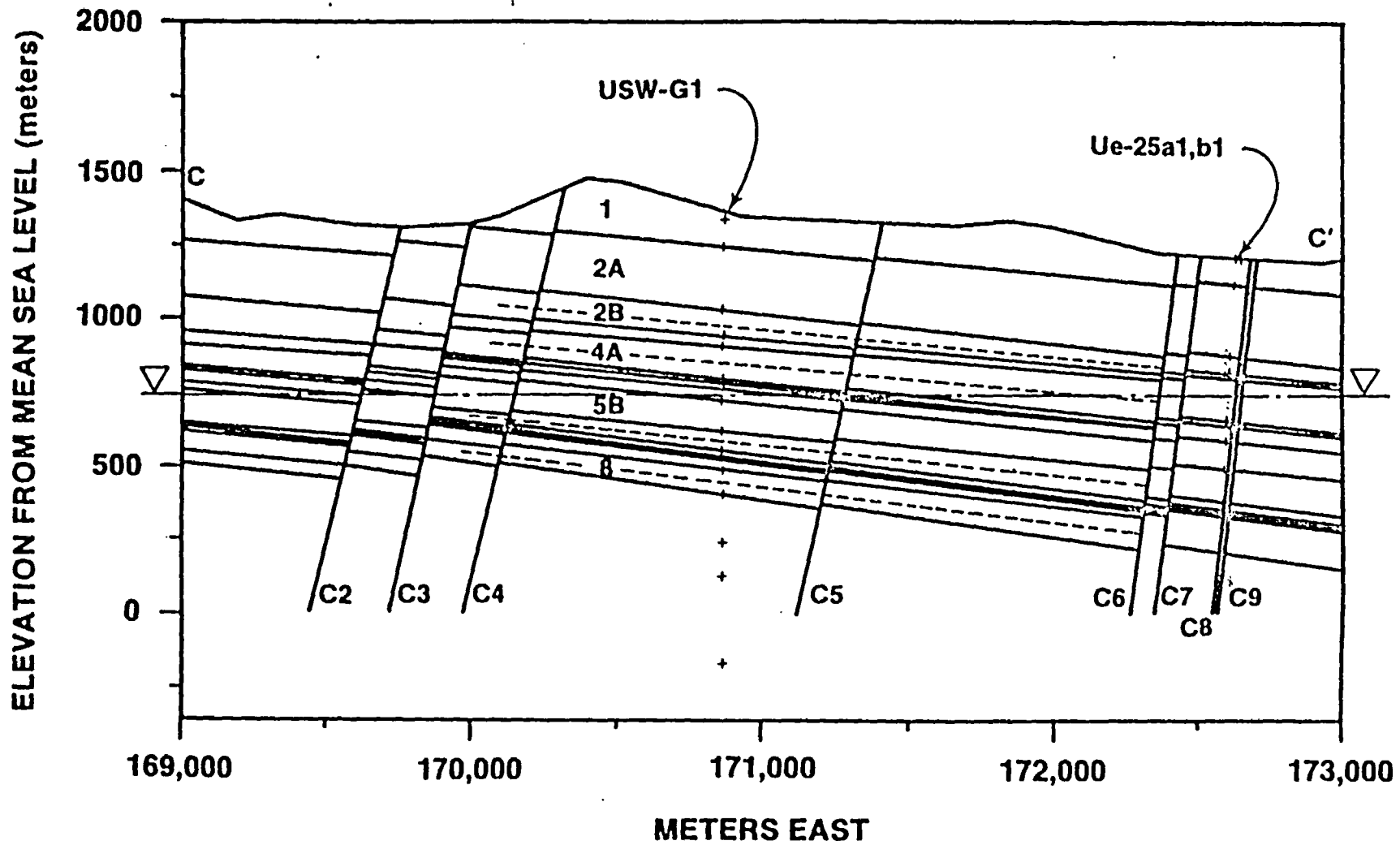


Figure 2. C-C' Cross Section of the Thermal/Mechanical Stratigraphy. (Dotted lines indicate possible repository locations; inverted triangles indicate position of static water table.)

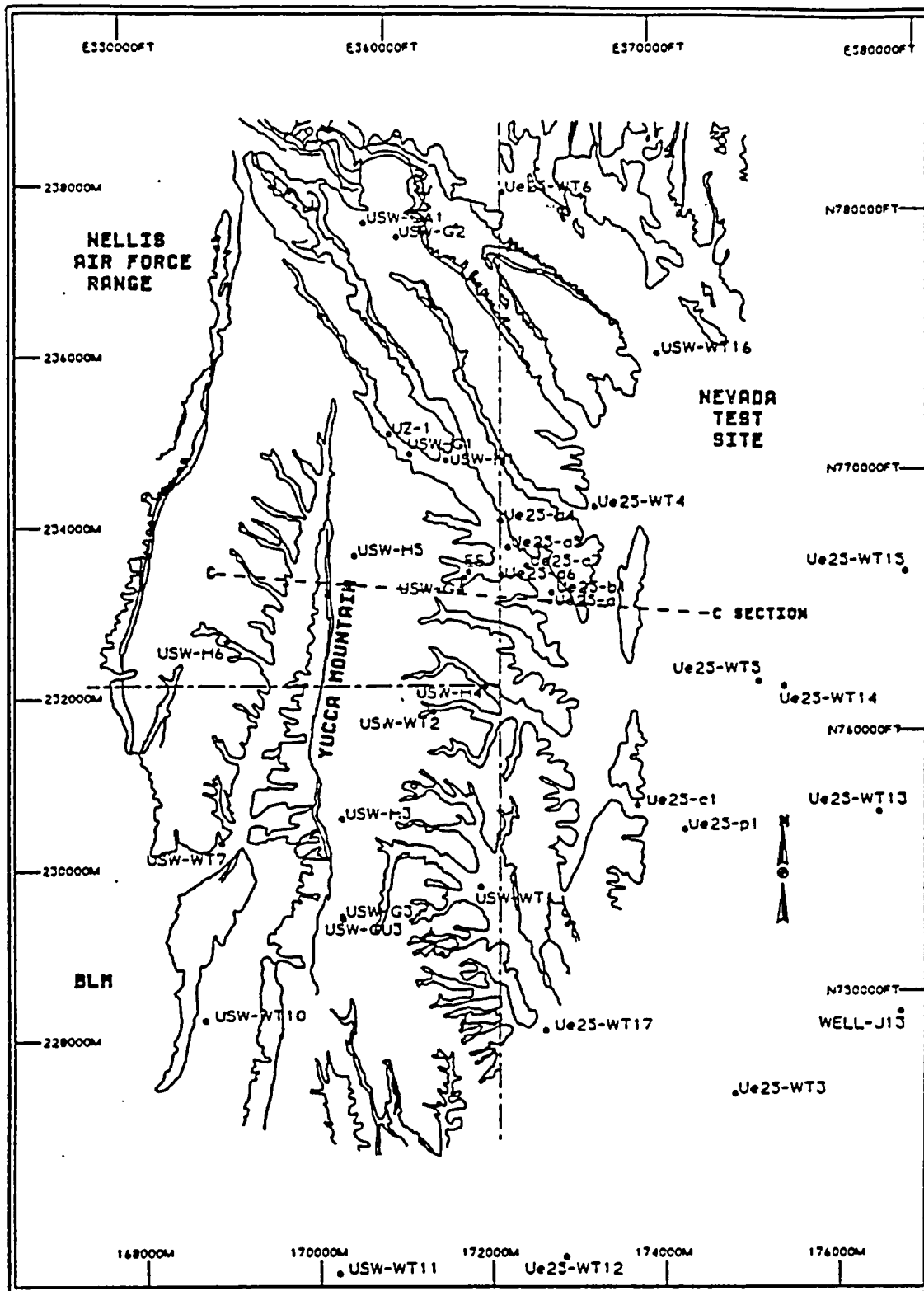


Figure 3. Map of Yucca Mountain Showing the Location of the C-C' Cross Section and Its Relation to Various Drill Holes.

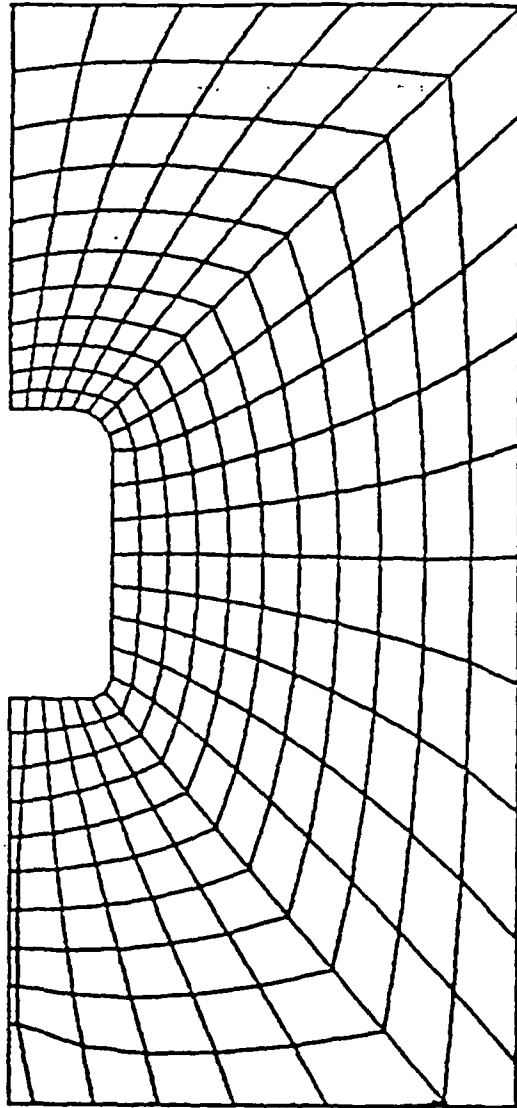


Figure 4. A Portion of the Finite-Element Mesh Used in Near-Field Thermal/Mechanical Calculations.

SYSTEM COMPONENT		OPERATIONAL PERIOD	CONTAINMENT PERIOD	ISOLATION PERIOD
NEAR FIELD	ROOM: ROOF, RIB, FLOOR	OPERATIONAL SERVICEABILITY	NO CONSTRAINT	NO CONSTRAINT
	ENVIRONMENT	TO BE DETERMINED	NO CONSTRAINT	NO CONSTRAINT
	FLOOR BACKFILL	T < 100°C T < 100°C	NO CONSTRAINT NO CONSTRAINT	NO CONSTRAINT NO CONSTRAINT
	PILLAR	SAFETY FACTOR > 1.5	NO CONSTRAINT	NO CONSTRAINT
	MINERAL DEHYDRATION/ ALTERATION	T < 150°C	NO CONSTRAINT	NO CONSTRAINT
ENGINEERED SYSTEM	NO RADIONUCLIDE RELEASE AT BOUNDARY	NO RADIONUCLIDE RELEASE AT BOUNDARY	<10 ⁻⁵ PER NUCLIDE PER YEAR	

Figure 5. Preliminary Technical Constraints for the Near Field.

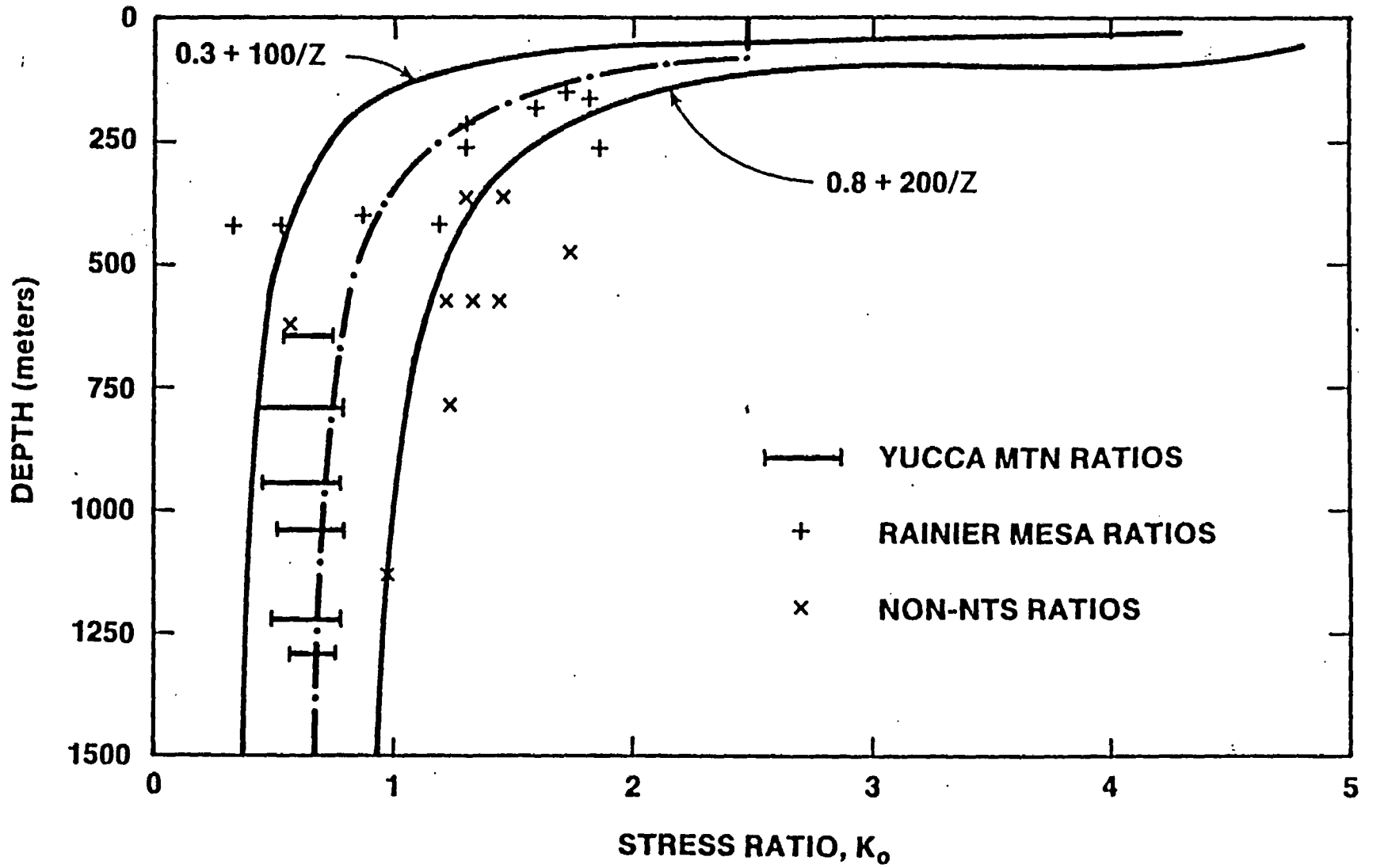


Figure 6. Ratio of Horizontal to Vertical Stress (K_0) as a Function of Depth. (Dotted line indicates values used in this analysis.)

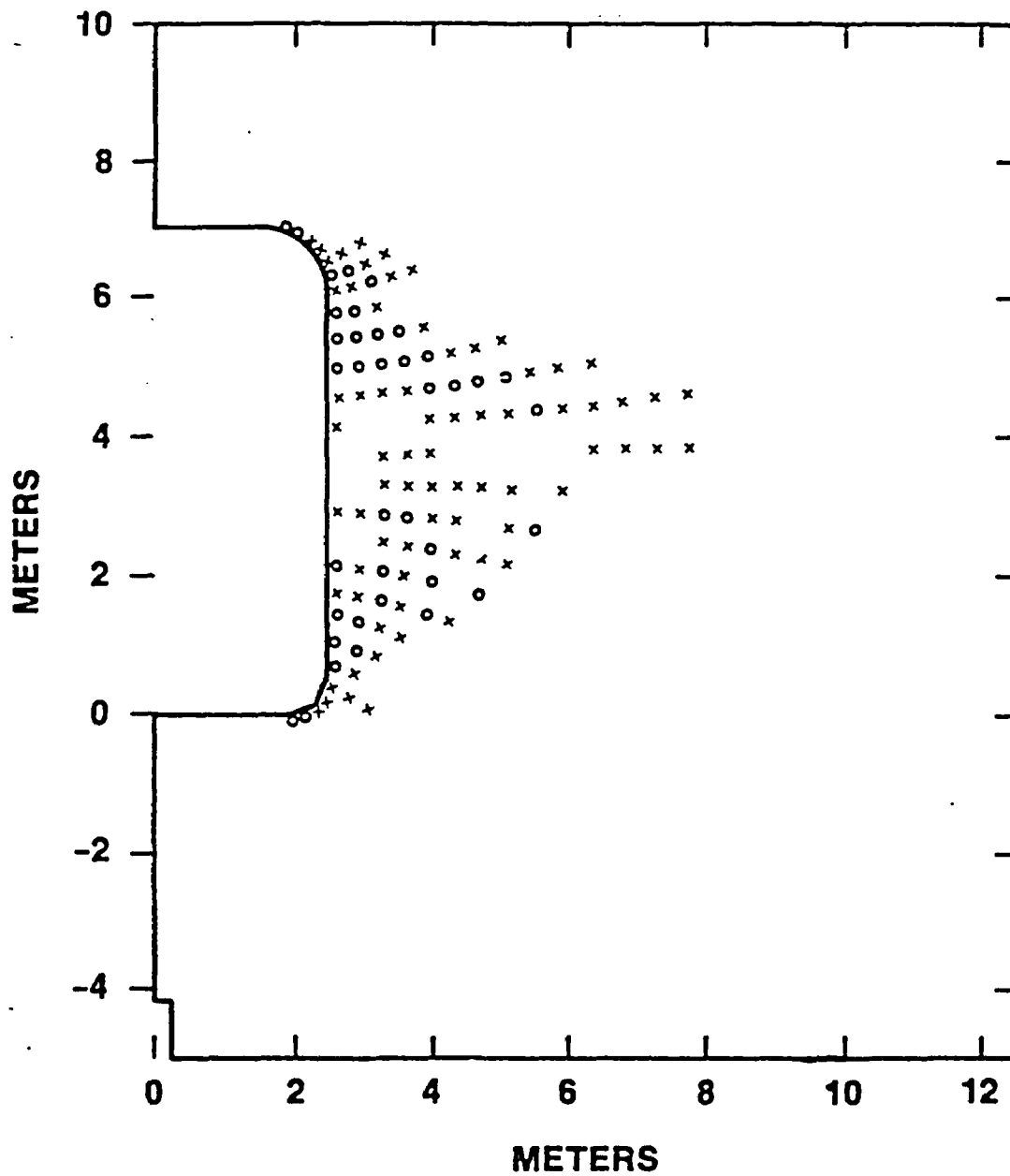


Figure 9. Joint Movement at 50-Year Time Step in the Calico Hills. (Limit Case: x - joint slip, o - joint opening.)

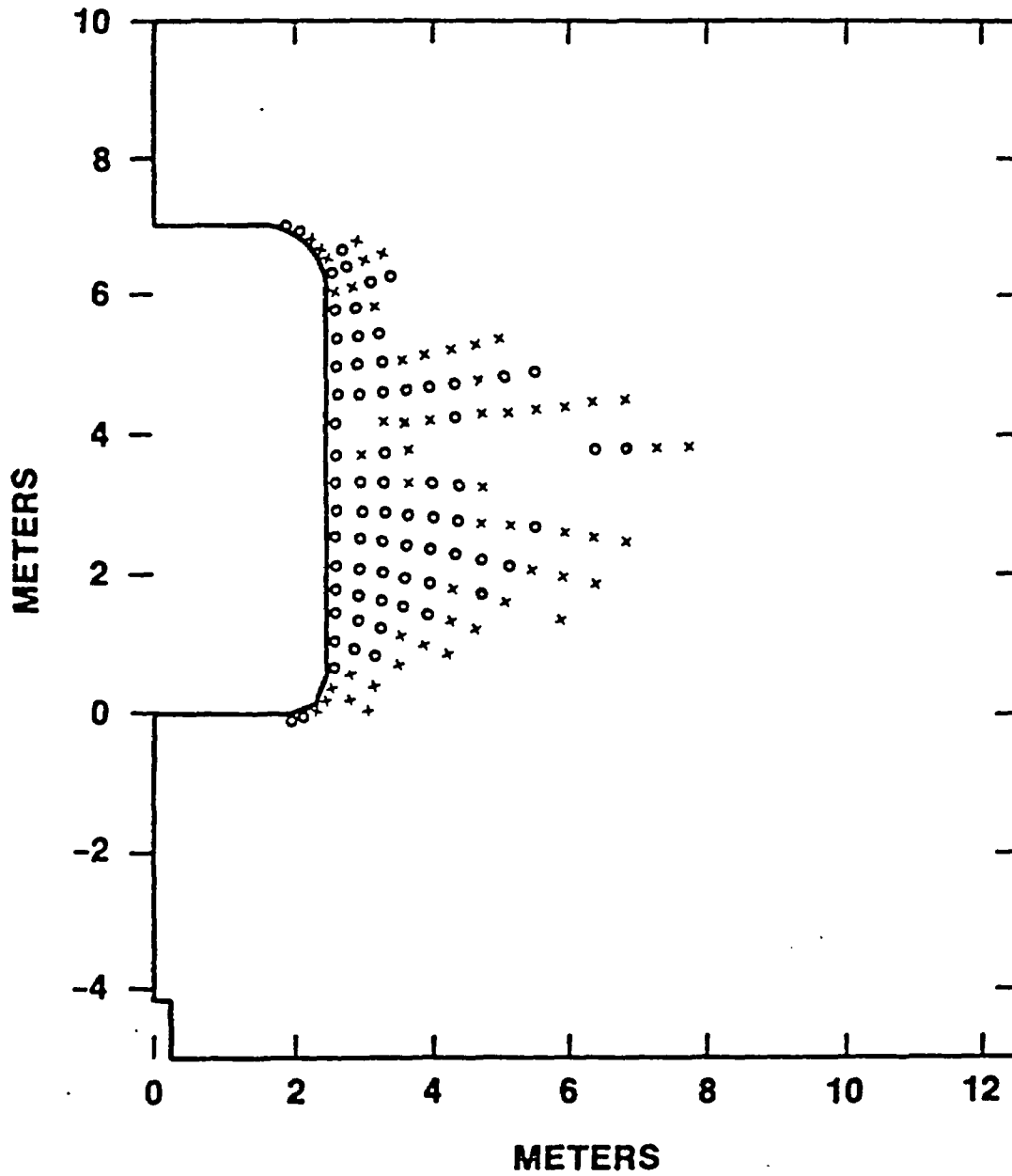


Figure 10. Joint Movement at 100-Year Time Step in the Calico Hills.
 (Limit Case: x - joint slip, o - joint movement.)

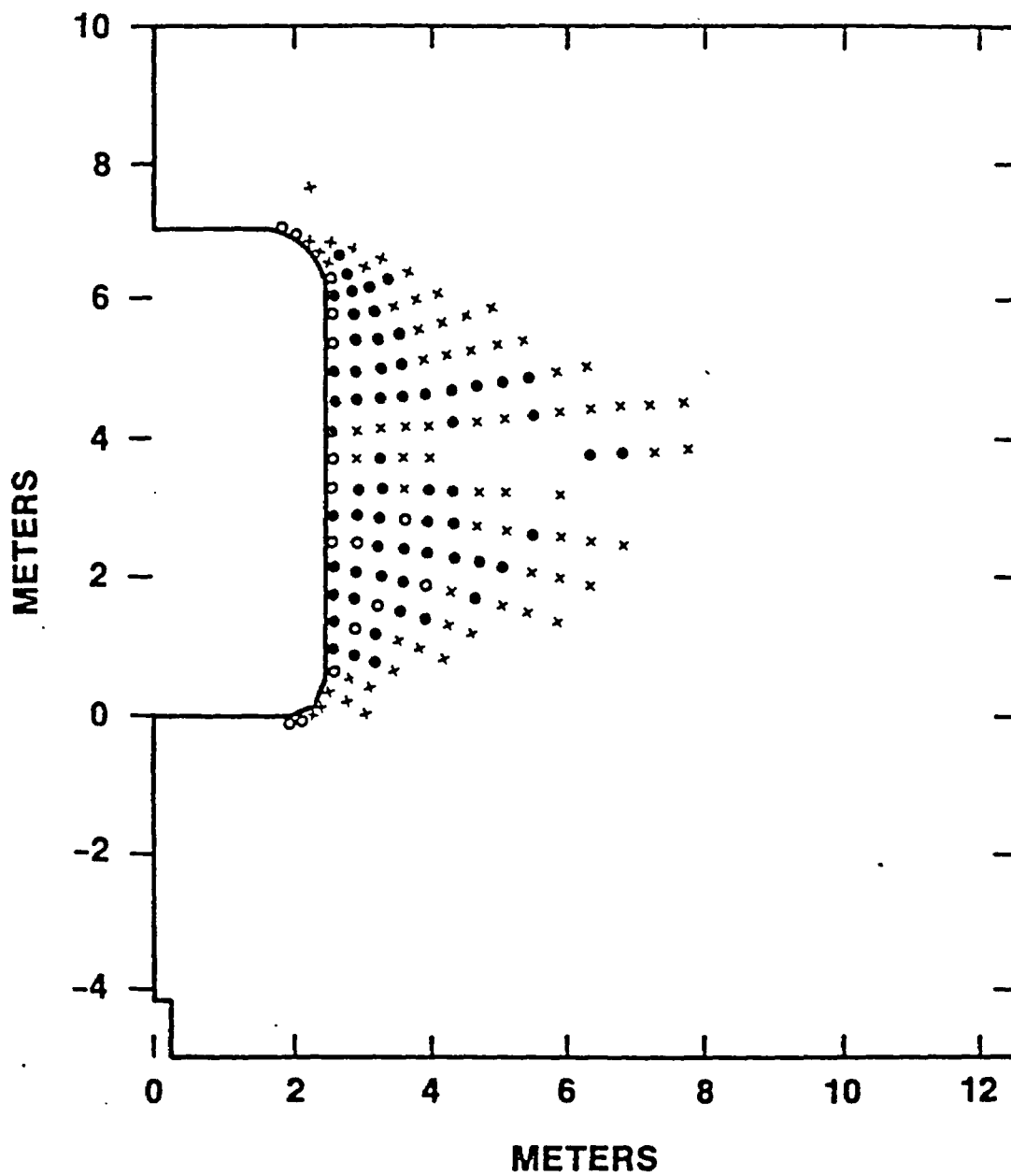


Figure 11. Cumulative Joint Movement in First 100 Years in Calico Hills. ((Limit Case: x - joint slip, o - joint opening, • - joint slip and opening.)

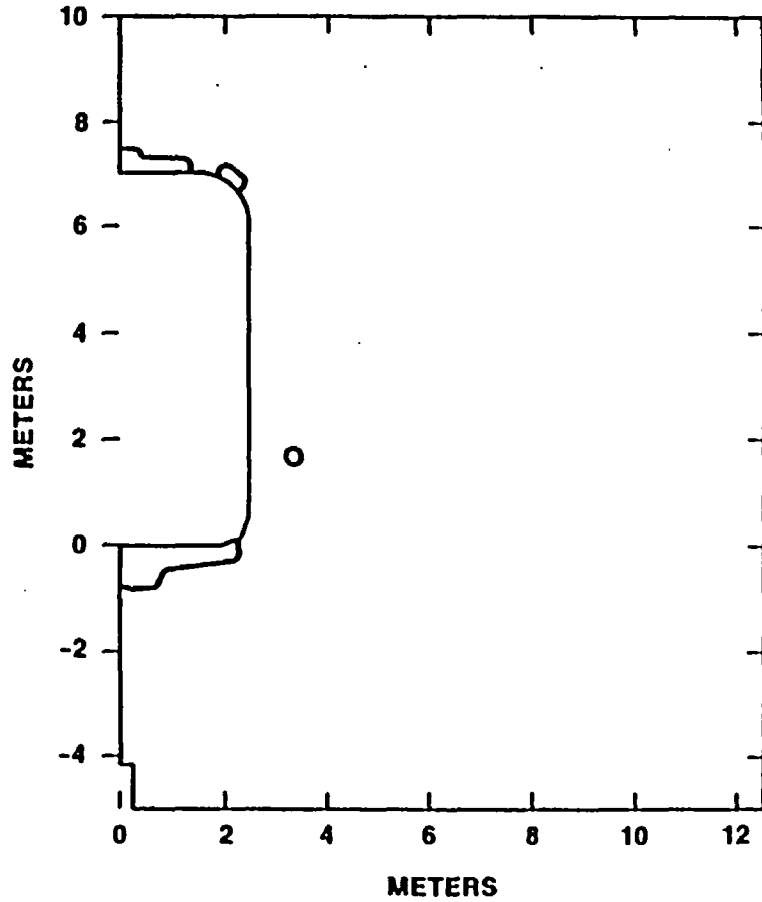


Figure 12. Calico Hills Matrix Fracturing Due to Excavation (None) and 100 Years of Heating (Average properties).

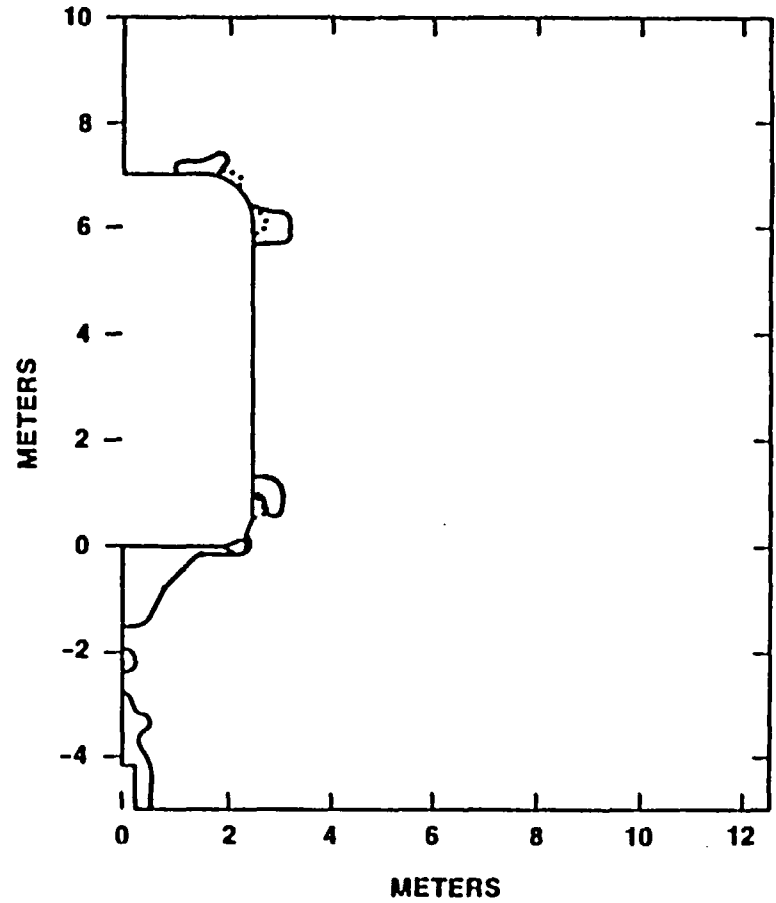


Figure 13. Calico Hills Matrix Fracturing Due to Excavation (Dotted line) and 100 Years of Heating (Solid line). (Limit properties.)

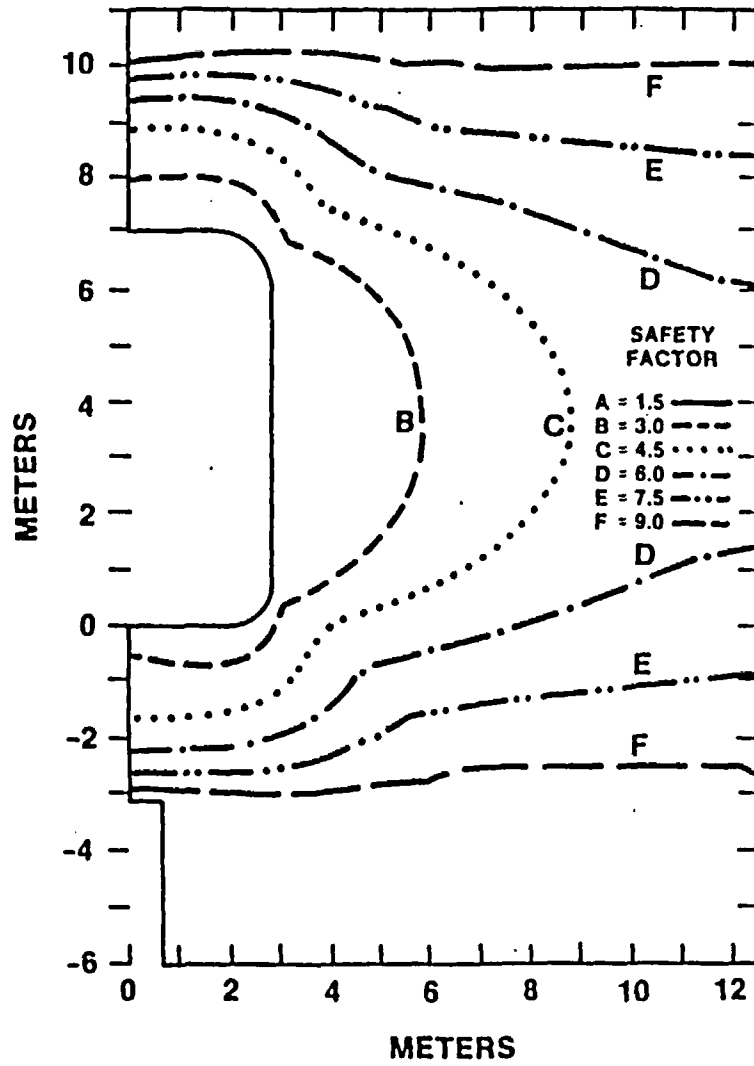


Figure 14. Matrix Factor of Safety Contours for the Calico Hills (Average properties) at Excavation.

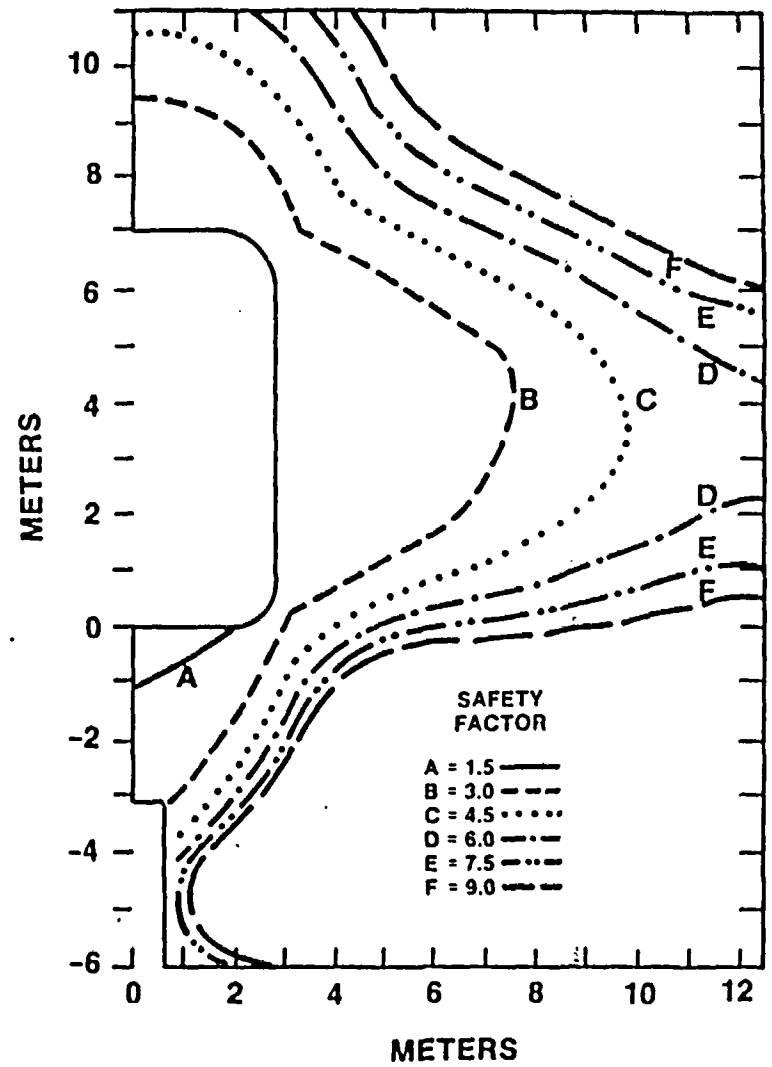


Figure 15. Matrix Factor of Safety Contours for the Calico Hills (Average properties) at 50 years.

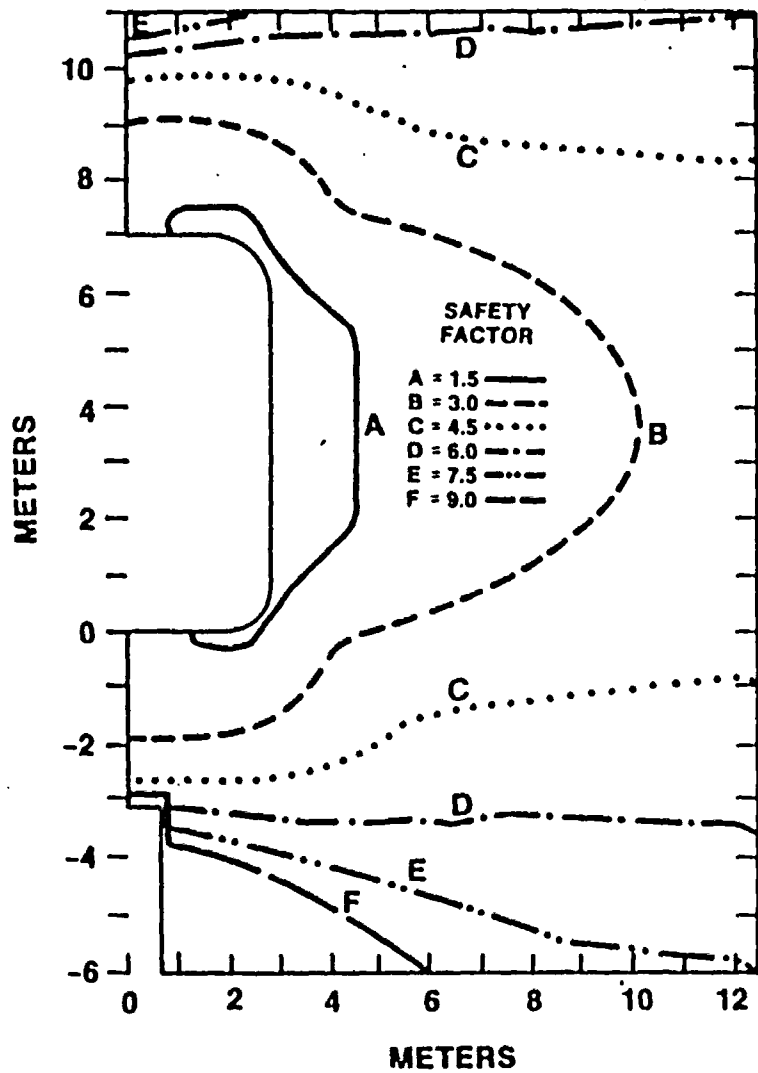


Figure 16. Matrix Factor of Safety Contours for the Calico Hills (Limit properties) at Excavation.

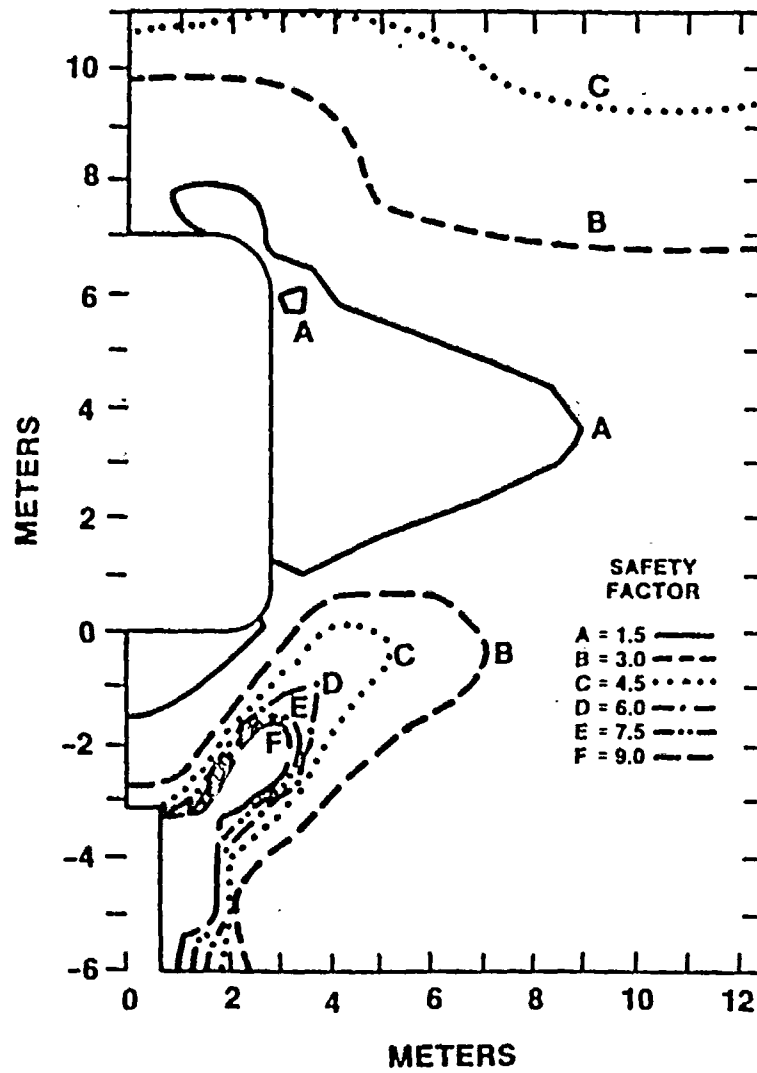


Figure 17. Matrix Factor of Safety Contours for the Calico Hills (Limit properties) at 50 years.

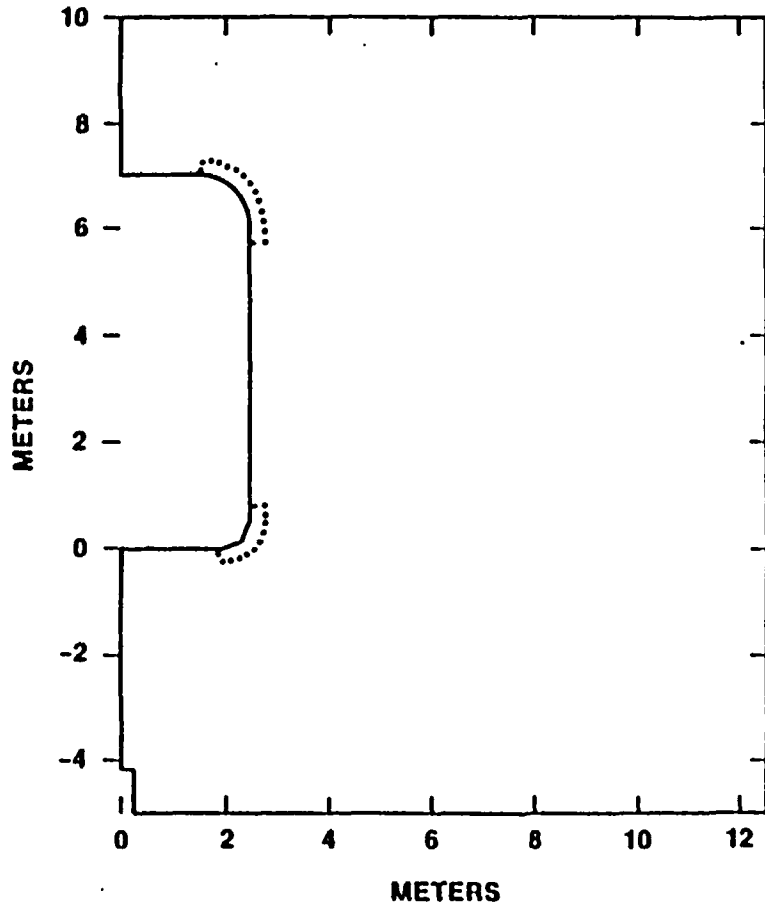


Figure 18. Fractured Matrix Regions for the Calico Hills (Limit properties) at Excavation. (No joints.)

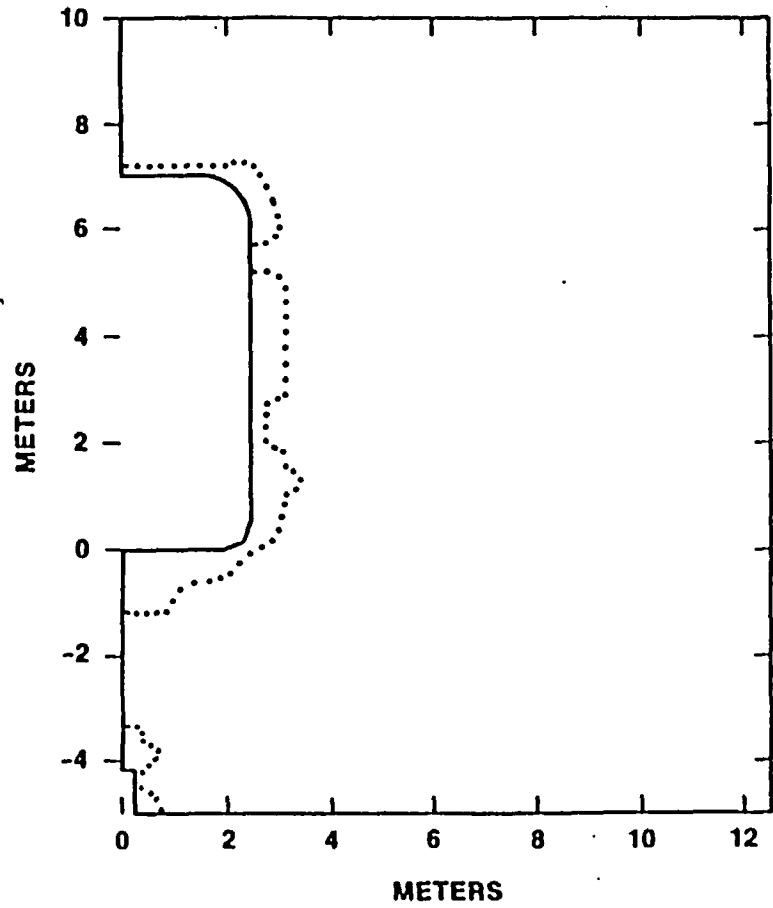


Figure 19. Fractured Matrix Regions for the Calico Hills (Limit properties) at 100 Years. (No joints.)

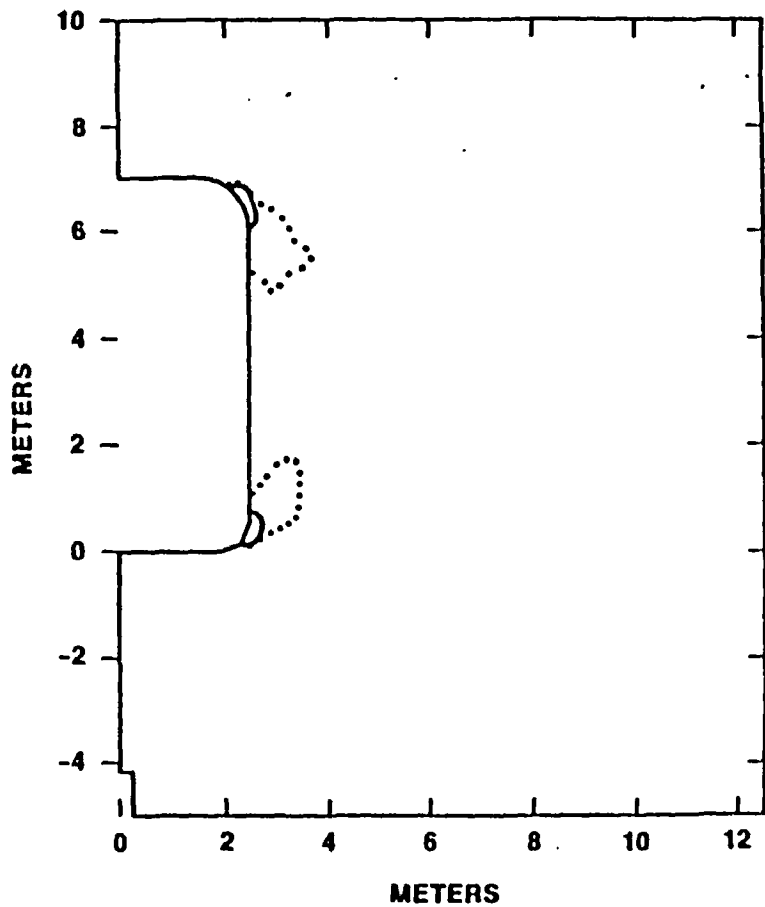


Figure 20. Joint Movement for Topopah Spring at Excavation. (Solid line--average properties, dotted line--limit properties.)

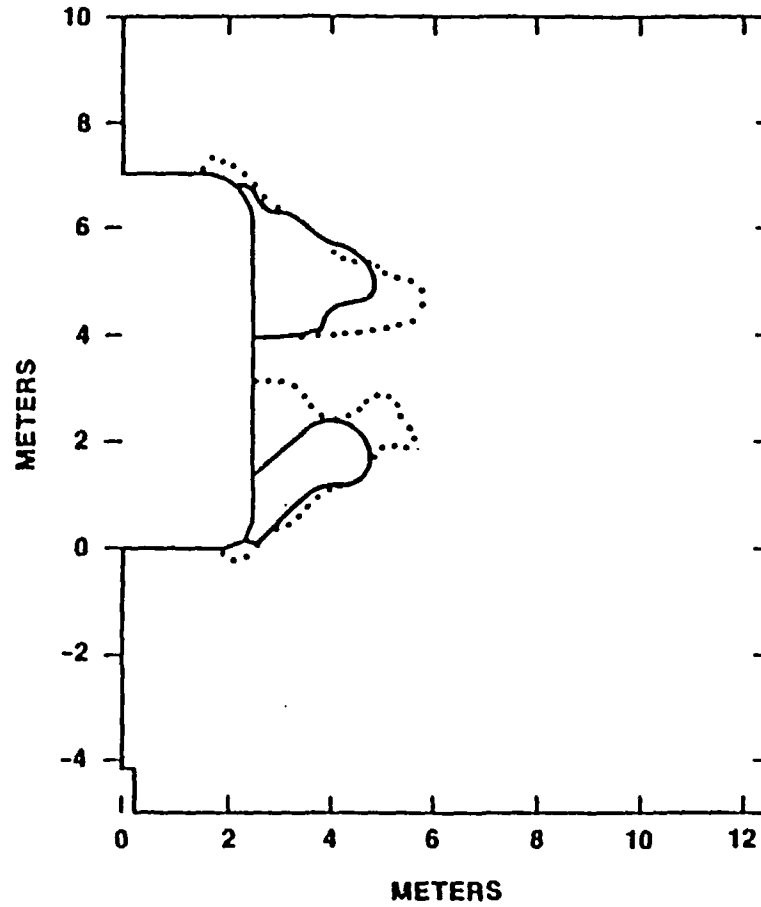


Figure 21. Cumulative Joint Movement for Topopah Spring to 100 Years. (Solid line--average properties, dotted line--limit properties.)

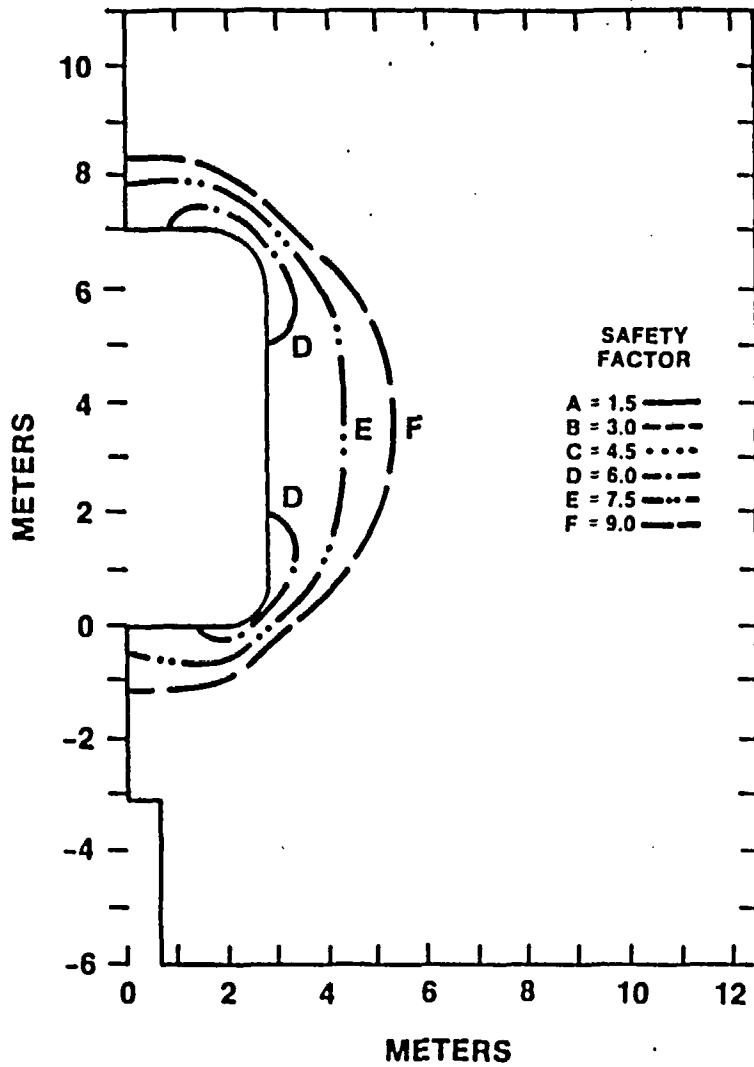


Figure 23. Matrix Factor of Safety Contours for Topopah Spring (Average properties) at Excavation.

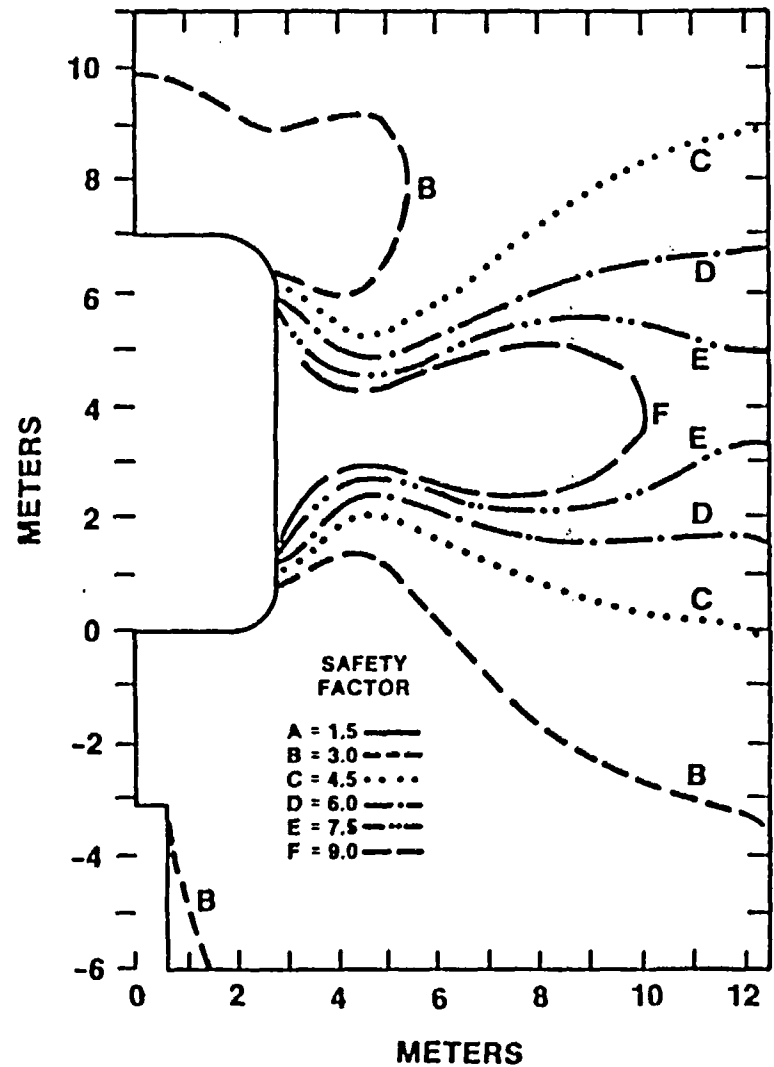


Figure 24. Matrix Factor of Safety Contours for Topopah Spring (Average properties) at 50 Years.

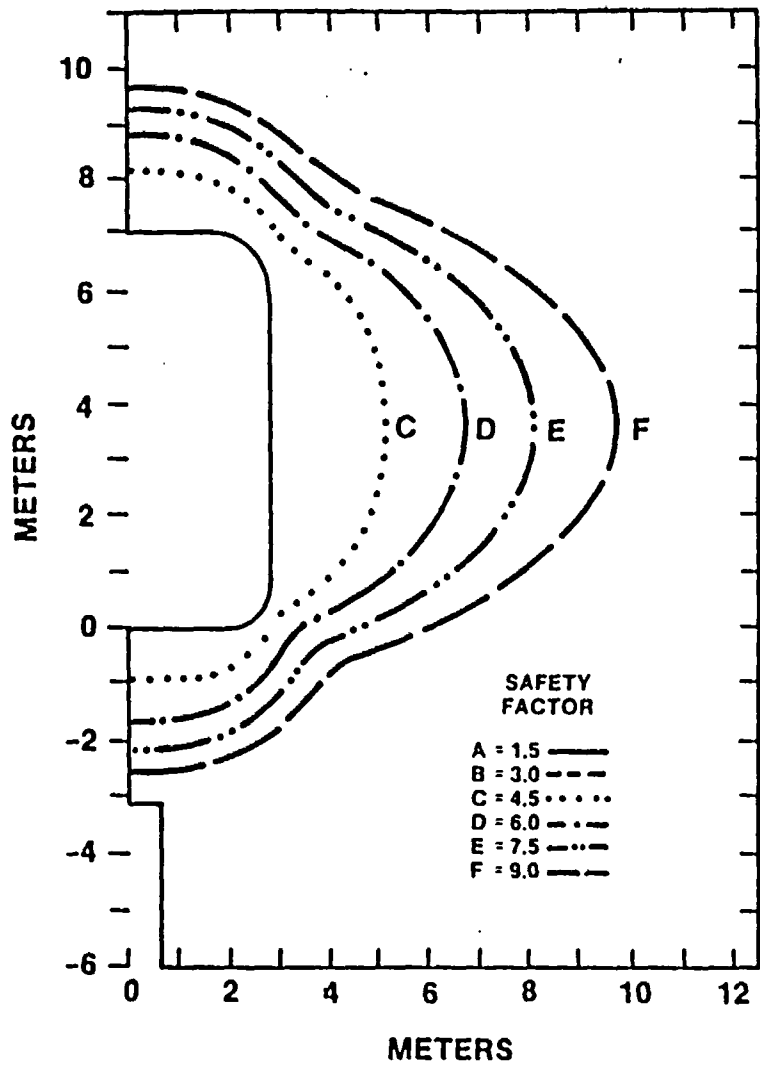


Figure 25. Matrix Factor of Safety Contours for Topopah Spring (Limit properties) at Excavation.

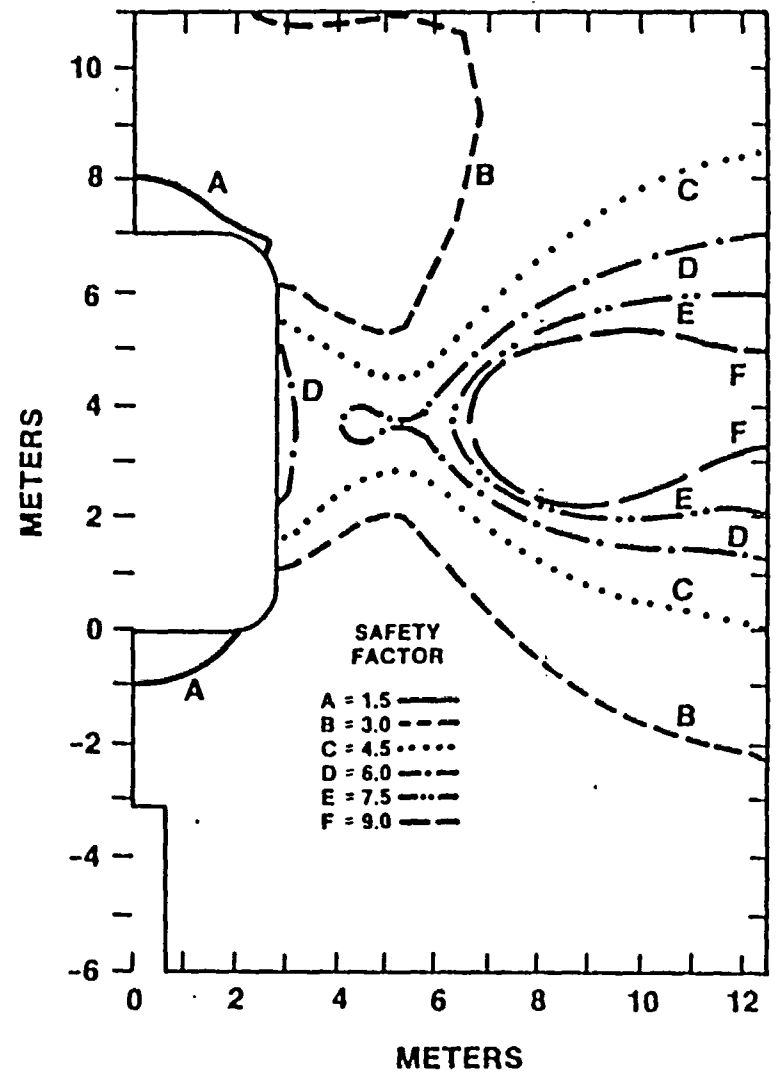


Figure 26. Matrix Factor of Safety Contours for Topopah Spring (Limit properties) at 50 Years.

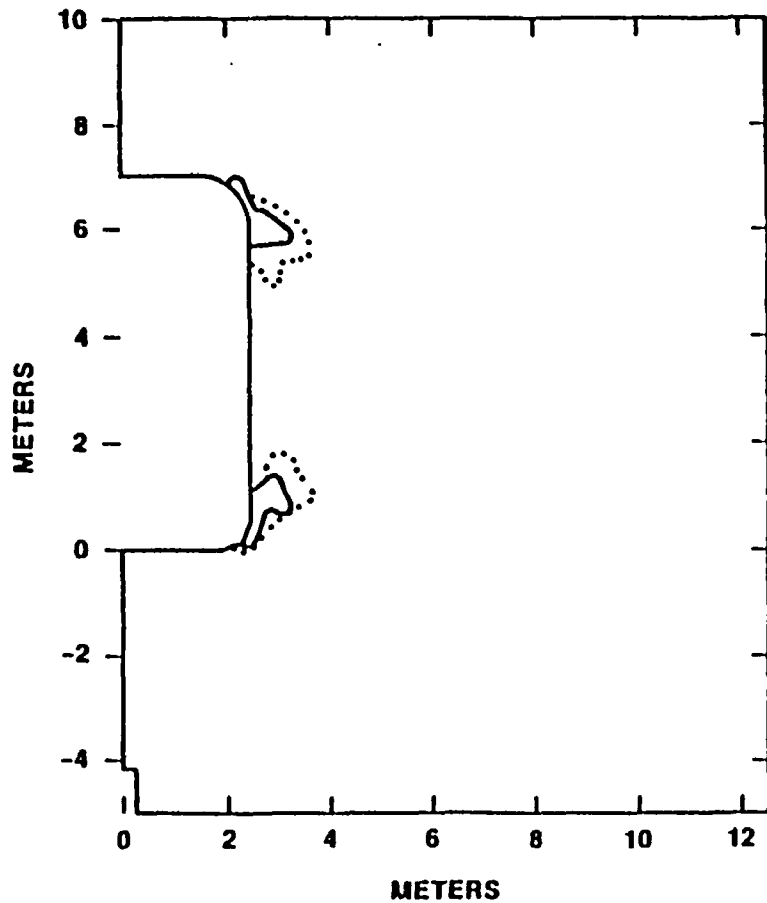


Figure 27. Joint Movement for Bullfrog at Excavation. (Solid line--average properties, dotted line--limit properties.)

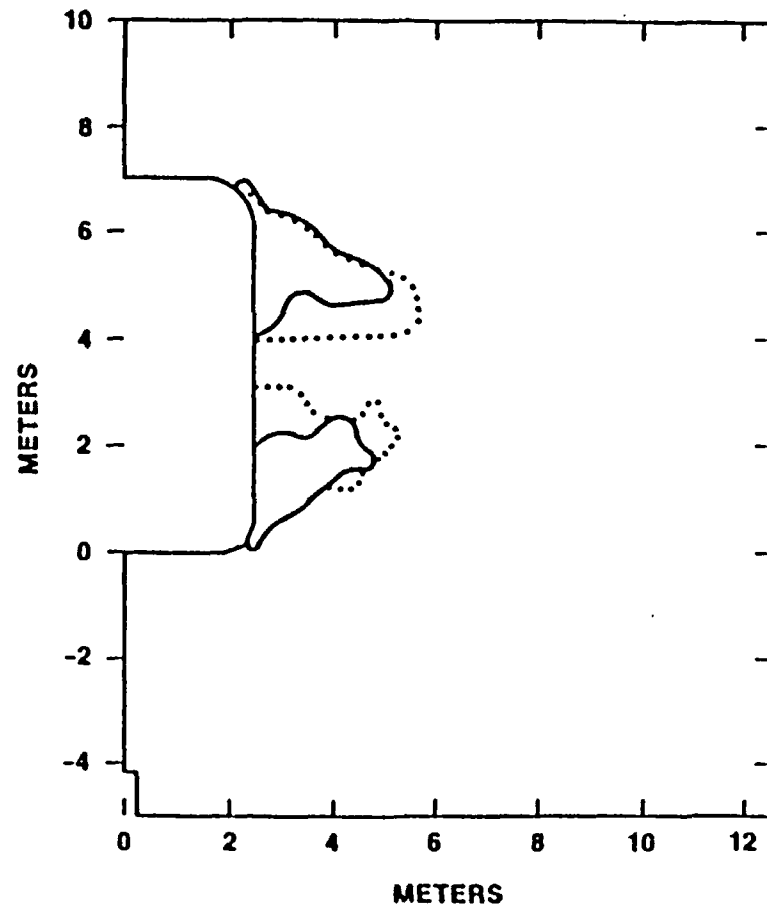


Figure 28. Cumulative Joint Movement for Bullfrog to 100 Years. (Solid line--average properties, dotted line--limit properties.)

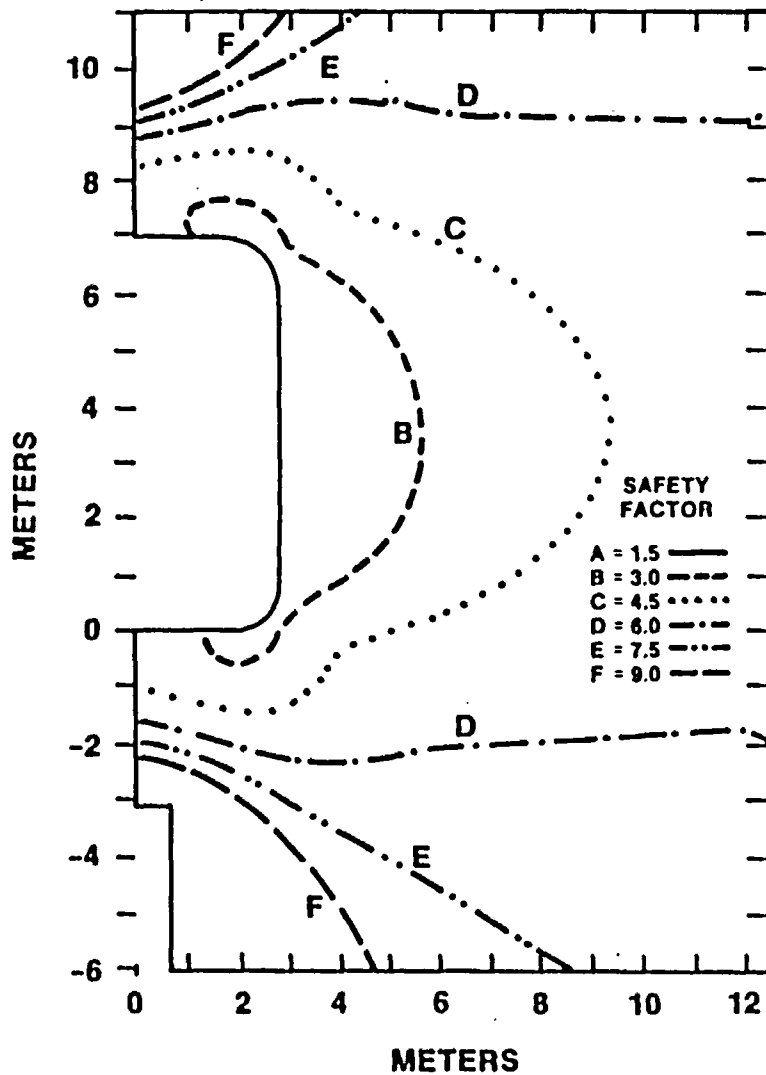


Figure 29. Matrix Factor of Safety Contours for Bullfrog (Average properties) at Excavation.

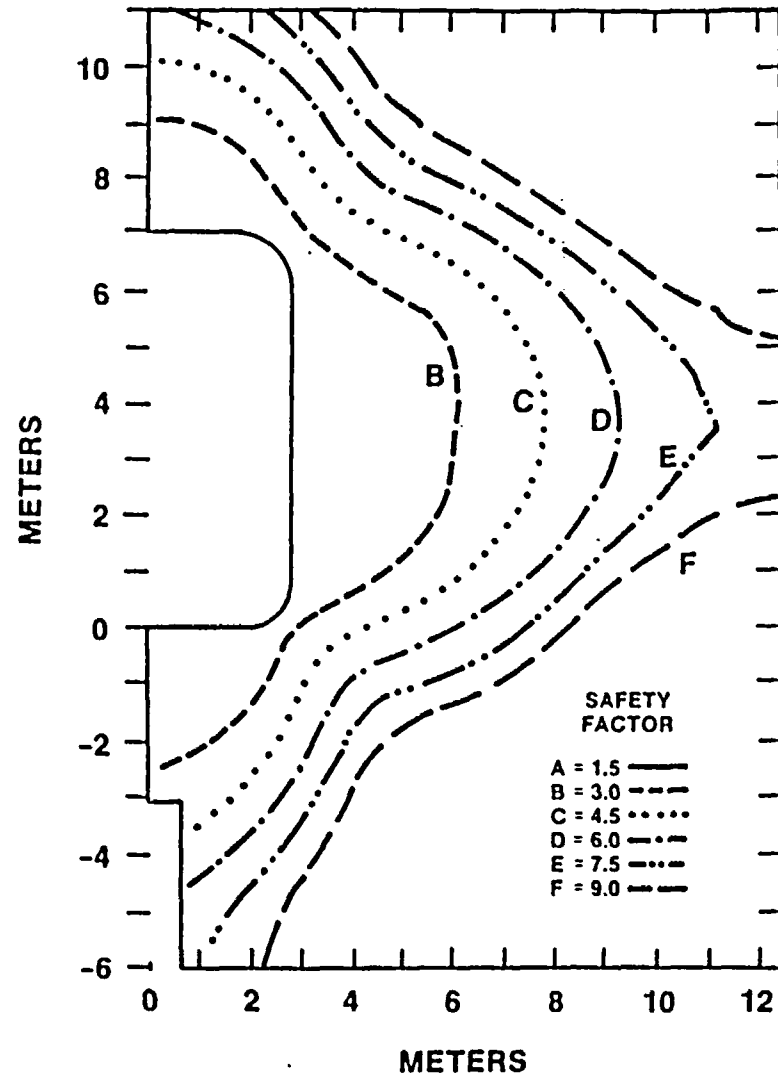


Figure 30. Matrix Factor of Safety Contours for Bullfrog (Average properties) at 50 Years.

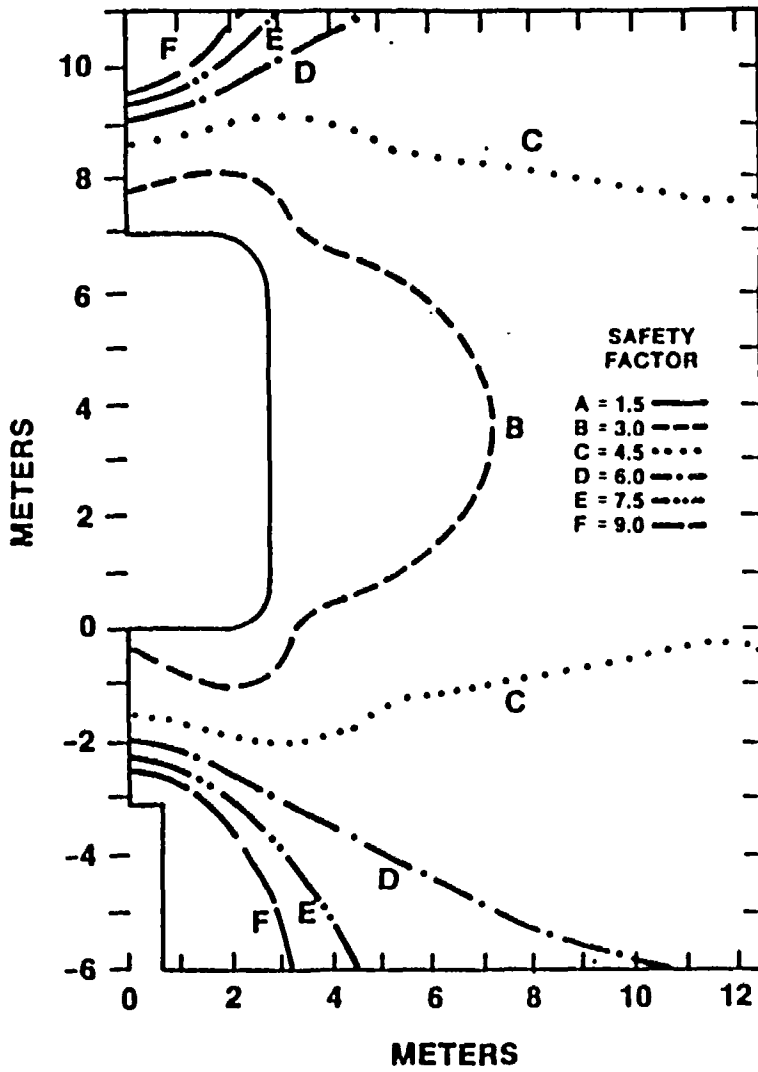


Figure 31. Matrix Factor of Safety Contours for Bullfrog (Limit properties) at Excavation.

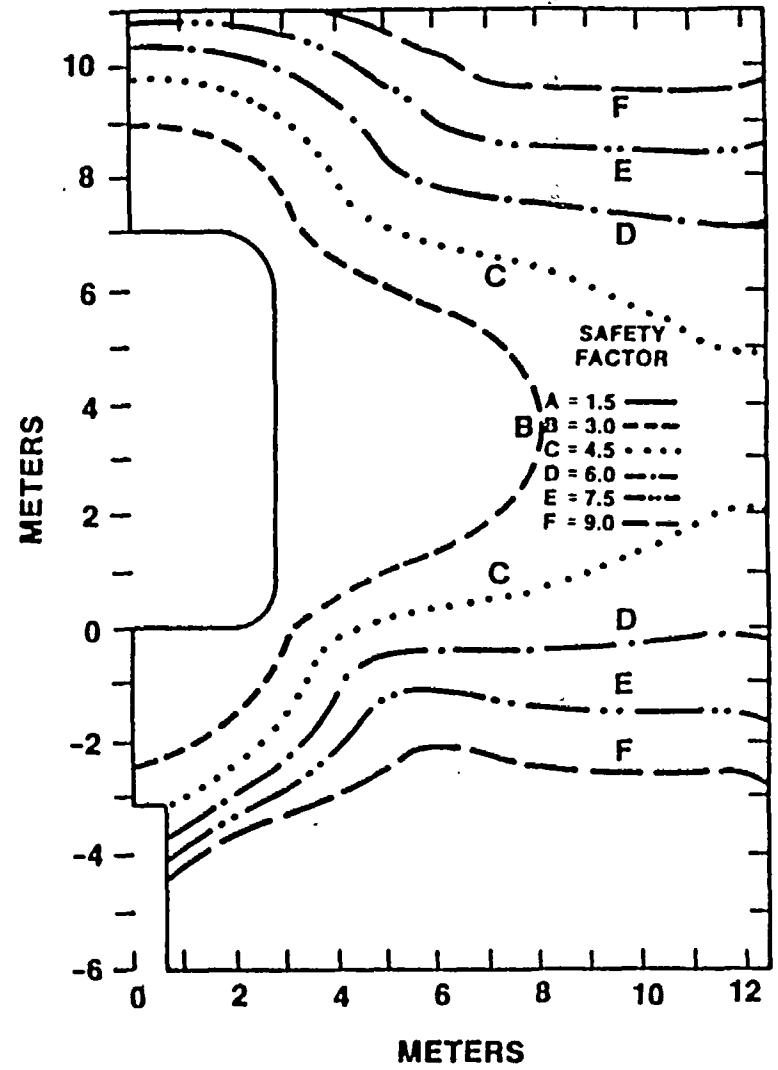


Figure 32. Matrix Factor of Safety Contours for Bullfrog (Limit properties) at 50 Years.

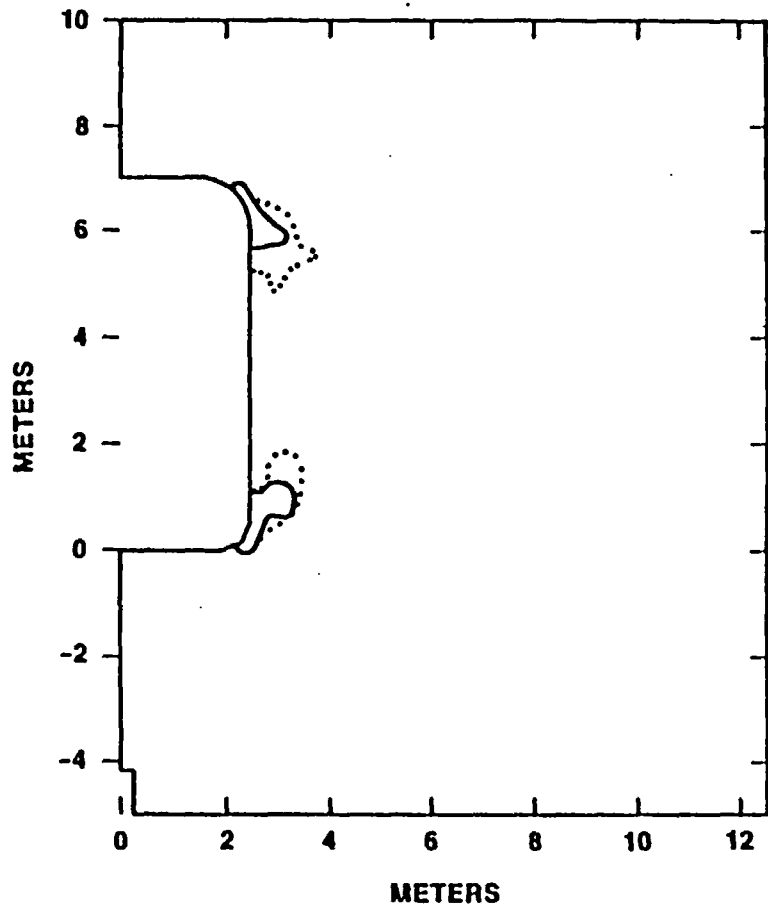


Figure 33. Joint Movement for Tram at Excavation. (Solid line--average properties, dotted line--limit properties.)

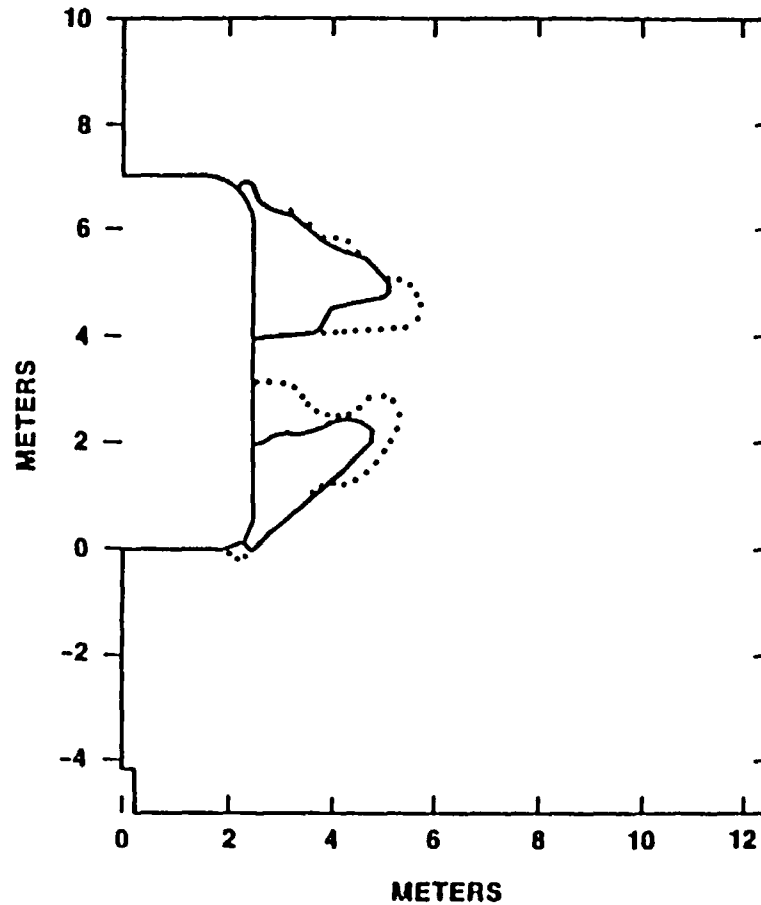


Figure 34. Cumulative Joint Movement for Tram to 100 Years. (Solid line--average properties, dotted line--limit properties.)

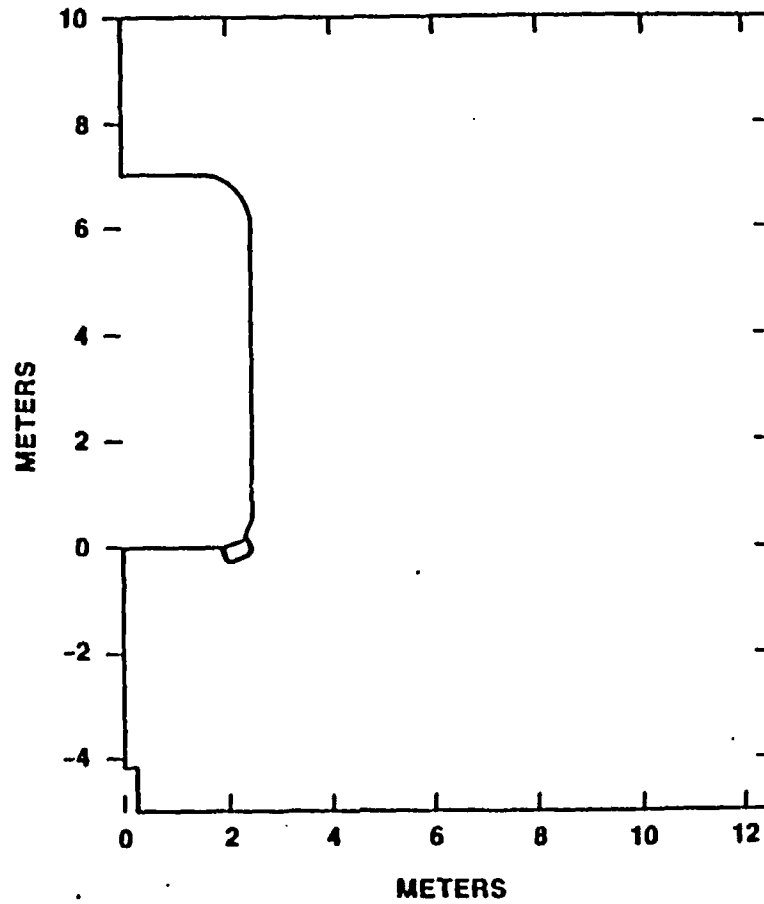


Figure 35. Fractured Matrix Region for Tram to 100 Years (Limit properties).

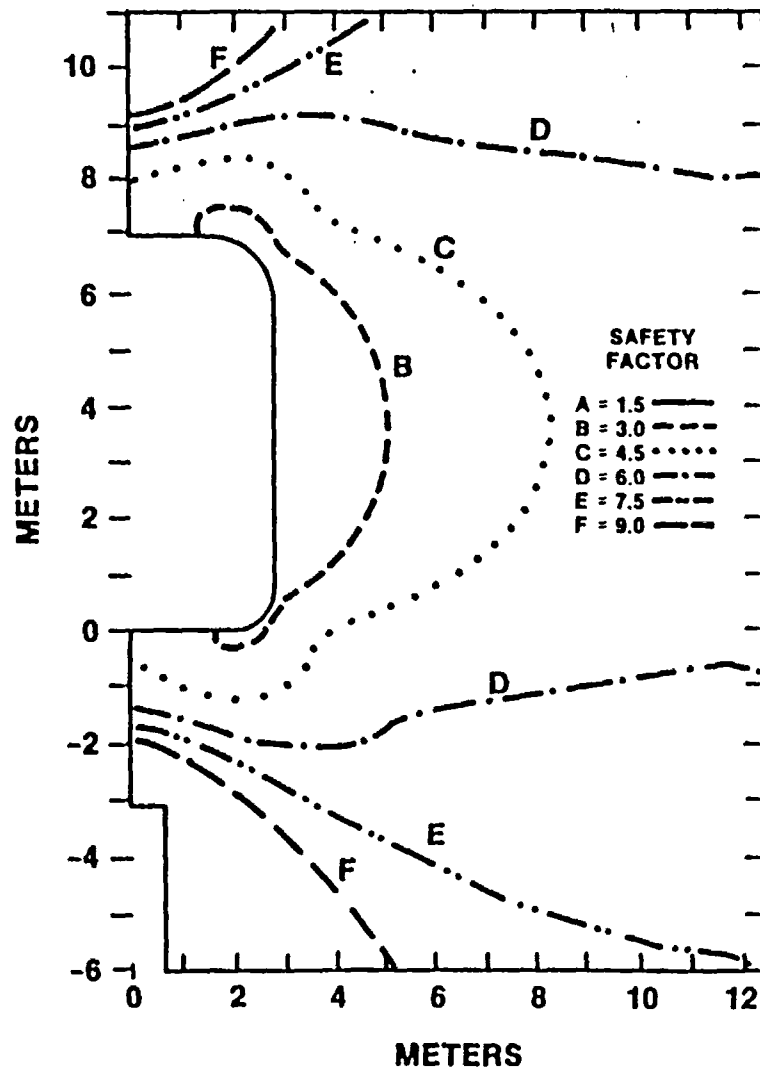


Figure 36. Matrix Factor of Safety Contours for Tram (Average properties) at Excavation.

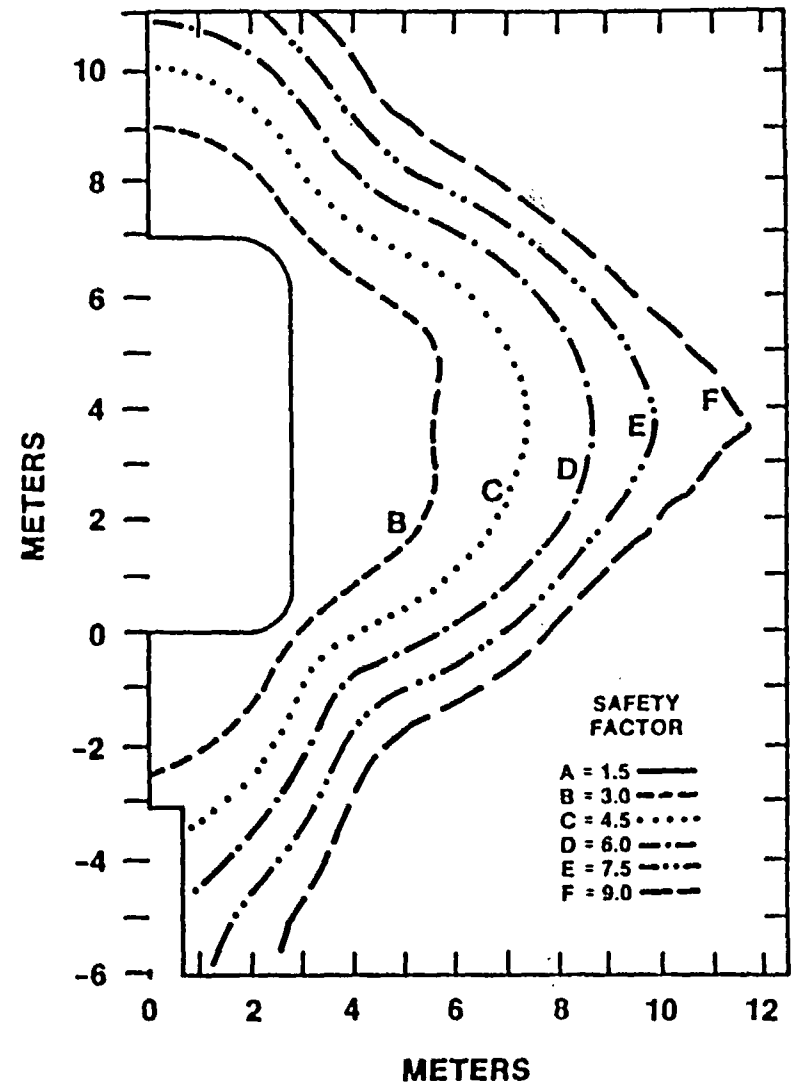


Figure 37. Matrix Factor of Safety Contours for Tram (Average properties) at 50 Years.

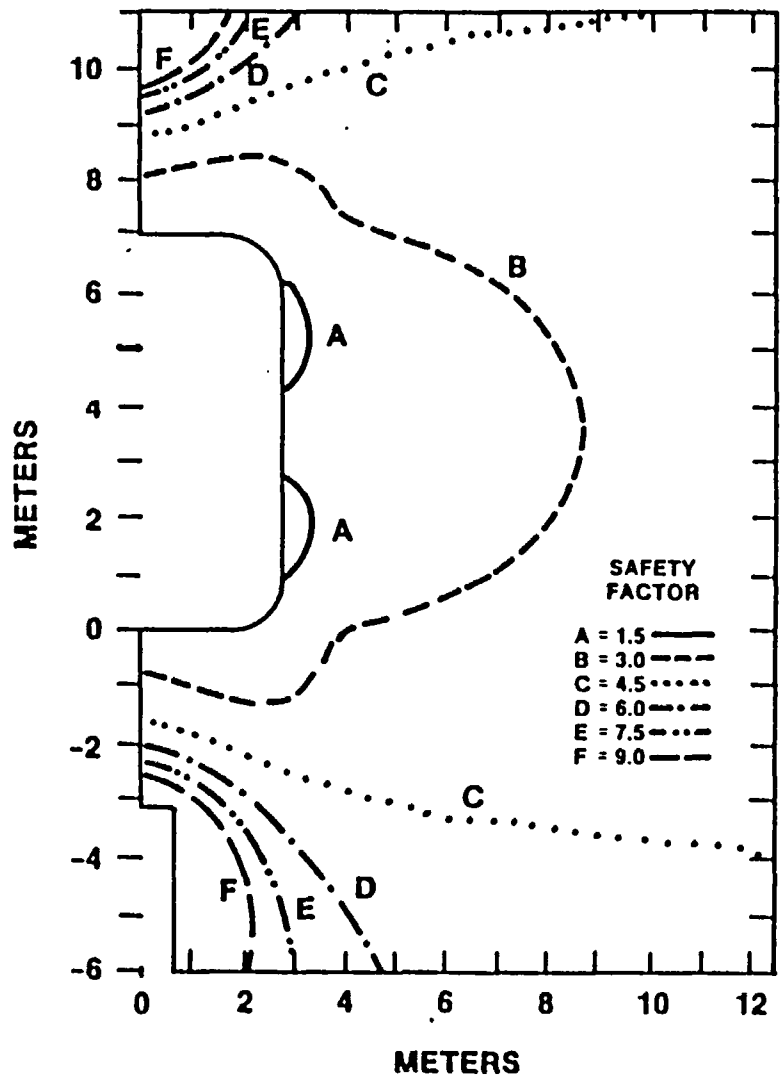


Figure 38. Matrix Factor of Safety Contours for Tram (Limit properties) at Excavation.

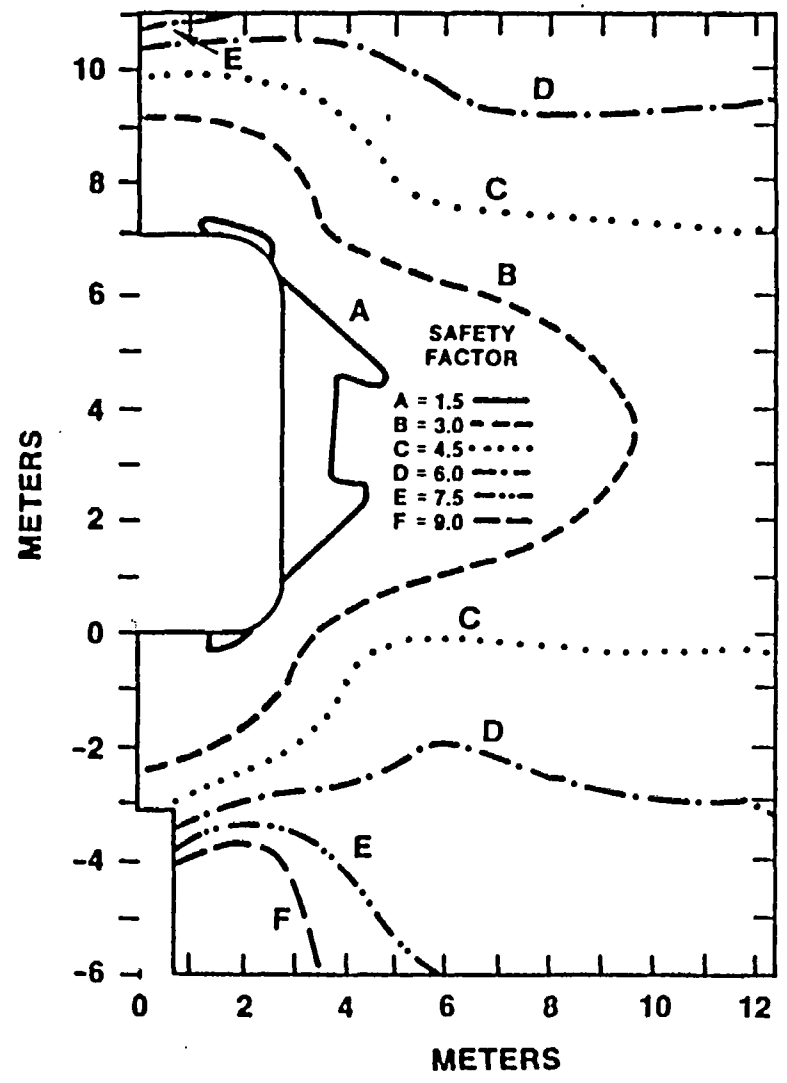


Figure 39. Matrix Factor of Safety Contours for Tram (Limit properties) at 50 Years.

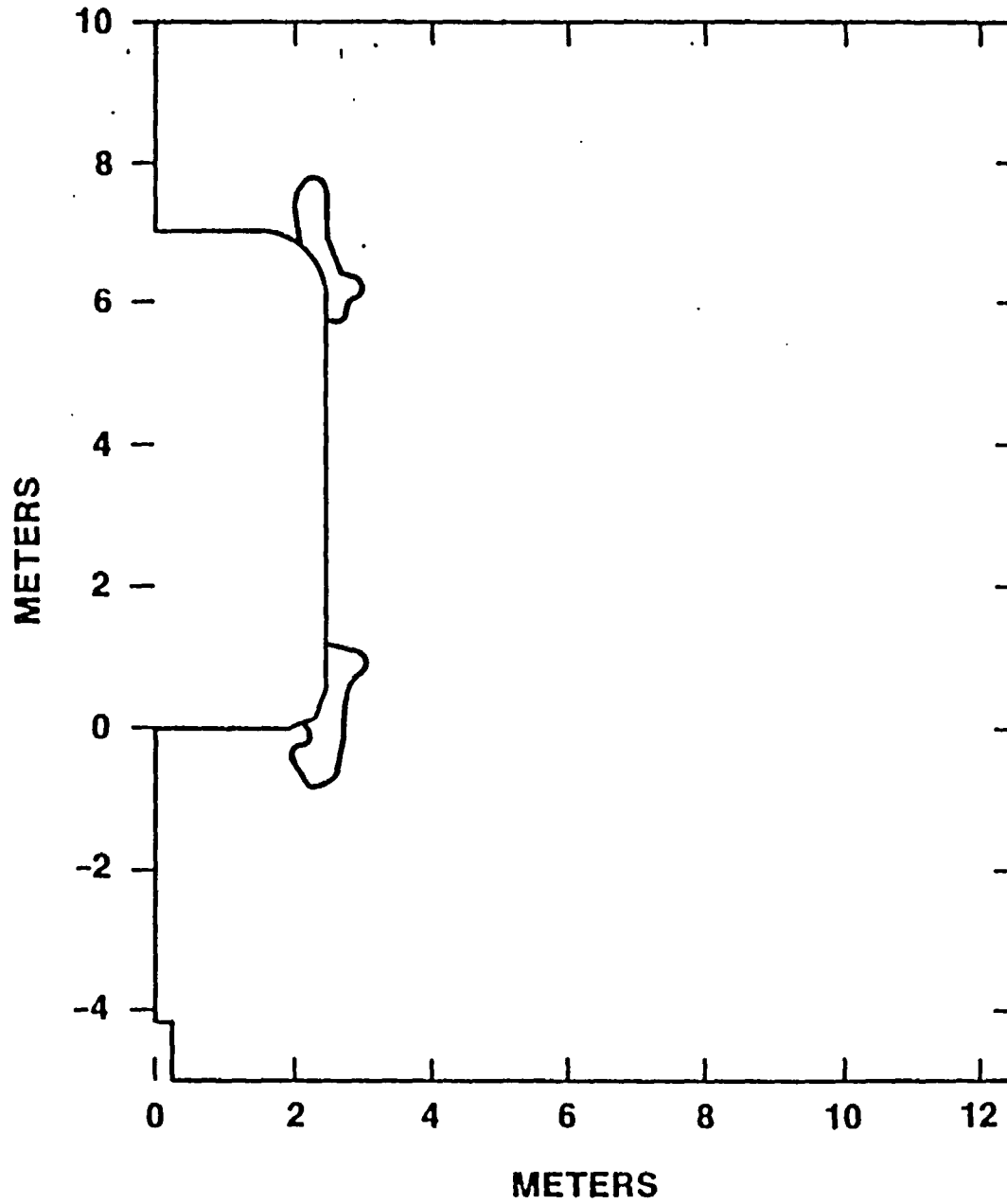


Figure 40. Joint Movement for Grouse Canyon at Excavation.

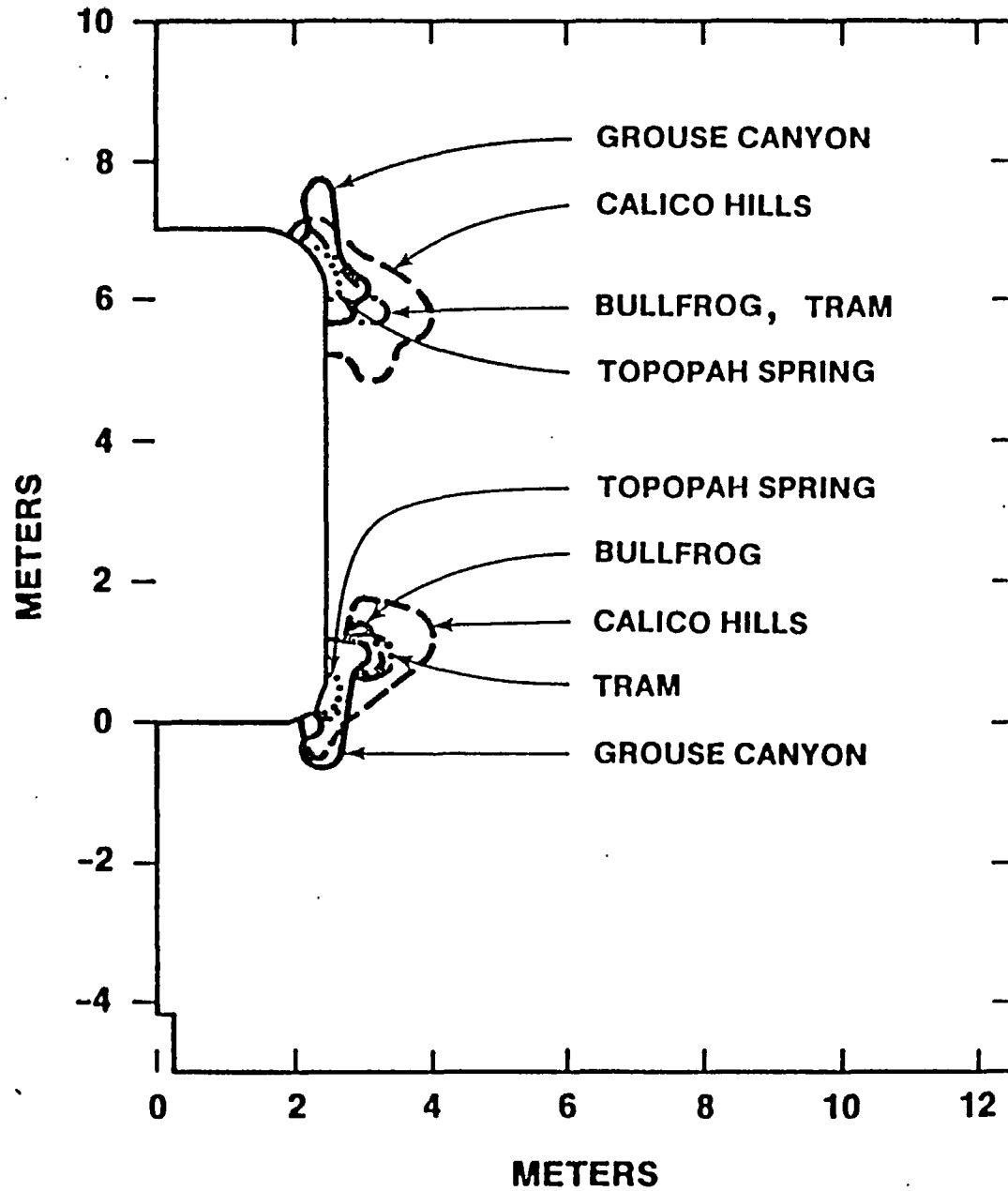


Figure 41. Comparison of Regions of Predicted Joint Movement in the Four Potential Units With Grouse Canyon at Excavation.

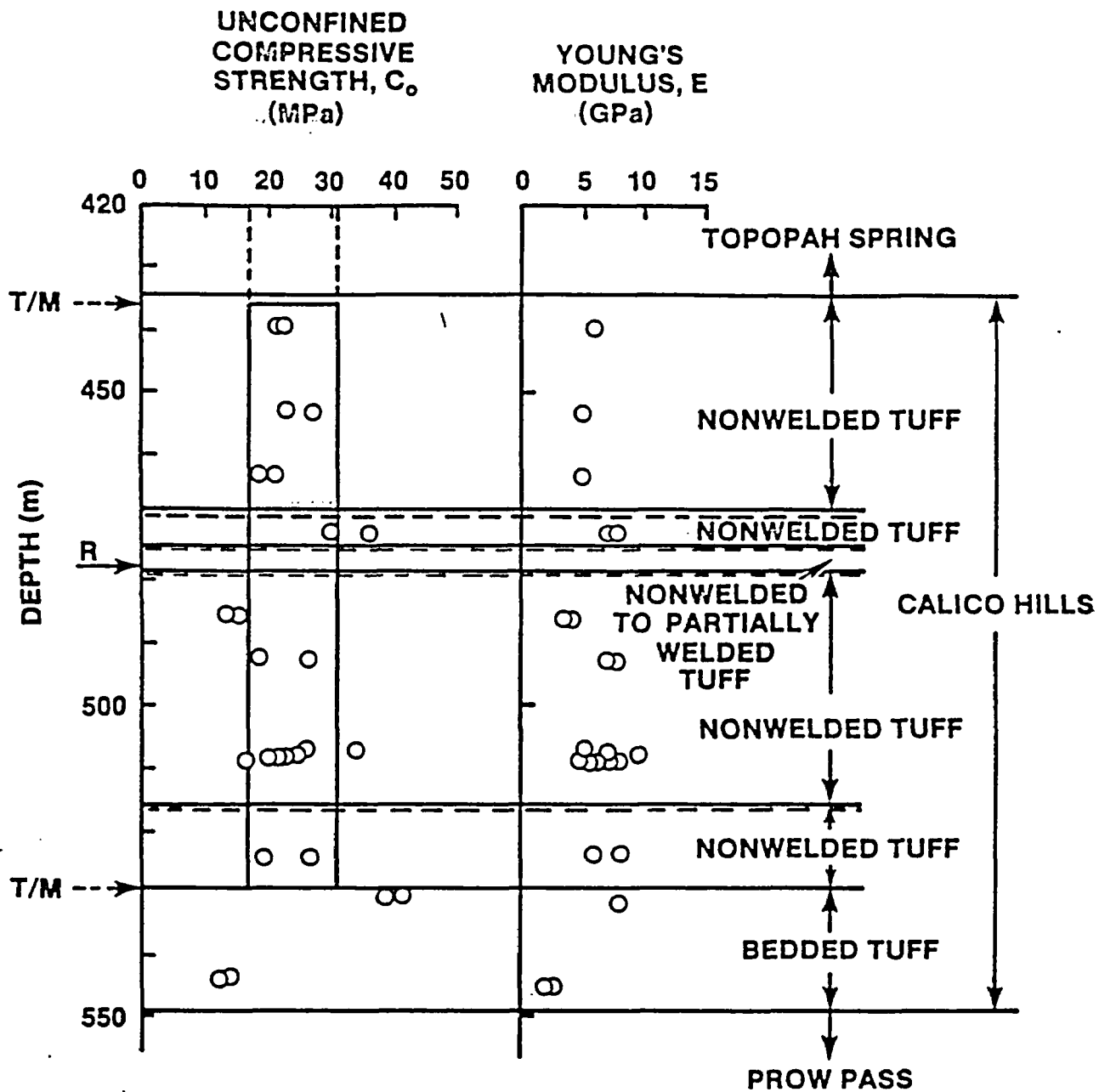


Figure 42. Sample Mechanical Properties Versus Sample Depth for the Calico Hills. (Tests on saturated samples at room temperature.)

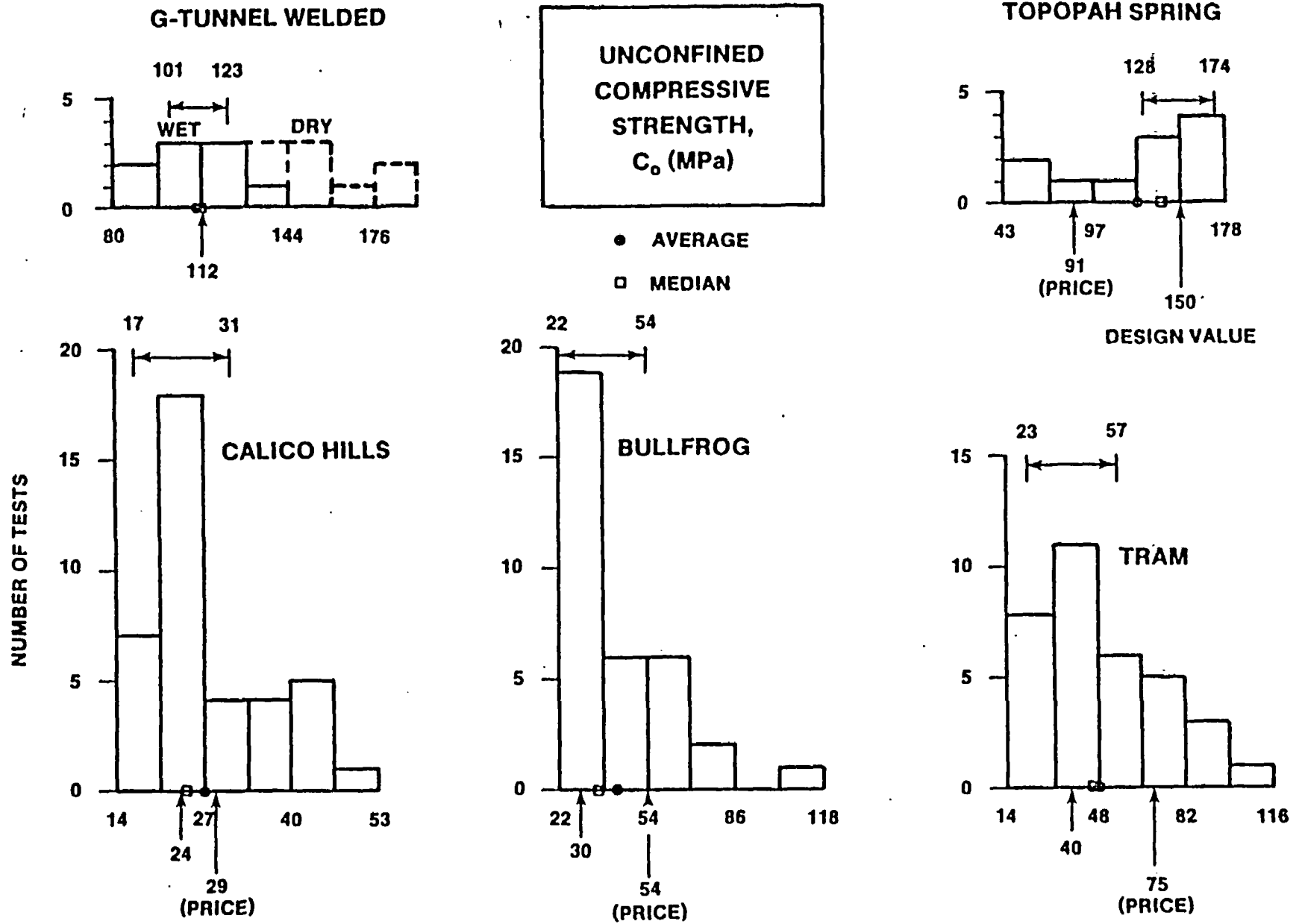
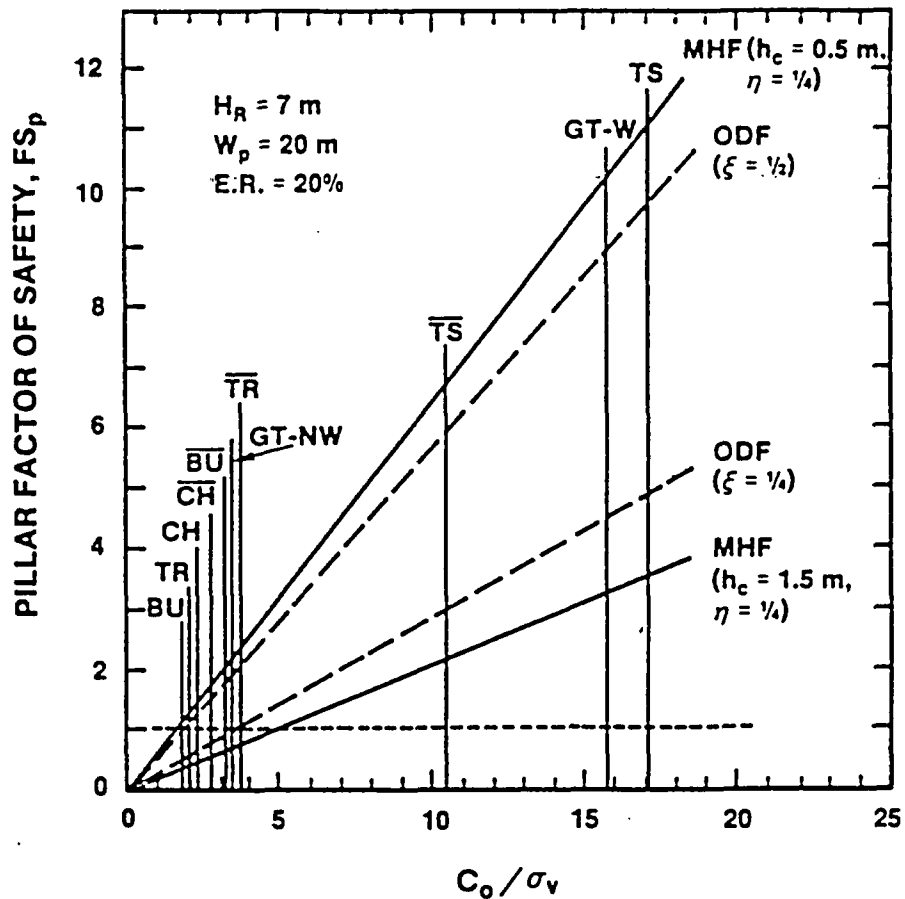


Figure 43. Frequency Plots of Unconfined Compressive Strength. (The mean of the greatest frequency range is shown for each unit along with the value suggested by Price.¹⁵)



$$FS_p = \xi f (W_p/H_R) \frac{C_0}{\bar{\sigma}_v}$$

MHF = MODIFIED HUSTRULID FORMULA: $\xi = (h/h_c)^\eta$

ODF = OBERT & DUVAL FORMULA: $\xi = 0.5$ OR 0.25

W_p = PILLAR WIDTH (20 m)

H_R = ROOM HEIGHT (7 m)

C_0 = UNCONFINED COMPRESSIVE STRENGTH OF ROCK

$\bar{\sigma}_v$ = AVERAGE VERTICAL PILLAR STRESS

h = HEIGHT OF TEST SPECIMEN

h_c = HEIGHT OF REFERENCE SPECIMEN AT WHICH NO FURTHER REDUCTION IN STRENGTH IS OBSERVED

η = EMPIRICAL CONSTANT

E.R. = EXTRACTION RATIO (20%)

Figure 44. Pillar Factor of Safety Determined According to Two Different Techniques.

TS - Topopah Spring

TR - Tram

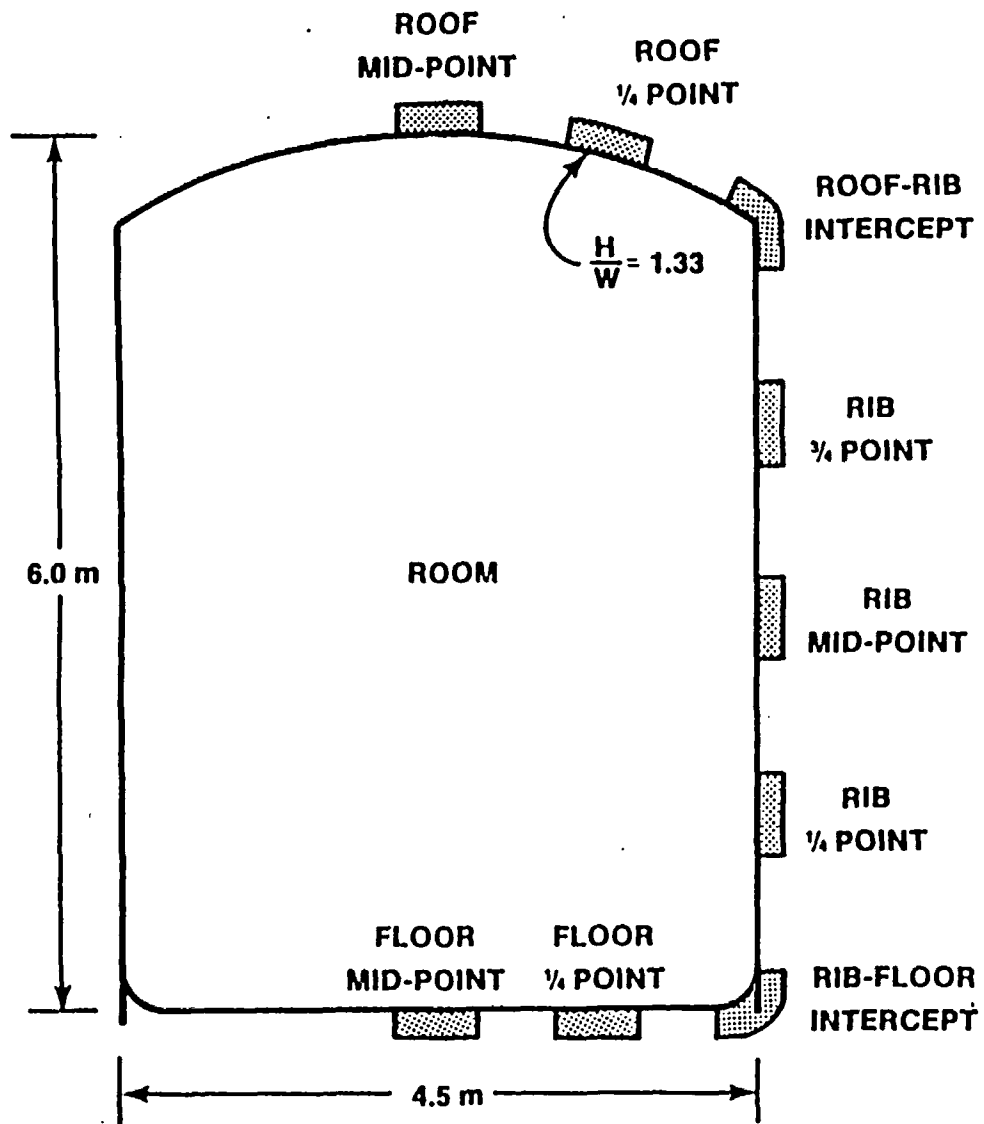
CH - Calico Hills

GT-W - G-Tunnel, Welded

BU - Bullfrog

GT-NW - G-Tunnel, Nonwelded

(An overhead bar, (TS), indicates Price's data¹⁵ while a plain symbol indicates value based on mean of sample frequency data.)

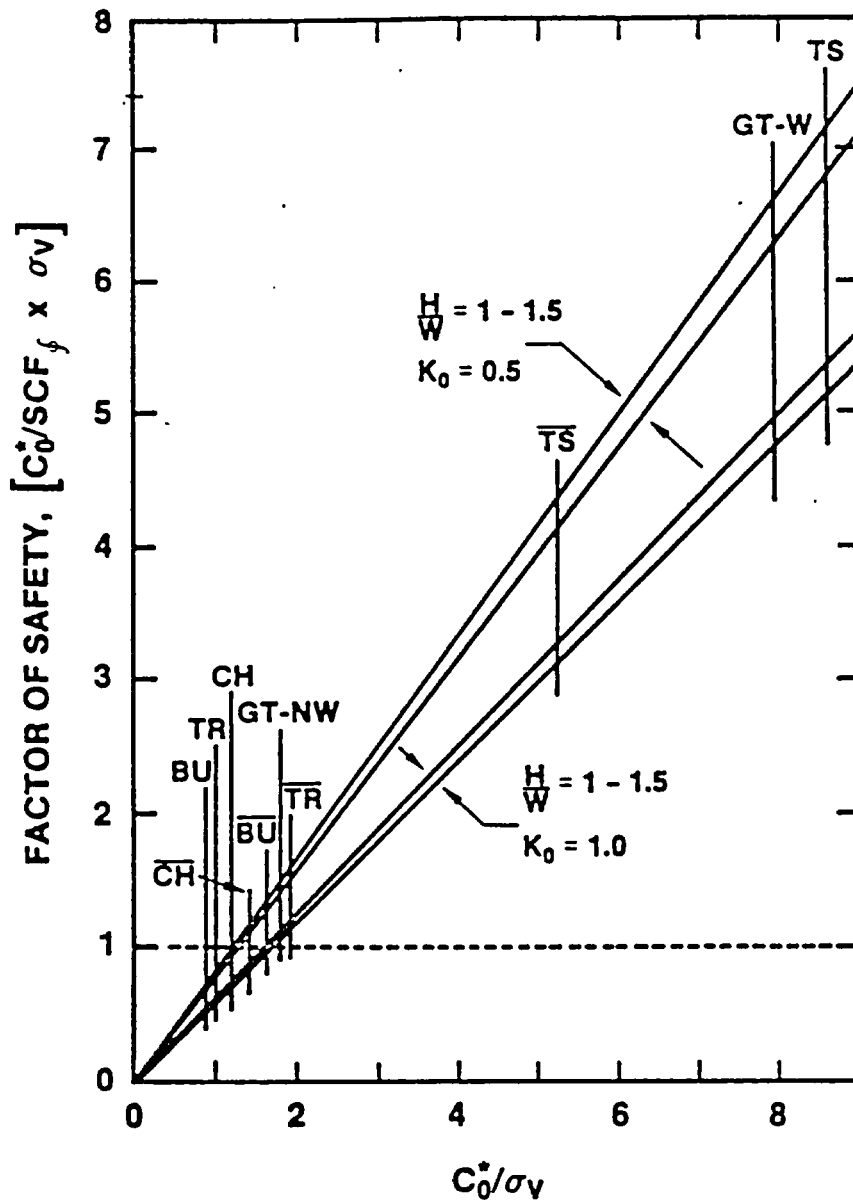


**AVERAGE STRESS CONCENTRATION
FACTOR FOR ROOM**

$$SCF_f = \frac{\int_0^L SCF(l) dl}{\int_0^L dl}$$

L = CIRCUMFERENCE OF ROOM

Figure 45. Schematic Showing the Manner in Which the Average Factor of Safety for the Room was Calculated.



$$K_0 = \frac{\sigma_{\text{HORIZONTAL}}}{\sigma_{\text{VERTICAL}}}$$

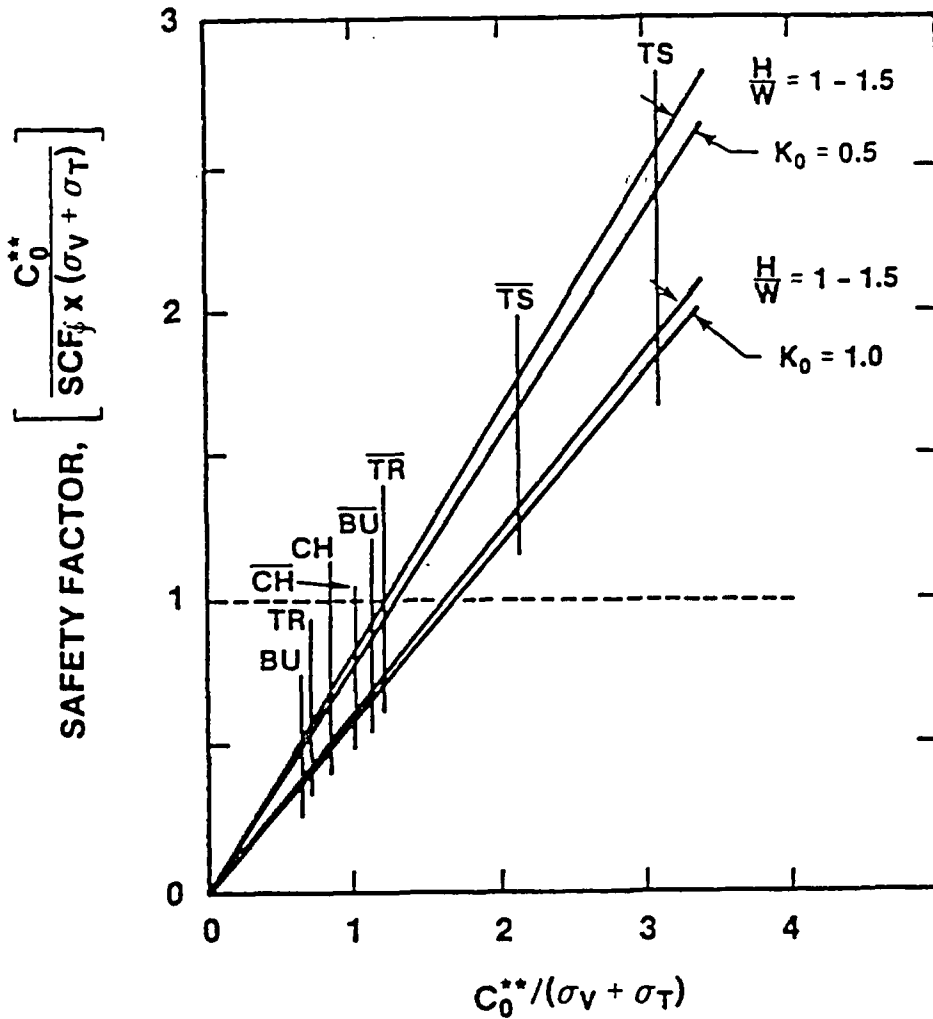
W = ROOM WIDTH (4.5 m)

H = ROOM HEIGHT

$C_0^* = 50\% C_0$

σ_v = OVERBURDEN (VERTICAL) STRESS

Figure 46. Average Factor of Safety for an Unheated Room Expressed as a Function of the Ratio of the Reduced Unconfined Compressive Strength to the Vertical Stress (Symbol explanation in Figure 43).



$$K_0 = \frac{\sigma_{\text{HORIZONTAL}}}{\sigma_{\text{VERTICAL}}}$$

W = ROOM WIDTH (4.5 m)

H = ROOM HEIGHT

$$C_0^{**} = 40\% C_0$$

$$E^{**} = 40\% E$$

σ_v = OVERBURDEN (VERTICAL) STRESS

$$\sigma_T = \alpha_T E^{**} (100 - T_{\text{ambient}})$$

Figure 47. Average Factor of Safety for a Heated Room Expressed as a Function of the Ratio of the Reduced Unconfined Compressive Strength to Sum of the Vertical and Thermal Stresses (Symbol explanation in Figure 43).

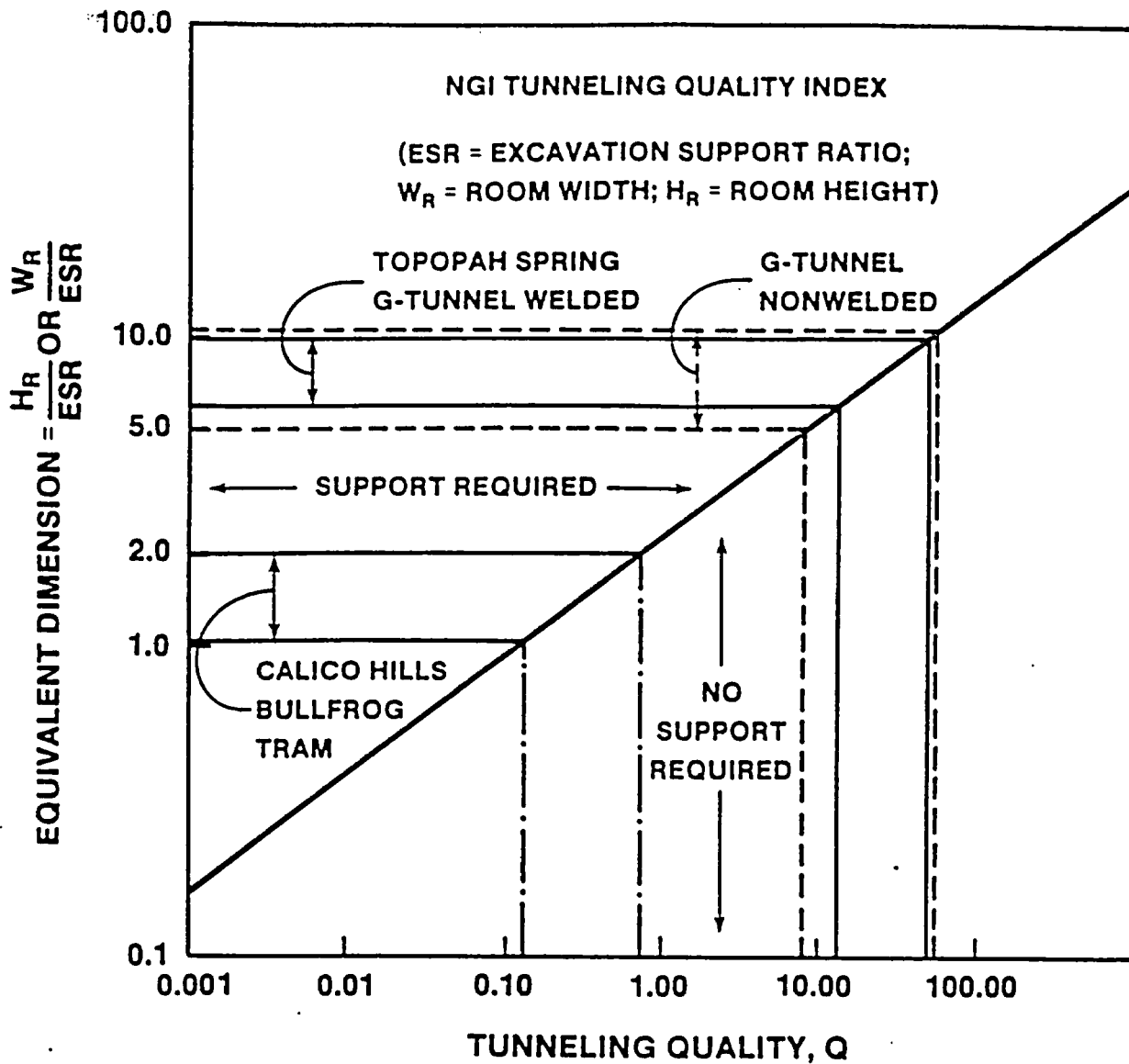


Figure 48. Tunneling Quality Index for the Four Units at Yucca Mountain and the Two Units at G-Tunnel.

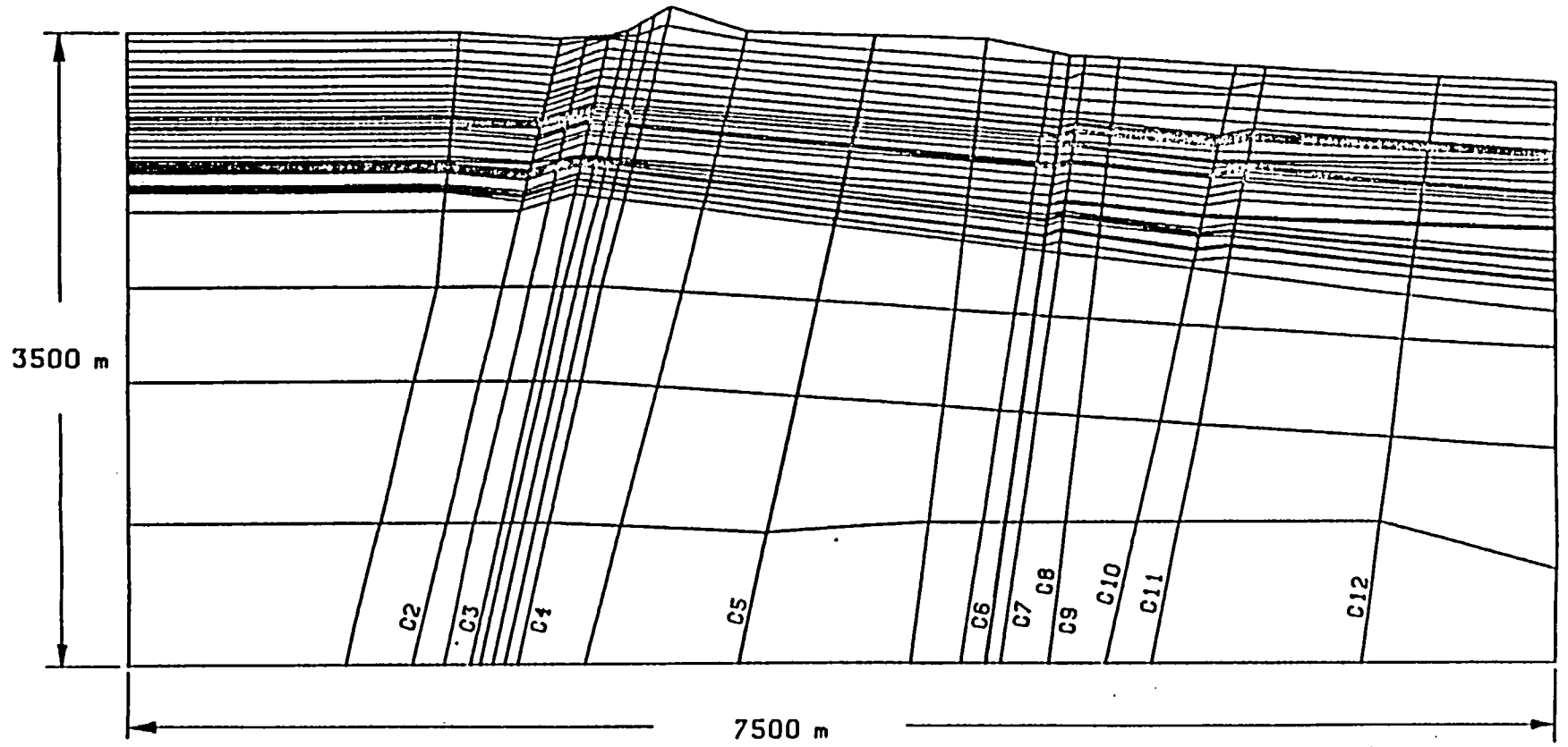


Figure 49. Finite Element Mesh Used in Far-Field Thermal/Mechanical Calculations.

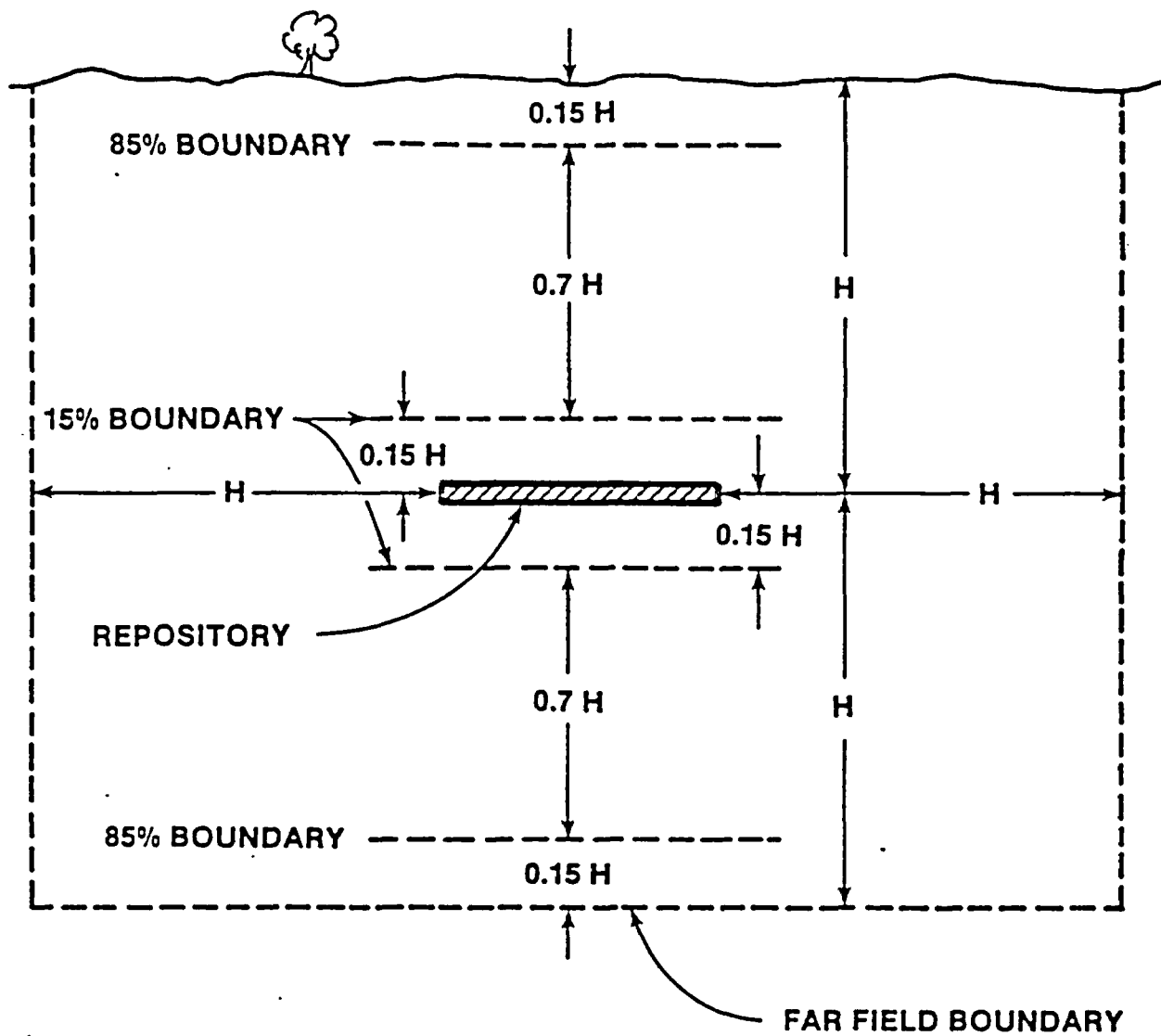
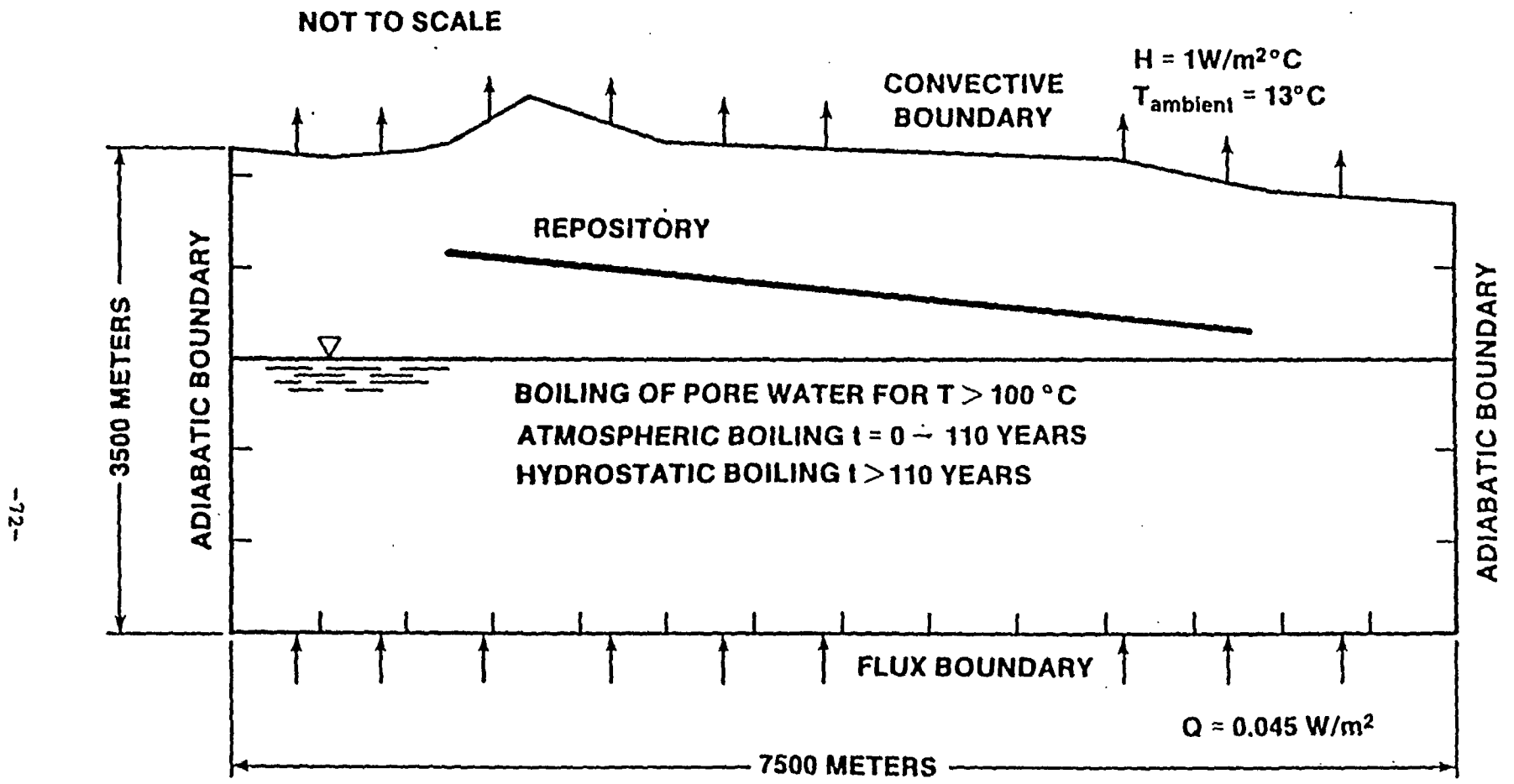


Figure 50. Schematic Diagram Showing Position of Boundaries.

SYSTEM COMPONENT		OPERATIONAL PERIOD	CONTAINMENT PERIOD	ISOLATION PERIOD
FAR FIELD	SHAFT	OPERATIONAL SERVICEABILITY	NO CONSTRAINT	
		INTERSECT NO MAJOR FAULTS		
	SEALS:			
	SHAFT AND BOREHOLE		EFFECTIVE PERMEABILILTY = TUFF*	
	ROCKMASS:			
	MECHANICAL BEHAVIOR		NO NEW FRACTURES*	
	MINERAL DEHYDRATION/ ALTERATION		T < 150°C*	
SURFACE UPLIFT AND SUBSIDENCE		< NATURAL ANALOGS		
SURFACE TEMPERATURE INCREASE		ΔT < 6°C (COMPARABLE TO NATURAL VARIATIONS)		
THERMALLY PERTURBED GROUNDWATER FLOW		TRAVEL TIME TO ACCESSIBLE ENVIRONMENT > 1000 YEARS		

*THESE CONSTRAINTS APPLY TO THE "INTACT" (70% REGION) ROCKMASS

Figure 51. Far-Field Preliminary Technical Constraints.



-72-

Figure 52. Thermal Model Conceptualized.

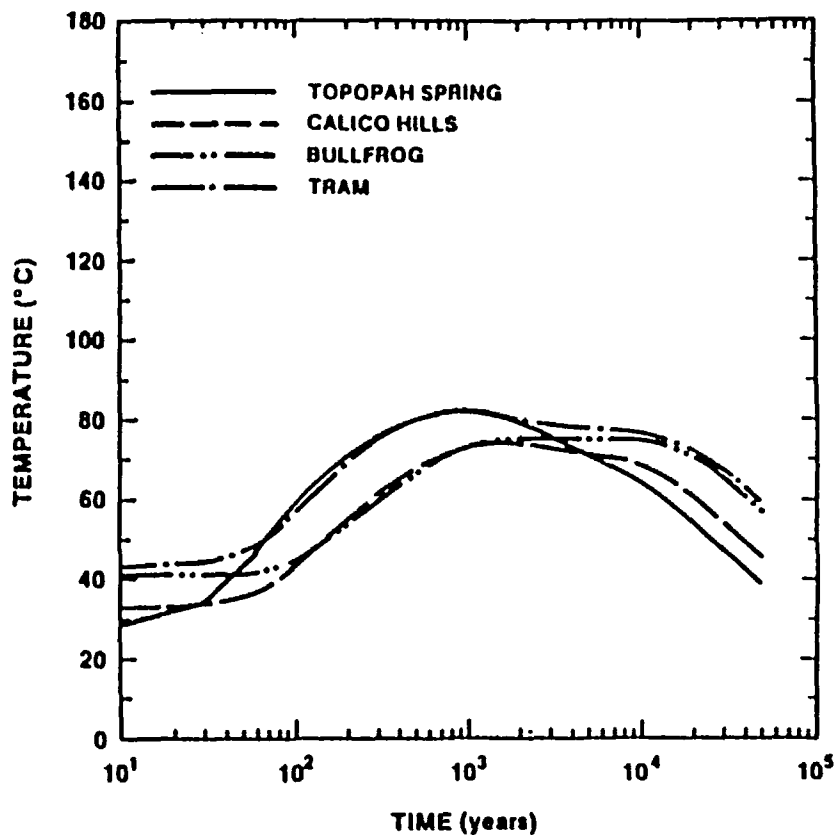


Figure 53. Thermal History of the 15% Boundary Below the Repository Horizons (Average properties).

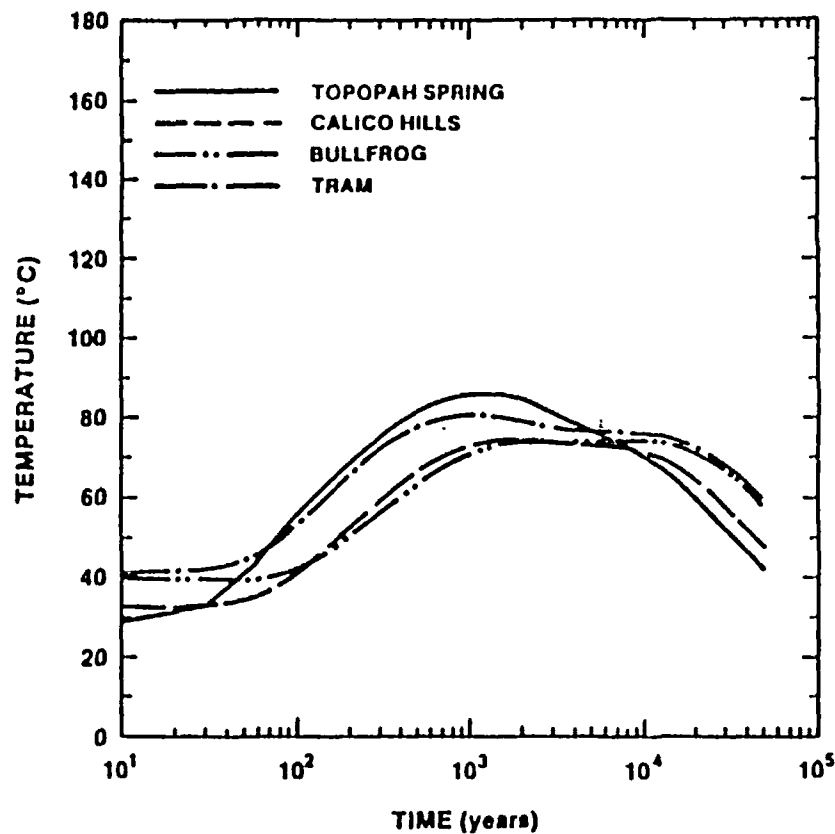


Figure 54. Thermal History of the 15% Boundary Below the Repository Horizons (Limit properties).

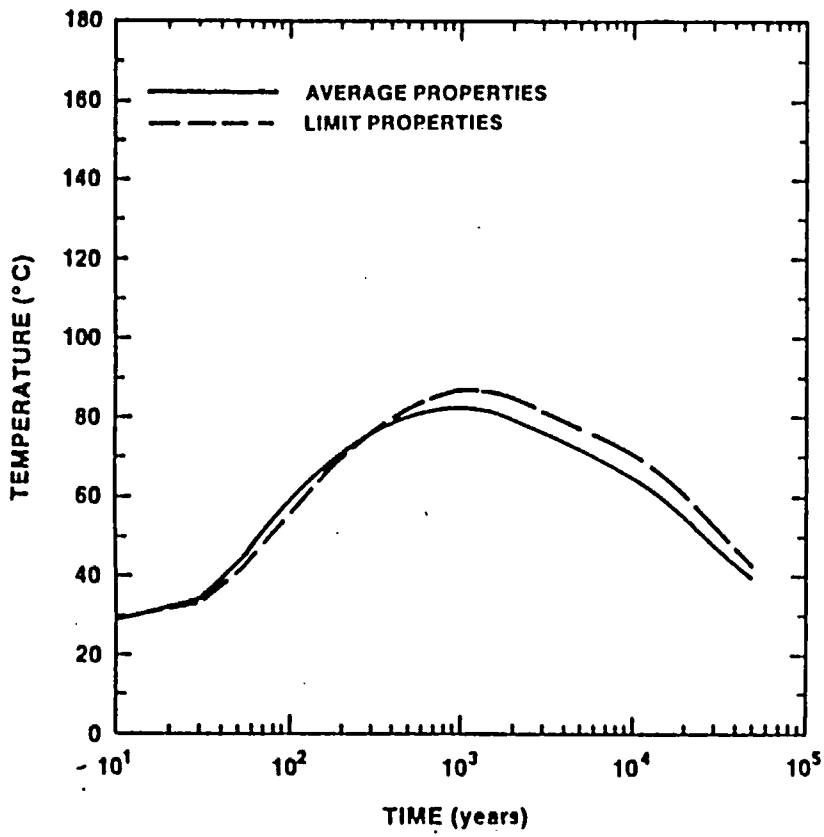


Figure 55. Thermal History of the 15% Boundary Below the Topopah Spring Repository Horizon.

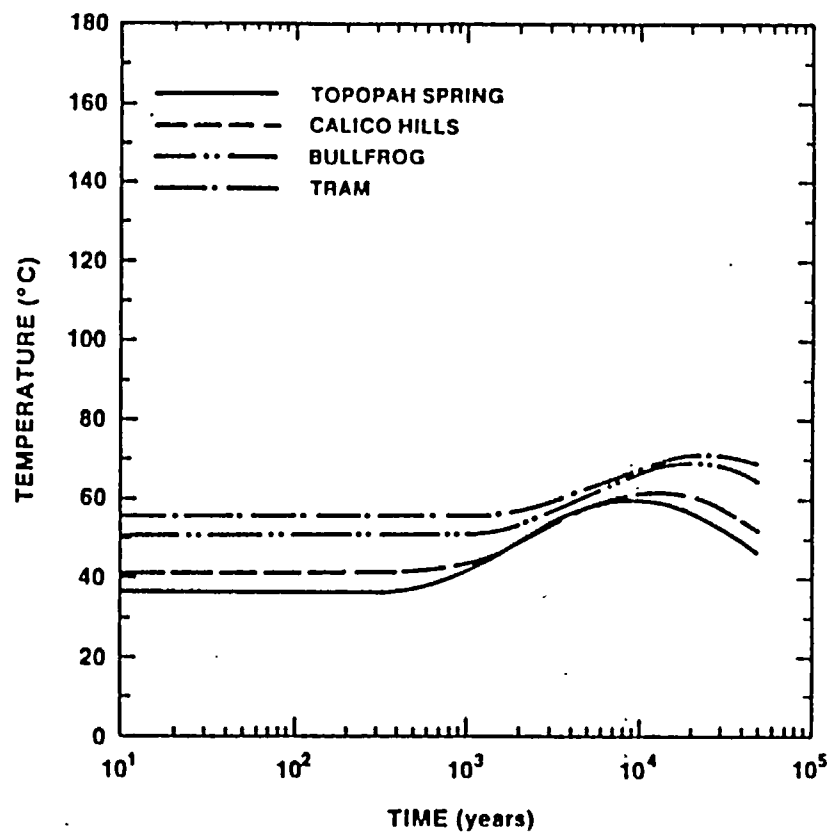


Figure 56. Thermal History of the 85% Boundary Below the Repository Horizons (Average properties).

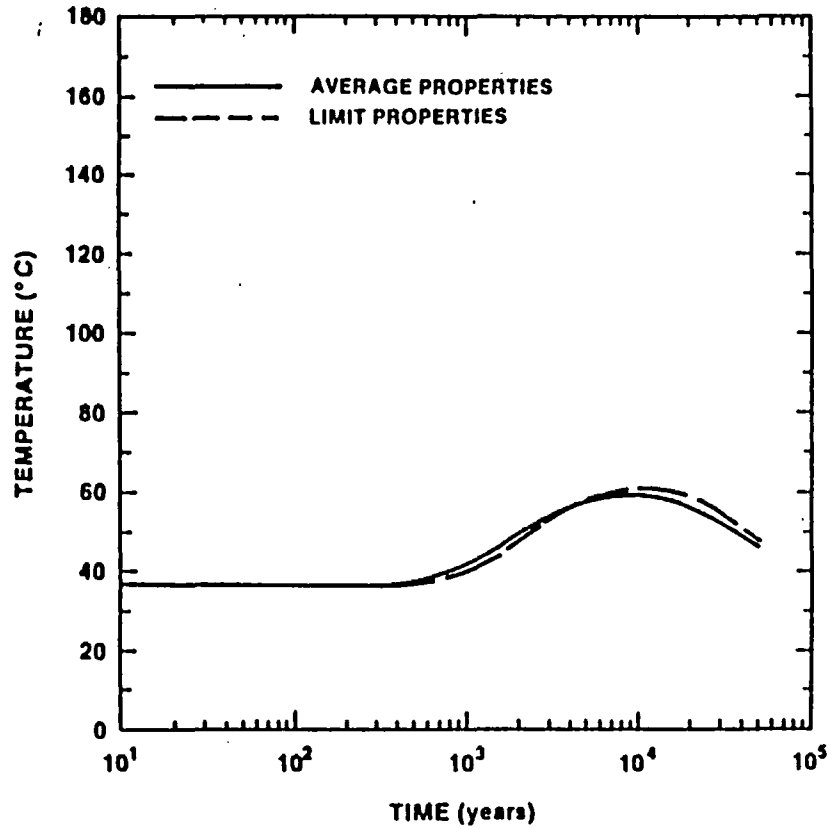


Figure 57. Thermal History of the 85% Boundary Below the Topopah Spring Repository Horizon.

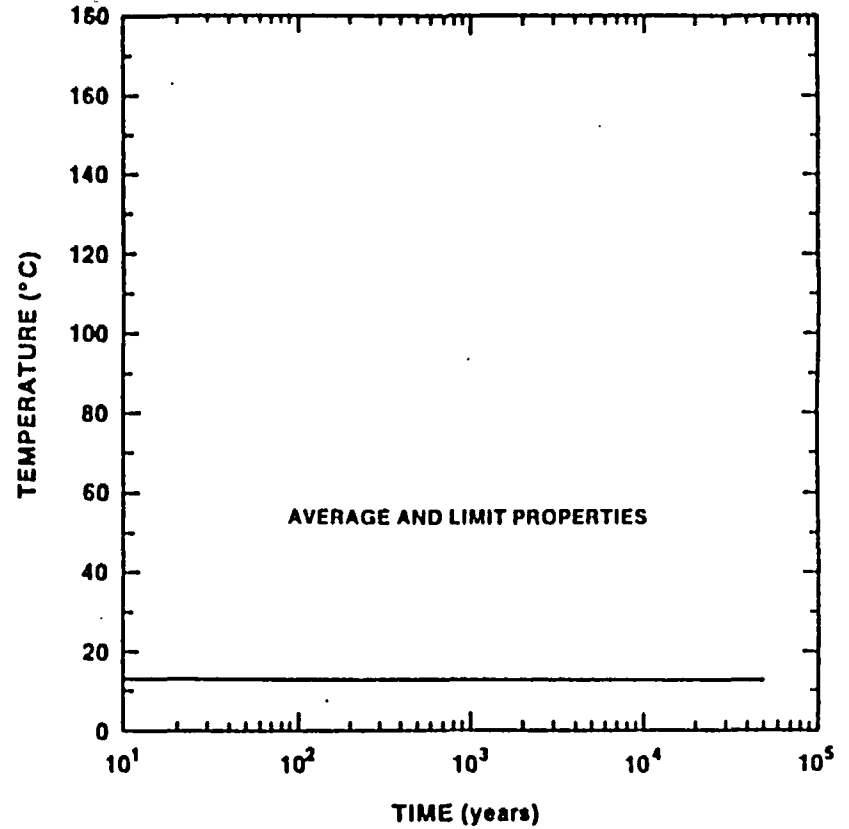


Figure 58. Thermal History 3 m Below Ground Surface When the Repository is Located in the Topopah Spring Horizon. (Max $\Delta T = 0.6^\circ\text{C}$ at time = 3,000 years.)

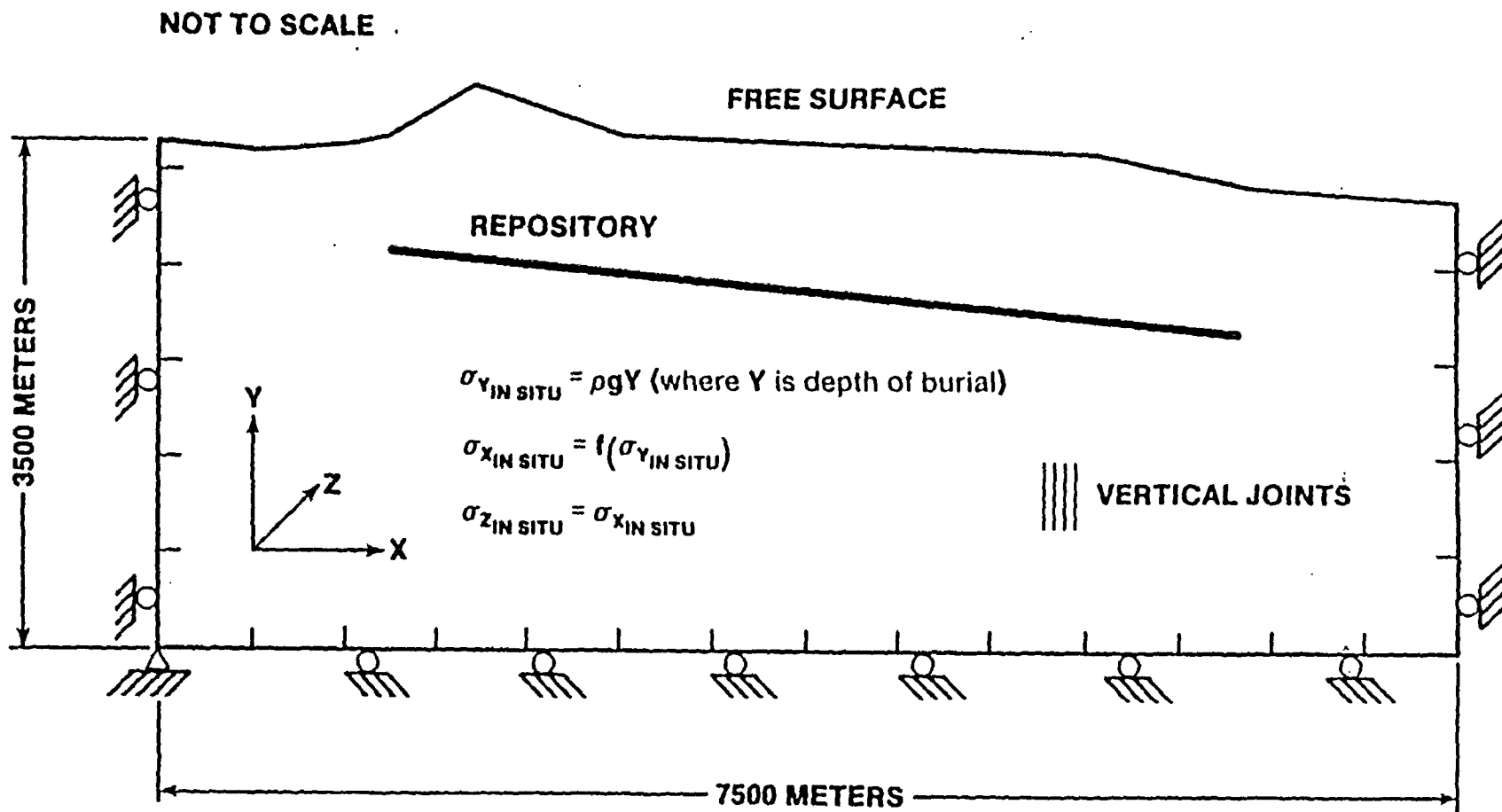


Figure 59. Mechanical Model Conceptualized.

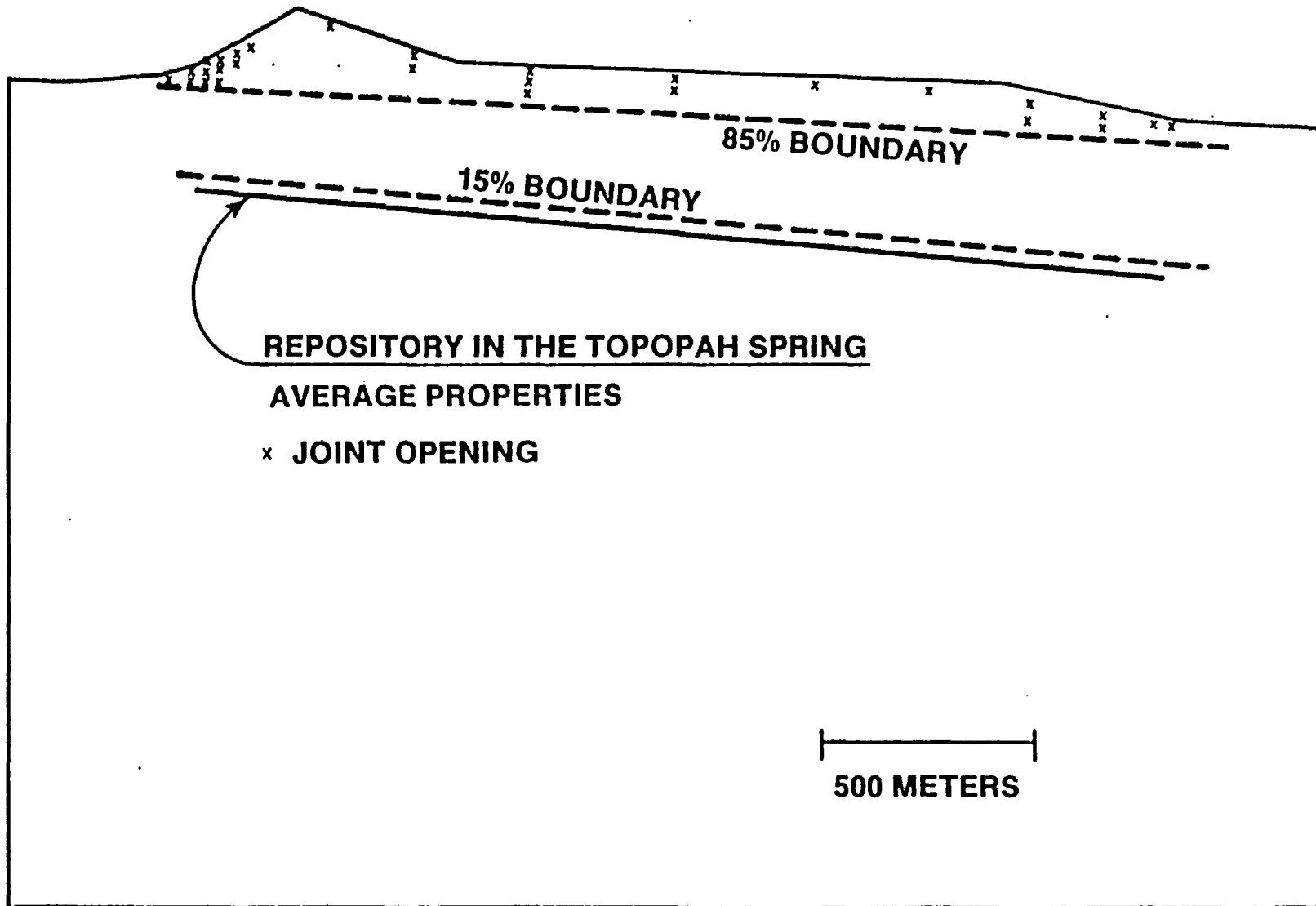


Figure 60. Far-Field Joint Opening With the Repository in the Topopah Spring (Average properties throughout the section).

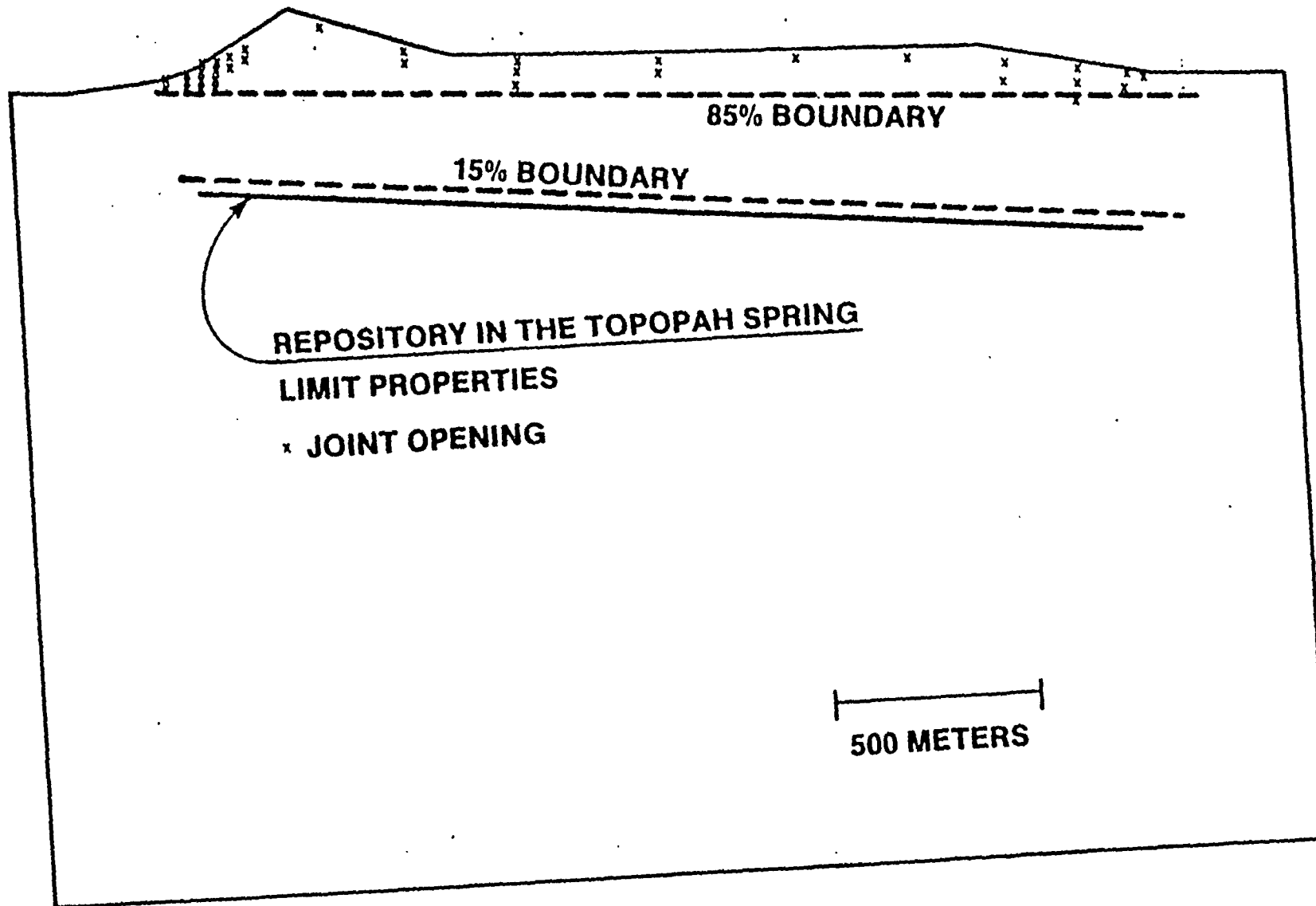


Figure 61. Far-Field Joint Opening With the Repository in the Topopah Spring (Limit properties throughout the section).

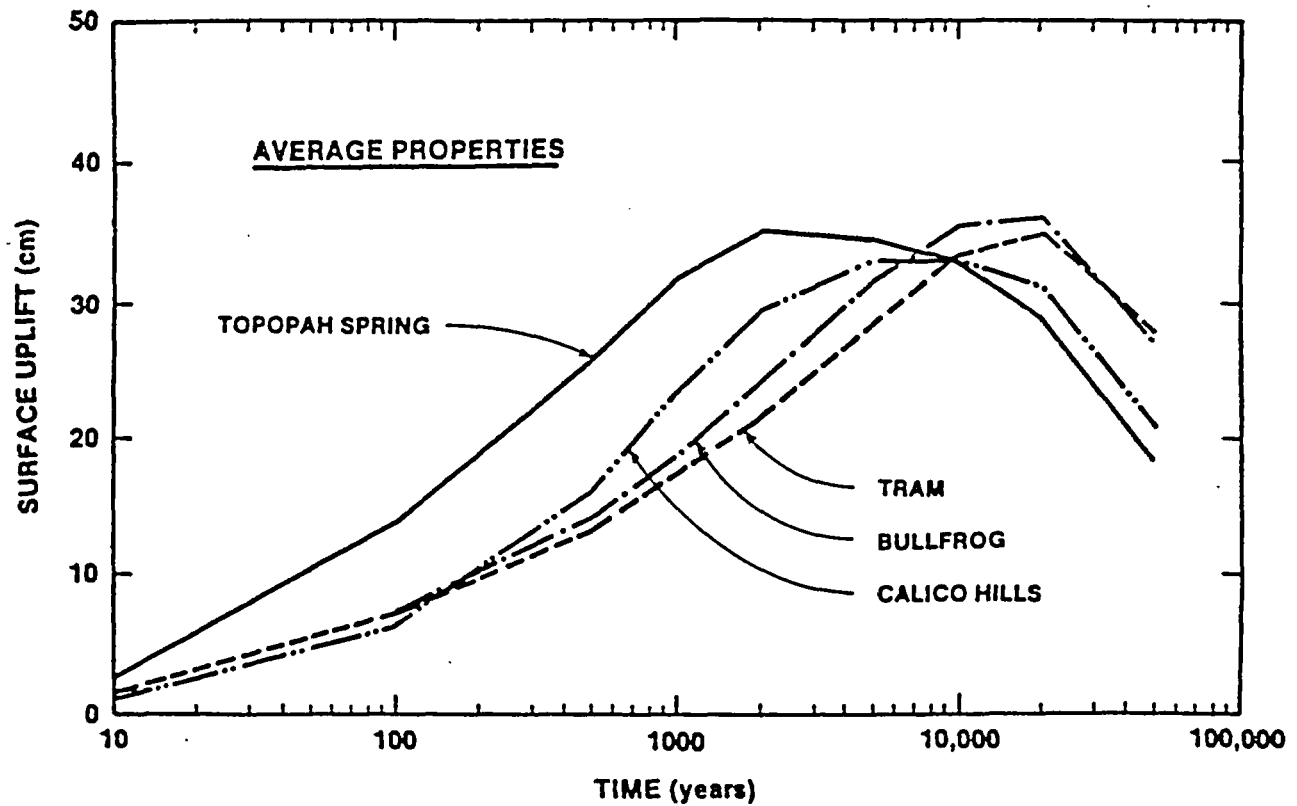


Figure 62. Surface Uplift Resulting From a Repository Emplaced in the Designated Units (Average properties throughout the section).

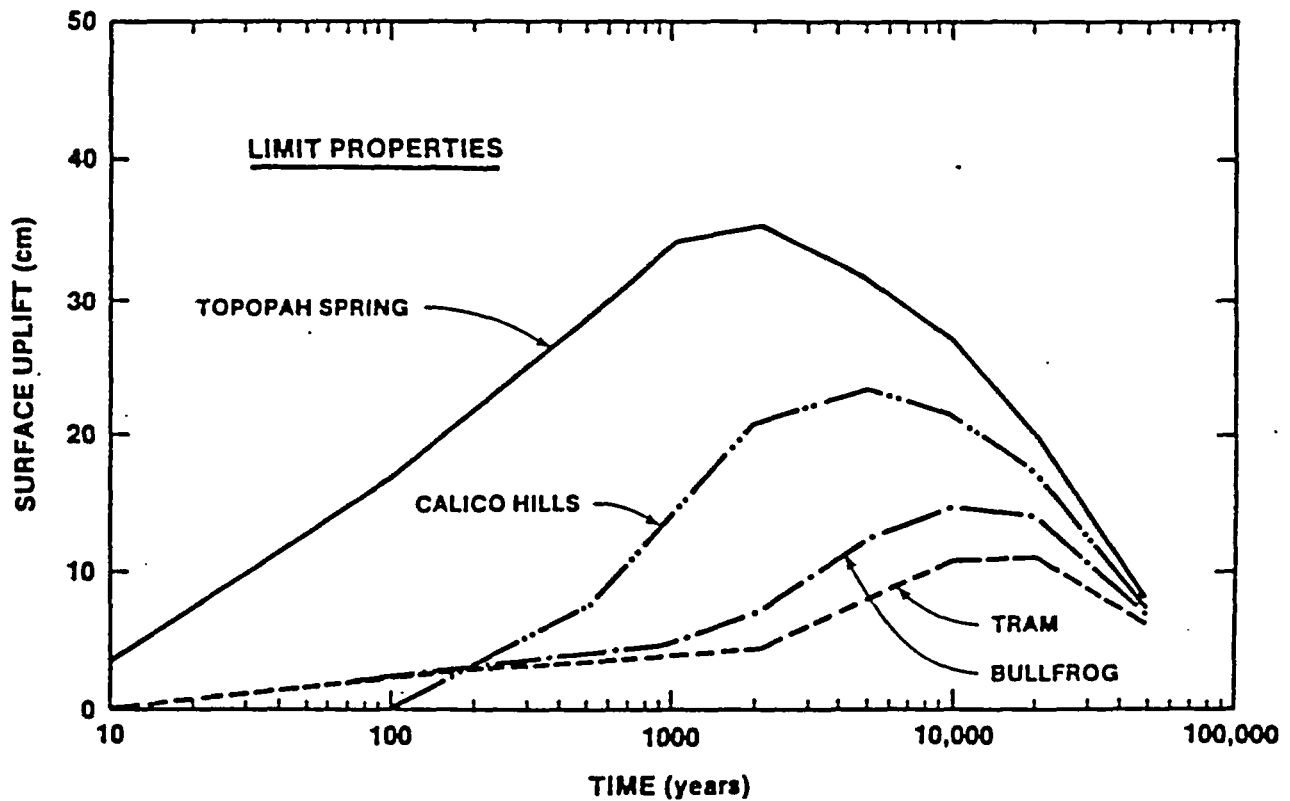


Figure 63. Surface Uplift Resulting From a Repository Emplaced in the Designated Units (Limit properties throughout the section).

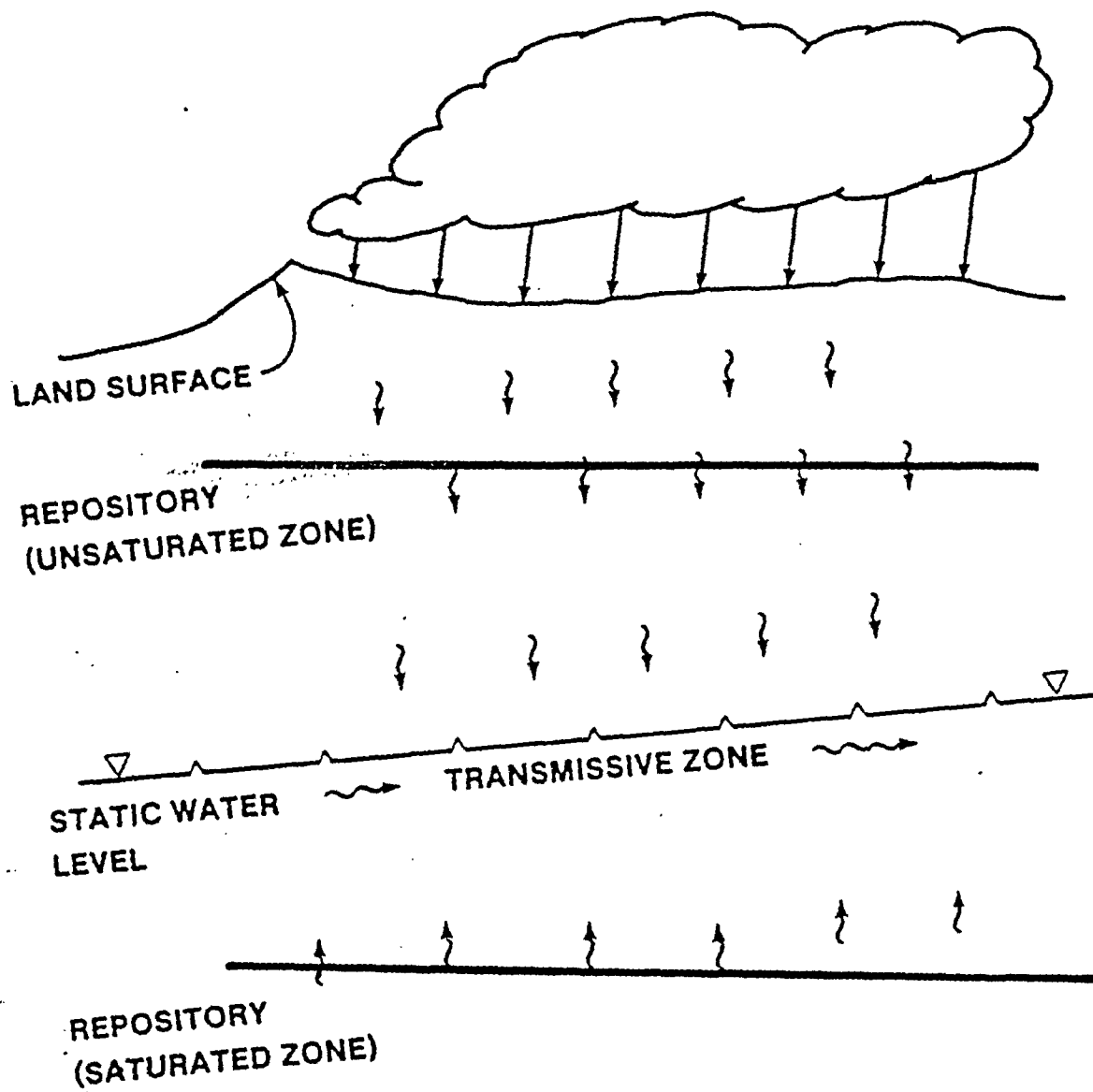
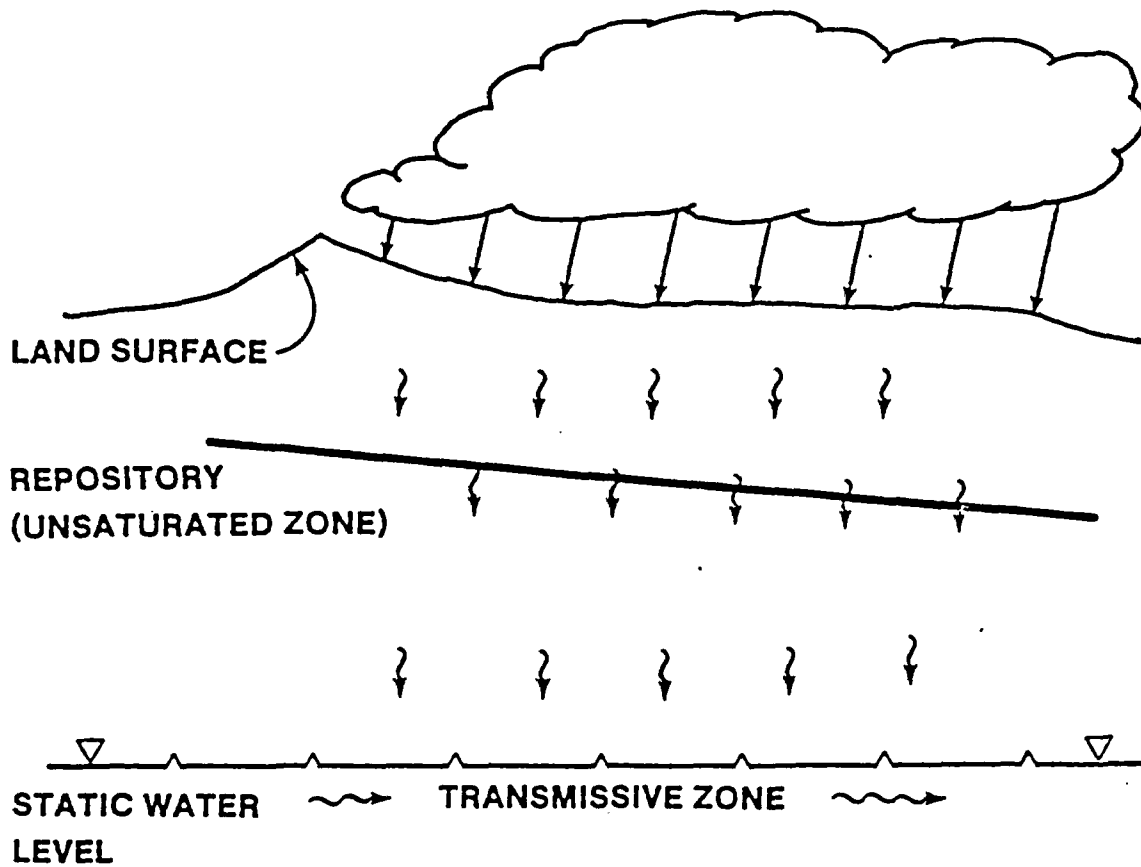


Figure 64. Conceptual Model for Groundwater Flow.



STEADY STATE VERTICAL INFILTRATION

$$\text{FLUID FLUX} = \frac{3 \text{ l}}{\text{m}^2 \text{ yr}} = 3 \frac{\text{ mm}}{\text{ yr}}$$

$$\text{VELOCITY} = \frac{\text{FLUX}}{\text{EFFECTIVE POROSITY } (\phi_E)}$$

Figure 65. Conceptual Steady-State Infiltration Model for the Unsaturated Zone.

DISTRIBUTION LIST

J. W. Bennett (RW-20)
Acting Associate Director
Geologic Repository Deployment
U. S. Department of Energy
Washington, D. C. 20545

Ralph Stein (RW-21)
Acting Deputy Associate Director
Geologic Repository Deployment
U. S. Department of Energy
Washington, D. C. 20545

J. G. Vlahakis (RW-21)
Geologic Repository Deployment
U. S. Department of Energy
Washington, D.C. 20545

C. R. Cooley (RW-24)
Acting Director
Geosciences & Technology Division
Geologic Repository Deployment
U. S. Department of Energy
Washington, D.C. 20545

M. W. Frei (RW-23)
Acting Director
Engineering & Licensing Division
Geologic Repository Deployment
U.S. Department of Energy
Washington, D.C. 20545

J. J. Fiore (RW-22)
Acting Director
Program Management Division
Geologic Repository Deployment
U.S. Department of Energy
Washington, D.C. 20545

E. S. Burton (RW-25)
Acting Director
Siting Division
Geologic Repository Deployment
U.S. Department of Energy
Forrestal Building
Washington, D.C. 20585

T. P. Longo (RW-22)
Geologic Repository Deployment
U. S. Department of Energy
Washington, D. C. 20545

Cy Klingsberg (RW-24)
Geologic Repository Deployment
U. S. Department of Energy
Washington, D. C. 20545

J. E. Shaheen (RW-25)
Geologic Repository Deployment
U. S. Department of Energy
Forrestal Building
Washington, D.C. 20585

Chief, High-Level Waste Technical
Development Branch
Division of Waste Management
U. S. Nuclear Regulatory Commission
Washington, D.C. 20555

NTS Project Manager
High-Level Waste Technical
Development Branch
Division of Waste Management
U. S. Nuclear Regulatory Commission
Washington, D.C. 20555

Document Control Center
Division of Waste Management
U.S. Nuclear Regulatory Commission
Washington, D.C. 20555

J. O. Neff, Program Manager
National Waste Terminal
Storage Program Office
U.S. Department of Energy
505 King Avenue
Columbus, OH 43201

C. H. George (RW-3)
Geologic Repository Deployment
U.S. Department of Energy
Washington, D.C. 20545

ONWI Library (5)
Battelle
Office of Nuclear Waste Isolation
505 King Avenue
Columbus, OH 43201

O. L. Olson, Project Manager
Basalt Waste Isolation Project Office
U.S. Department of Energy
Richland Operations Office
P.O. Box 550
Richland, WA 99352

E. B. Ash
Rockwell International Atomics
Rockwell Hanford Operations
Richland, WA 99352

A. A. Metry, Program Manager
Roy F. Weston, Inc.
2301 Research Blvd., 3rd Floor
Rockville, MD 20850

G. Tomsic
Utah Dept. of Community
Economic Development
Room 6290, State Office Bldg.
Salt Lake City, UT 89114

A. Johnson
414 West Ninth Street
Carson City, NV 89701

R. R. Loux, Jr.
Nuclear Waste Project Office
Office of the Governor
State of Nevada
Capitol Complex
Carson City, NV 89710

N. E. Carter
Battelle
Office of Nuclear Waste Isolation
505 King Avenue
Columbus, OH 43201

S. A. Mann, Manager
Crystalline Rock Project Office
U.S. Department of Energy
9800 S. Cass Avenue
Argonne, IL 60439

L. D. Ramspott (3)
Technical Project Officer
Lawrence Livermore National
Laboratory
P.O. Box 808
Mail Stop L-204
Livermore, CA 94550

D. C. Hoffman
Los Alamos National Laboratory
P.O. Box 1663
Mail Stop E-515
Los Alamos, NM 87545

D. T. Oakley (3)
Technical Project Officer
Los Alamos National Laboratory
P.O. Box 1663
Mail Stop F-671
Los Alamos, NM 87545

T. Hay, Executive Assistant
Office of the Governor
State of Nevada
Capitol Complex
Carson City, NV 89710

R. W. Lynch
Sandia National Laboratories
P. O. Box 5800
Organization 6300
Albuquerque, NM 87185

T. O. Hunter (4)
Technical Project Officer
Sandia National Laboratories
P. O. Box 5800
Organization 6310
Albuquerque, NM 87185

K. Street, Jr.
Lawrence Livermore National
Laboratory
P.O. Box 808
Mail Stop L-209
Livermore, CA 94550

A. R. Hakl, Manager
Westinghouse Electric Corporation
Waste Technology Services Division
Nevada Operations
P.O. Box 708
Mail Stop 703
Mercury, NV 89203

W. W. Dudley, Jr. (3)
Technical Project Officer
U.S. Geological Survey
P.O. Box 25046
Mail Stop 418
Federal Center
Denver, CO 80225

J. A. Cross, Manager
Las Vegas Branch
Fenix & Scission, Inc.
P.O. Box 15408
Las Vegas, NV 89114

M. E. Spaeth (3)
Technical Project Officer
Science Applications, Inc.
2769 South Highland Drive
Las Vegas, NV 89109

W. S. Twenhofel
820 Estes Street
Lakewood, CO 80215

D. L. Vieth, Director (8)
Waste Management Project Office
U.S. Department of Energy
P.O. Box 14100
Las Vegas, NV 89114

D. F. Miller, Director
Office of Public Affairs
U.S. Department of Energy
P.O. Box 14100
Las Vegas, NV 89114

D. A. Nowack (14)
Office of Public Affairs
U.S. Department of Energy
P.O. Box 14100
Las Vegas, NV 89114

B. W. Church, Director
Health Physics Division
U.S. Department of Energy
P.O. Box 14100
Las Vegas, NV 89114

A. E. Gurrola, General Manager
Energy Support Division
Holmes & Narver, Inc.
P.O. Box 14340
Las Vegas, NV 89114

H. D. Cunningham
General Manager
Reynolds Electrical &
Engineering Co., Inc.
P.O. Box 14400
Mail Stop 555
Las Vegas, NV 89114

P. T. Prestholt
NRC Site Representative
Federal Building
Room 323
300 Las Vegas Blvd. South
Las Vegas, NV 89101

Louelle Clark
Battelle Northwest Labs
Richland, WA 99352

W. R. McDonnell
Operational Planning Division
E.I. DuPont de Nemours & Co., Inc.
Savannah River Laboratory
Aiken, SC 29808

RE/SPEC, Inc. (6)
P.O. Box 725
Rapid City, SD 55709
Attn: P. F. Gnirk
J. L. Ratigan
S. Key
T. Brandshaug
A. Melo
D. K. Parrish

F. H. Dove
Battelle Pacific Northwest
Laboratory
P.O. Box 999
Richland, WA 99352

W. A. Hustrulid
Dept. of Mining Engineering
Colorado School of Mines
Golden, CO 80401

Scott-Ortech, Inc. (2)
12567 West Cedar Dr.
Lakewood, CO 80228
Attn: J. L. Ash
W. E. Craig

J. L. Younker (50)
Science Applications, Inc.
2769 S. Highland Dr.
Las Vegas, NV 89101

1500 W. Herrmann
1510 J. W. Nunziato
1520 T. B. Lane
1522 R. L. Johnson
1524 W. N. Sullivan
1524 R. K. Thomas
1542 B. M. Butcher
1542 R. H. Price
6311 L. W. Scully
6311 R. I. Brasier
6311 A. W. Dennis
6311 T. W. Eglinton
6311 J. L. Jackson
6311 H. R. MacDougall
6311 J. T. Neal
6311 P. D. O'Brien

6311 L. G. Perrine (2)
6311 C. G. Shirley
6311 V. J. Stephens
6311 K. D. Young
6312 F. W. Bingham
6312 J. W. Braithwaite
6312 N. K. Hayden
6312 J. K. Johnstone (20)
6312 B. S. Langkopf
6312 Y. T. Lin
6312 R. R. Peters (5)
6312 S. Sinnock
6312 J. G. Yeager
6313 J. R. Tillerson
6313 J. A. Fernandez
6313 F. B. Nimick
6313 R. M. Zimmerman
6313 G. K. Beall
6313 A. J. Mansure
6314 R. E. Stinebaugh
6330 J. T. Henderson
3141-1 C. M. Ostrander (5)
3151 W. L. Garner (3)
8424 M. A. Pound